

# Master thesis

submitted for the degree of  
Master

**Technical University of Applied Sciences Wildau**

**Faculty of Engineering and Natural Sciences**

**Mechanical Engineering M. Eng.**

**Title (german):** Konzentrierende Solarenergie: Vergleich und Bewertung innovativer Parabolrinnenkollektor-Konzepte für die Anwendung im großen Maßstab

**Title:** Concentrated Solar Power: A comparison and evaluation of innovative parabolic trough collector concepts for large scale application

Author: José Rolando Fredriksson Chaves

Student number: 121042235

Study group: MM/15

Supervisor: Prof. Dr. rer. nat. Lutz Giese

Second assessor: Prof. Dr. rer. nat. Michael Herzog

Institute advisor: Dipl. Ing. Martin Eickhoff  
German Aerospace Center (DLR)  
Institute for Solar Research

Submitted on: 11.08.2019

# Master thesis

Application received: 18.01.2019

Name:	José Rolando Fredriksson Chaves	Student number:	121042235
Study programme:	Maschinenbau	Study group:	MM/15
First examiner:	Prof. Dr. rer. nat. Lutz Giese	Start of work:	11.02.2019
Second examiner:	Prof. Dr. rer. nat. Michael Herzog	Submission Date:	14.07.2019
Presenter of topic:	German Aerospace Center [DLR]/ Deutsches Zentrum für Luft- und Raumfahrt	Company advisor:	Martin Eickhoff
		Street:	Paseo de Almería, 73, 2
		Code and City:	E-04001 Almería

## Title (German)

Konzentrierte Solarenergie: Vergleich und Bewertung von innovativen Parabolrinnenkollektor-Konzepten für die Anwendung im großen Maßstab

## Title

Concentrated Solar Power: A comparison and evaluation of innovative parabolic trough collector concepts for large scale application

## Goal

Define the state of the art on parabolic trough concepts for solar thermal energy generation and present an emphasis on future trends. Identify innovative concepts that cover performance requirements and offer a cost-effective character\*.

## Contents requirements / specific tasks

- Extensive literature research to identify known innovative collector concepts
- Describe the working principle of the technology and of important components (e.g. reflectors, heat transfer fluid, absorber tubes, bearing structures, among others).
- Detailed description of these collector concepts based on literature and direct contact with the manufacturers (or users)
- Creation of an evaluation matrix for a comparative analysis and define the comparison criteria
- Analytical evaluation of the collector concepts using information from literature research and from direct contacts with the manufactures (or users)

## Thesis Language

English

Consultation: on appointment with university advisor

Prof. Dr. rer. nat. Lutz Giese (University lecturer)	Prof. Dr. rer. nat. Michael Herzog (Second assessor)	José Rolando Fredriksson Chaves (Student)	<i>Approved</i> (Examination board)
---	---	---	--

Submission date \_\_\_\_\_

Nondisclosure  Yes  No



## **Bibliographical Description and Presentation**

### **Title in English:**

Concentrated Solar Power: A comparison and evaluation of innovative parabolic trough collector concepts for large scale application

### **Title in German:**

Konzentrierende Solarenergie: Vergleich und Bewertung innovativer Parabolrinnenkollektor-Konzepte für die Anwendung im großen Maßstab

Master thesis, 2019, 99 Pages

54 Figures; 23 Tables; 2 Annexes (from which: 1 Supplement of Master Thesis)

University of Applied Sciences Wildau, Faculty of Engineering and Natural Sciences, Wildau

### **Objective:**

Define the state of the art on parabolic trough concepts for solar thermal energy generation and present an emphasis on future trends. Identify innovative concepts that cover performance requirements and offer a cost-effective character

### **Content:**

The thesis presents relevant components that define the performance of parabolic trough collectors, among them: mirror materials, receivers, structures and heat transfer fluids. The collectors are respectively categorized according to their features. Criteria are defined for the analysis and evaluation. The cycle of selected collector loops is simulated for thermo-oil and molten salt collectors, to attain the thermal gain potential. The economic impact of up scaling effects and implementation of molten salts as heat transfer fluid is highlighted. An evaluation matrix according to the VDI2225 guideline of the Association of German Engineers (VDI) is conducted.

**Keywords:** Concentrated Solar Power, Parabolic Trough Collector, Innovation, Molten Salt, Technical-Economic Value, Renewable Energy

**Statutory Declaration:**

I hereby declare that I have prepared the present thesis independently and have used only the specified sources and resources.

Berlin, 11<sup>th</sup> August 2019

---

José Rolando Fredriksson Chaves

**Disclaimer:**

This thesis was prepared by the author in cooperation between the Institute for Solar Research of the DLR and the University of Applied Sciences Wildau. Neither the author nor the DLR, nor the University of Applied Sciences Wildau, nor their employees, make any warranty, expressed or implied, or assume any legal liability or responsibility for the accuracy, completeness or usefulness of any information given in this thesis.

If the reader finds any error, incompleteness or ambiguity, please help to improve the document by sending your comments to José Fredriksson ([eng.fredriksson@gmail.com](mailto:eng.fredriksson@gmail.com))

## **Acknowledgments**

Special thanks for the transmitted know-how for this thesis to the institute advisor, Dipl. Ing. Martin Eickhoff from the Institute for Solar Research of the German Aerospace Center (DLR), as well as to the first supervisor, Prof. Dr. rer. nat. Lutz Giese and to the second assessor, Prof. Dr. rer. nat. Michael Herzog from the University of Applied Sciences Wildau.

I am also very thankful to Erik Fredriksson and Dr. Robert Schmidt for the corrections and comments on the content.

Last but not least, thanks to the department of the Institute for Solar Research in Almería, Spain, for supporting the internal survey about parabolic trough collectors.

## List of Contents

<b>List of Tables .....</b>	<b>VII</b>
<b>List of Figures .....</b>	<b>VIII</b>
<b>List of Abbreviations and Symbols .....</b>	<b>XI</b>
<b>Summary .....</b>	<b>XV</b>
<b>1. Introduction.....</b>	<b>1</b>
1.1 Problem Statement .....	2
1.2 Objectives and Tasks.....	3
1.3 Methodology .....	4
1.4 Thesis Structure.....	4
<b>2. State of the Art .....</b>	<b>5</b>
2.1 Geometry and Concentration Ratio.....	10
2.2 Mirror Materials .....	12
2.3 Receivers .....	16
2.4 Heat Transfer Fluid .....	19
2.5 Collector Efficiency .....	23
2.5.1 Optical Losses .....	25
2.5.2 Thermal Losses .....	27
2.5.3 Parasitic Energy Losses in the Solar Field.....	29
<b>3. Parabolic Trough Collector Concepts .....</b>	<b>30</b>
3.1 Category: Historical Collectors .....	32
3.2 Category A: Conventional Collectors .....	34
3.3 Category B: Metal Structures & Sheet Reflectors .....	38
3.4 Category C: Non-Metallic Materials.....	39

3.5	Category D: Enclosed Aperture Collectors .....	41
3.6	Category E: Fixed Focus .....	42
3.7	Technical Overview .....	45
<b>4.</b>	<b>Value Analysis and Evaluation.....</b>	<b>49</b>
4.1	Comparison Criteria .....	49
4.1.1	Optical Performance .....	49
4.1.2	Thermal Performance.....	56
4.1.3	Parasitic Consumption .....	65
4.1.4	Global Efficiency by Heat Transfer Fluid .....	71
4.1.5	Costs Scenario.....	74
4.1.6	Scaling Potential .....	80
4.1.7	Structure .....	84
4.2	Evaluation Matrix.....	89
4.3	Evaluation Results.....	93
4.4	Evaluation Discussion .....	95
<b>5.</b>	<b>Conclusion and Outlook.....</b>	<b>98</b>
<b>6.</b>	<b>Bibliography .....</b>	<b>100</b>
<b>Annex A</b> .....	<b>A-1</b>	
<b>Annex B</b> .....	<b>B-1</b>	

## List of Tables

Table 1.	Overview on current reflector materials for parabolic trough collectors.....	14
Table 2.	Heat transfer fluid requirements [15] .....	20
Table 3.	Characteristics of nitrate/nitrite salts and Therminol VP-1 [28] .....	21
Table 4.	Densities and Young´s module of diverse materials [17].....	39
Table 5.	Example mixture of an UHPC composition [2006] .....	40
Table 6.	Overview of Category A: Conventional Parabolic Trough Collectors.....	46
Table 7.	Overview of Category B: Alternative Structures & Sheet Reflectors and Category C: Alternative Materials.....	47
Table 8.	Overview of Category D: Enclosed Aperture and Category E: Fix Focus of different Parabolic Trough Collector.....	48
Table 9.	Ranking of reflector types for large scale application of parabolic troughs .....	50
Table 10.	Peak optical efficiency of different parabolic trough collectors.....	51
Table 11.	Incidence Angle Modifier at the example of an EuroTrough and SkyFuel collector [48] [49].....	52
Table 12.	Required PTC aperture length to reach operational temperature of thermo-oil T=400°C.....	58
Table 13.	Simulation results of different PTC loops and relevant parameters for the computation with Thermo-Oil as HTF.....	62
Table 14.	Simulation results of different parabolic trough collector loops and relevant parameters for the computation with Molten Salt as heat transfer fluid.....	64
Table 15.	Parasitic power consumption due to the HTF pump of the solar field with Thermo-Oil as HTF.....	68
Table 16.	Parasitic power consumption due to the HTF pump of the solar field with molten salt as HTF.....	69
Table 17.	Collector efficiencies with Thermo-Oil and Molten Salt as heat transfer fluid.....	71
Table 18.	Case study of thermo-oil vs. molten salt power plant with EuroTrough (ET) and UltimateTrough (UT) collectors. [9] .....	75
Table 19.	Specific solar field cost estimation with different PTC.....	77
Table 20.	Intercept factor of innovative parabolic trough concepts .....	84
Table 21.	Specific total weight and maximal operational wind speed .....	86
Table 22.	Evaluation metrics of the criteria and sub-criteria.....	91

Table 23.	Evaluation matrix of innovative parabolic trough collector concepts for large scale application .....	92
-----------	---	----

## List of Figures

Figure 1	Estimate renewables share total of final energy consumption, 2016 [4] .....	1
Figure 2	Worldwide overview of operating, planned and under construction CSP projects [6].....	2
Figure 3	a) General scheme on concentrating solar energy at the focal point of a PTC [10] b) One-axis tracking of the sun [11] .....	5
Figure 4	Scheme of a PTC Solar Power Plant, with three integrated blocks: Solar Field, Thermal Storage and Power Block [12] .....	6
Figure 5	Noor I Power Plant 160 MW, Ouarzazate Morocco (2016) and Noor II 200 MW (2017) [13] .....	7
Figure 6	HelioTrough Loop segmentation and dimensions.....	7
Figure 7	Main components of a parabolic trough collector with EuroTrough collector as example [11].....	8
Figure 8	Energy and components flow diagram in a parabolic trough solar field and three current applications .....	9
Figure 9	Geometrical parameters and geometrical concentration ratio of a parabolic trough.....	10
Figure 10	Dependence of the focal spot size on the rim angle [15].....	11
Figure 11	Schematic representation of direct and diffuse reflection on a mirror surface [16] .....	12
Figure 12	Hemispherical reflectance spectra of different material samples according to standard ASTM G173-03 [16].....	15
Figure 13	a) Components of a receiver tube at the example of a PTR70 Schott receiver b) Integrated elements to enhance longevity and performance.....	16
Figure 14	Multi-layer coating of the absorber tube .....	17
Figure 15	Reflectance of a spectral selective coating, e.g. TaSi <sub>2</sub> , and spectral ranges of the solar radiation and the blackbody radiation at 700°C [23].....	17

Figure 16	Receiver for air as heat transfer fluid implemented used in the Airlight collector [25] .....	18
Figure 17	Direct storage system cycle overview using molten salts. The solar field cycle and the steam generation cycle are decoupled [31] .....	22
Figure 18	Calculation of the effective thermal energy in a PTC .....	23
Figure 19	Collector efficiency curve at the example of an LS-2 collector with empirical parameter values and DNI= 800 W/m <sup>2</sup> .....	24
Figure 20	Tracking case for an East-West- oriented PTC to explain the Incidence Angle Modifier IAM [33] .....	26
Figure 21	A one-dimensional heat balance on a receiver cross-section .....	28
Figure 22	Heat loss measurements for different receiver types [36] .....	28
Figure 23	Estimated energetic flow in a parabolic trough power plant [37] .....	29
Figure 24	Genealogy of selected parabolic trough collectors categorized into the main conventional and innovative concepts with a further subdivision according to their prevalent feature.....	30
Figure 25	Augustine Mouchout’s an John Ericsson’s schematic parabolic trough collector [39] .....	32
Figure 26	Front sight and back sight of a collector row at the Solar Engine One power plant in Al Meadi, Egypt 1912 [39].....	33
Figure 27	Reflector facets [41] .....	34
Figure 28	Double torque box, torque box, torque tube, space frame [42] .....	35
Figure 29	Assembly jig of a torque box structure [43] and assembly jig of a torque tube structure [44] .....	35
Figure 30	Flexible interconnection elements [41] .....	36
Figure 31	Time line conventional collectors and module’s dimensions.....	37
Figure 32	Self-supporting fiber glass reinforced sandwich structure [45].....	40
Figure 33	Enclosed collector concepts. (left) HelioTube [Heliovis AG], (center) Airlight [R. Presley], (right) Glasspoint.....	41
Figure 34	Conventional version vs. fixed focus mechanism. ....	42
Figure 35	Mass distribution in a parabolic trough with the rotation axis at focal length $f$ from its vertex. ....	44
Figure 36	Images of specular beam diversion of different material samples. [16].....	50
Figure 37	Incidence Angel Modifier curves with and without cosine losses .....	52

Figure 38	End losses curves of different collectors neglecting the spacing between the modules of a SCA.....	54
Figure 39	Shade losses of different PTCs.....	55
Figure 40	PTR70 specific heat loss curve fit with a polynomial of 3 <sup>rd</sup> order (red) and 2 <sup>nd</sup> (black). A 1.14 factor defines the Ø80mm loss curve and 1.34 respectively for Ø94mm. ....	56
Figure 41	Required collector length of different PTC to achieve operational temperatures with VP-1.....	59
Figure 42	Performance comparison of different PTC loops with Thermo-Oil.....	62
Figure 43	Performance comparison of different PTC loops with Molten Salt .....	63
Figure 44	Scheme of a conventional loop. (i) Receiver piping, (ii) cross-over piping with ball-joints, (iii) 90°-elbows.....	66
Figure 45	Pressure drop and parasitic consumption of different PTC loops with Thermo-Oil (VP-1) VS. Molten Salt as HTF .....	70
Figure 46	Global conversion efficiency at the example of the UltimateTrough and MS-Trough with Thermo-Oil and Molten Salt.....	72
Figure 47	Solar Field cost of Andasol I (50 MW) power plant with EuroTrough collectors .....	74
Figure 48	Specific solar field cost estimate for different parabolic trough collectors. Supplement Table 19.....	76
Figure 49	Dimensions comparison of innovative parabolic trough collector modules and timeline of innovations .....	80
Figure 50	Effective aperture area estimate of a collector loop with subtracted receiver area .....	82
Figure 51	Possible concentration ratio of different PTC for different receiver diameters: Ø70, Ø80, Ø94 & Ø140 mm.....	82
Figure 52	Designed concentration ratio of innovative parabolic trough collectors .....	83
Figure 53	Degraded inflatable collector, due to a possible crack of the plastic film. Coordinates: 30°13'01.7"N 9°08'57.5"W .....	88
Figure 54	S-Diagram for the evaluation of innovative parabolic trough collectors.....	93

## List of Abbreviations and Symbols

Symbol	Unit	Definition
$\alpha_{st}$	mm/m·K	thermal expansion coefficient
$\alpha$	-	absorptance
$a_p, a_{col}$	m	aperture width of collector
$A_{eff}$	m <sup>2</sup>	effective aperture area
$A_{rec}$	m <sup>2</sup>	projected area of receiver
$A_{col}$	m <sup>2</sup>	aperture area of collector
$b_{1,2}$	-	correlation factors
$C / C_g$	-	concentration ratio/ geometrical concentration ratio
$c_1$	W/m <sup>2</sup> K	linear loss coefficient
$c_2$	W/m <sup>2</sup> K <sup>2</sup>	quadratic loss coefficient
$d$	m	tube's inner diameter
$d_{row}$	m	collector row distance
$d_{abs}$	m	absorber diameter
$\cos(\theta_i)$		cosine losses
$c_p$	J/kg·K	specific heat capacity factor
$\Delta p$	bar	overall pressure drop
$\Delta p_{receiver}$	bar	pressure drop in the receivers
$\Delta p_{obstacles}$	bar	pressure drop in obstacles
$\Delta p_{crossover}$	bar	pressure drop in crossover components
$\Delta p_{HTF}$	bar	pressure loss in the solar field
$\Delta T$	K	temperature difference
$\Delta L_{th}$	mm	thermal length difference
$K$	-	incidence angle modifier with cosine losses
$\lambda$	-	friction coefficient for a turbulent stream
$L$	m	length
$L_{Loop}$	m	loop length
$l_{rec}$	m	receiver length
$l_{col}$	m	collector length
$f:$	m	focal length
$f_m:$	m	mean focal length

*List of Abbreviations and Symbols*

---

$G_{b,ap}$	$W/m^2$	direct irradiance on the collector's aperture
$G_{im}$	$W/m^2$	radiant flux at the focal line
$T_{SF,in/out}$	$^{\circ}C$	solar field inlet/outlet temperature
DNI	$W/m^2$	Direct Normal Irradiance
M	kg	mass
$\dot{m}_{HTF}$	kg/s	mass flow of heat transfer fluid
$\dot{m}_{design}$ :	kg/s	mass flow at design
$n$	-	number of obstacles
$n_{row}$	-	number of rows
$\eta_{pump}$ :	-	heat transfer fluid pump efficiency
$\eta_{carnot}$		Carnot efficiency
$\eta_{global}$	-	global efficiency of solar power plant
$\eta_{opt,peak}$	-	peak optical efficiency
$\eta_{opt,0^{\circ}}$		peak optical efficiency
$\eta_{end}$	-	end loss efficiency factor
$\eta_{shade}$	-	shade loss efficiency factor
$\eta_{clean}$	-	cleanness efficiency factor
$\eta_{col}$ :	-	collector efficiency
$\eta_{SF}$	-	solar field efficiency
$\eta_{th}$	-	thermal efficiency
$P_{el}$	$W_{el}$	thermal-to-electric power
$P_{HTF}$	$W_{el}$	electric power consumption of heat transfer fluid pump
$P_{parasitic}$	%	rate of parasitic power consumption
$\rho_{mean}$	$kg/m^3$	mean density of heat transfer fluid
$\rho_{tot}$	-	total specular reflectance
$\rho$	$^{\circ}$	tracking angle
$S, S_f$	-	center of mass, center of mass on focal axis
$S', S''$	-	center of mass of an element
s		strength of concept
$\sigma_{spec}$	-	standard deviation of specular reflectance
$\Psi$	$^{\circ}$	rim angle
$T_m, \bar{T}$	K	mean temperature

*List of Abbreviations and Symbols*

---

$T_{amb}$	K	ambient temperature
$T_{in}, T_{out}$	°C	collector inlet and outlet temperature
$T_{i+1}(l)$	°C	outlet temperature in dependence of receivers length
$T_i$	°C	inlet temperature
$\tau$	-	transmittance
$\theta_i$	°	incidence angle
$\dot{q}_{loss}$	W/m	specific thermal losses
$\dot{Q}_{abs}$	W <sub>th</sub>	absorbed thermal energy
$\dot{Q}_{solar}$	W <sub>th</sub>	absorbed solar energy
$\dot{Q}_{SF}$	W <sub>th</sub>	solar field's thermal energy
$\dot{Q}_{eff}$	W <sub>th</sub>	effective thermal energy
$\dot{Q}_{loss}$	W <sub>th</sub>	thermal losses
X	-	technical value
$\xi_{90^\circ}$	-	pressure loss coefficient for 90°-elbows
Y	-	economic value
$\gamma$	-	intercept factor
$\dot{V}$	m <sup>3</sup> /h	volumetric flow
$\dot{V}_{HTF}$	m <sup>3</sup> /h	volumetric flow of heat transfer fluid

---

<b>Abbreviations</b>	<b>Definition</b>
BOP	balance of plant
BO-PET	biaxial orientated polyethylene terephthalate
C&I	commercial and industrial
CSP	concentrated solar power
DLR	Deutsches Zentrum für Luft- und Raumfahrt
DSG	direct steam generation
Eq.	equation
EOR	enhanced oil recovery
ET	EuroTrough
ETFE	ethylene tetrafluorethylene
HCE	heat collector element
HTF	heat transfer fluid
MS-Tr.	MS-Trough

N.A/n.a.	not available
NREL	National Renewable Energy Laboratory, USA
O&M	operations and maintenance
PS	polystyrol
PTC	parabolic trough collector
PTR	parabolic trough receiver
PU	polyurethane
PVC	polyvinylchloride
PVD	physical vapour deposition
SAM	system advisor model
SCA	solar collector assembly
SCE	solar collector element
SEGS	Solar Electric Generating Systems
SF	solar field
SKAL-ET	<u>scaled EuroTrough</u>
TRL	Technology Readiness Level
UHPC	ultra-high performance concrete
UT	UltimateTrough
VDI	Verein Deutscher Ingenieure/ Association of German Engineers

## Summary

The present thesis aims to define the state of the art of parabolic trough collectors and to identify the concepts in the framework of innovation's requirements. These are the increase of operating temperatures and of the plant's overall efficiency, as well as the cost reductions of the solar field by eliminating components and also the reduction of the parasitic power consumption [1].

The study is based on the investigation of 34 concepts. The collectors were classified according to their main structural features depending on their mechanisms or materials. The categories include conventional collectors (Category A), alternative structures and sheet reflectors collectors (Category B), non-metallic materials (i.e. sandwich composite structures and concrete), enclosed aperture collectors (Category D) and fix focus collectors (Category E).

In order to identify the potential among the collectors, an analysis is made of their optical and thermal properties, as well as of their structures and performance. For this comparative analysis, two conventional collectors are taken as the reference baseline, namely of both the EuroTrough and the UltimateTrough, to compare them against the innovations. This analysis also separates those collectors that operate with thermo-oils as heat transfer fluid and those that can operate with molten salts.

A total of 16 collectors were included in the analysis for later evaluation. The design engineering method of the guideline VDI2225 is used, which suggests the implementation of an evaluation matrix, where the analysed criteria can be integrated. For the assessment, a metric table of these criteria is additionally defined.

Results show that the collectors operating with molten salts, instead of thermo-oils, have a significant techno-economic potential, for instance, the MS-Trough, the UltimateTrough and the SkyFuelDSP. They also show that the inflatable Heliolis collector has an economic superiority once operating with thermo-oils.

The detailed description of the collectors, which correspond to the basis of this work, is included in Annex B or supplement of the thesis. In addition, Annex A includes the results of a previous survey carried out to estimate the scope of the current most known collectors.

## 1. Introduction

Concentrated solar power technologies became of relevance with the first parabolic trough solar power plants after the oil crisis in the 1980's, when the hazard of an energy shortage was feasible. Today the struggle of securing energy supplies remains and as fossil energy resources gradually deplete, renewable energies represent the alternative pathway [2]. The last report of the International Energy Agency sums up the current energetic consumption coverage by source, where 79.5% are provided by fossil fuels and 17.2% from renewables, as seen in Figure 1. It states that a significant impact on the global climate can be the consequence, if the fossil energy consumption tendency keeps being maintained [3]. In this context, the limitation of CO<sub>2</sub> and greenhouse gas emissions due to fossil fuels means, in fact, the greatest motivation to search for environmentally sustainable systems.

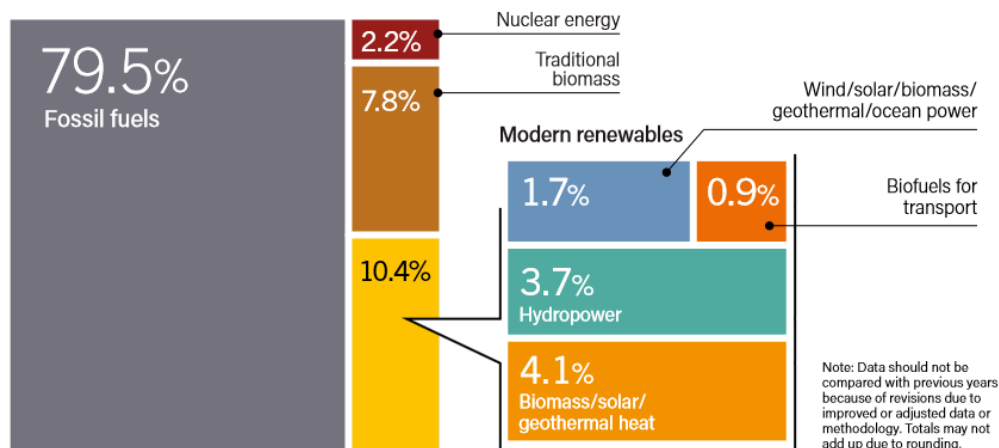


**Figure 1** Estimate renewables share total of final energy consumption, 2016 [4]

A modern political incentive is the resolution of the Paris Agreement in 2015, which took until the climate summit in Katowice (Poland) in December 2018, to put its targets into practice. With it, 174 countries confront with the task of maintaining the global average temperature increase at 2°C above pre-industrial levels [5]. To achieve this, mitigation of greenhouse gas emissions is the key strategy, which incentivises the drastic reduction of current and future emissions caused by transport, industry, electricity generation and individual consumption of fossil energy [2].

Solar thermal energy generation together with biomass and geothermal heat, correspond to only 4.1% of the global renewable sources share. Within the solar thermal branch, nevertheless, parabolic trough power plants remain with the greatest share of installed concentrating solar technologies. Worldwide it covers 66% of the concentrated solar power (CSP) projects, followed by solar towers (24%), Fresnel collectors (9%) and dish/Stirling collectors (1%) [6]. All together are covering 5.8 GW of the world's total energy consumption basis and in the near future additional power plants will supply further 3.8 GW, as shown in Figure 2. In this figure countries giving CSP a great impulse in the energy market like South Africa, Morocco, United Arab Emirates, India, Chile and China are shown.

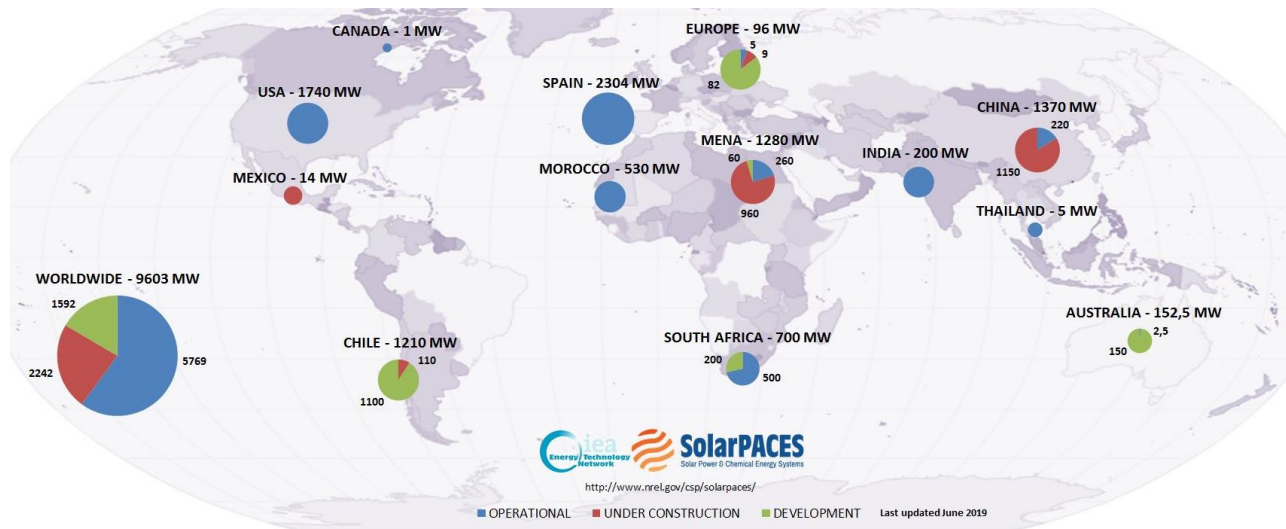


Figure 2 Worldwide overview of operating, planned and under construction CSP projects [6]

## 1.1 Problem Statement

The Sun is the richest disposal source of renewable energies, where its radiation can be used by photovoltaic technology to directly generate electricity or by concentrated solar thermal-to-electric systems.

On one hand photovoltaic technologies gained high importance in the market, due to the drastic decrease of its costs and the possibility to deploy solar fields at both, small scale and large scale in the megawatt range. With this, the price of photovoltaic panels decreased from the period between 2005 and 2014 from 40 €/ct/kWh to 9 €/ct/kWh and at adequate solar conditions even to

4-6 €/kWh [7]. On the other hand, for concentrated solar power technology with parabolic trough collector it has been more difficult to remain a cost effective alternative.

CSP experienced nevertheless a market breakthrough in the beginning of the 2000's, mainly due to the integration of solar thermal storage blocks in the solar field, which enables the disposition of energy to the grid even after sun hours. Thus the first power plant in Europe *Andasol 1* produced energy for 27 €/kWh in 2006, then the first in Morocco *Noor 1* for 18 €/kWh in 2013 and a near future hybrid power plant (PV+CSP) in Dubai *DEWA*, for 6.6 €/kWh<sup>1</sup> by 2021 [6]. Despite this, solar thermal power plants carry significantly higher financial investments and risk than photovoltaic deployments.

In parabolic trough power plants around 38.5% of the investments go to the solar field block [8]. Even though significant tariff reductions were achieved and projected, the potential of further reducing the costs of solar power plants is possible: first by up scaling effects, second by increasing operational temperatures and subsequently the global efficiency, and third through reduction of components in the solar field [9].

For that reason, the study aims to investigate the different types of current parabolic trough collector concepts that have the potential to meet these requirements. It is also intended to identify technologies that will enhance cost efficiency among solar plants, but also that will allow this technology to increase its competitive prevalence in the renewable energy market.

## 1.2 Objectives and Tasks

Derived from the problem statement, a task is to define the state of the art on parabolic trough concepts exclusively for large scale application, for instance, as in solar power plants and relevant industrial process heat applications. Additionally, innovative aspects among the collector concepts, which distinguish them from the state of the art, shall be identified. Furthermore, the task is to estimate the cost effectiveness of such collectors by analysing their components and performance. For the analysis relevant criteria are to be defined, so that a methodical evaluation can be conducted. As a comparison tool for the concepts, an evaluation matrix shall be created.

---

<sup>1</sup> 7.3\$/kWh converted in Euro currency

### 1.3 Methodology

An internal survey within the Institute of Solar Research of the DLR in Almería is accomplished to establish the scope of well-known collectors and also to identify the improvement potential of a parabolic trough. Then a survey on solar power plant projects is done, to track the conventionally implemented collector types on the globe. Once a number of collectors are encountered, a categorization according to their common properties is sorted out between conventional and innovative concepts. The exposition of the collectors' variety implies the description of the most relevant components. Therefore, a selection of the main elements is enlightened.

Furthermore, the evaluation matrix proposes a methodology according to the guideline VDI2225 of the Association of German Engineers (*german*: 'Verein Deutscher Ingenieure'). Sources of reference are literature, product datasheets, patents and communication with manufacturers, inventors or operators. This work contains the description of 34 parabolic trough collectors, where 16 of them are subjected to the evaluation.

### 1.4 Thesis Structure

**Chapter 2** first presents a general study of the essential components of a parabolic trough collector and their relations to the performance of a solar field. In **Chapter 3** a categorization between conventional and innovative technologies is summarized highlighting their main attributes. **Chapter 4** defines the criteria for the evaluation, followed by their corresponding argumentation. For the comparison, a conventional collector representing the state of the art is, chosen as a reference towards the innovative concepts. **Chapter 5** contains the conclusions of this study. In the **Annex**, a wide presentation of the researched parabolic trough collectors is attached and functions as the basis information for the comparison and evaluation procedures. Furthermore results on the aforementioned department internal survey study is presented, which can serve as a measure for the study's scope in regards to the included concepts.

## 2. State of the Art

### Working principle

Parabolic trough collectors (PTC) belong to line focusing systems. They concentrate the solar energy by reflecting the incident light rays to its focal point. At this height an absorber tube is placed containing a streaming fluid, the so called heat transfer fluid (HTF). Both elements have the necessary properties to gain the heat and transfer it from the inlet to the outlet of the tube (see Figure 3a). The one-axis tracking system enables the perpendicular facing of the collector's aperture to the sun, thus taking maximum advantage of the solar direct normal irradiance, as illustrated in Figure 3b.

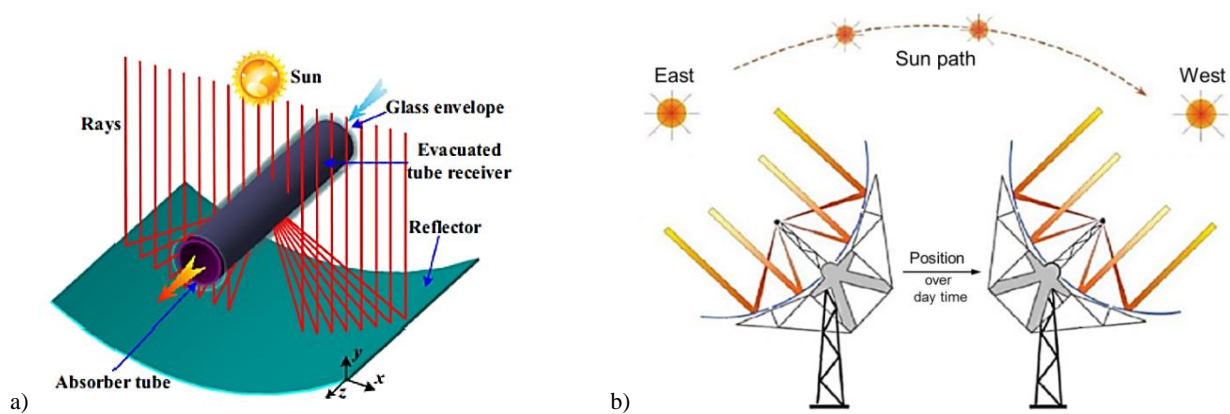


**Figure 3 a)** General scheme on concentrating solar energy at the focal point of a PTC [10] **b)** One-axis tracking of the sun [11]

This technology finds diverse applications and forms of implementation within two main branches: electricity generation and industrial process heat production.

Commonly parabolic power plants operate at temperatures ranging from 300°C to 500°C and in for industrial process heat generation between 100°C to 300°C. Some examples for the low temperature heat demand process: water desalination, climate & industrial control (heat/cold) and biogas heat assistance. Another alternative application, which needs large scale solar fields for steam generation to access on heavy crude oil reservoirs, is known as enhanced oil recovery (EOR).

The collectors presented in this thesis adapt to those different applications, but above all for commercial parabolic solar power plants to generate electricity. On large areas of about 200 hectares, e.g. Andasol I, solar fields are integrated into a conventional steam turbine cycle, either directly or indirectly. The entire or partial substitution of the fossil fuels heat source by the solar field makes the conceptual difference (see Figure 4).

Parabolic trough collectors take advantage of the Direct Normal Irradiance (DNI)<sup>2</sup> of the sun. The collectors transfer this thermal energy by concentration into heat transfer fluid and it is conducted into the steam cycle<sup>3</sup> to drive a steam turbine or it is led into the storage block. The thermal energy storage block gives solar power plants the characteristic of energy dispatchability, which enables the power block to operate after 6 to 12 hours without sun, thus giving access to electricity on demand to the grid.

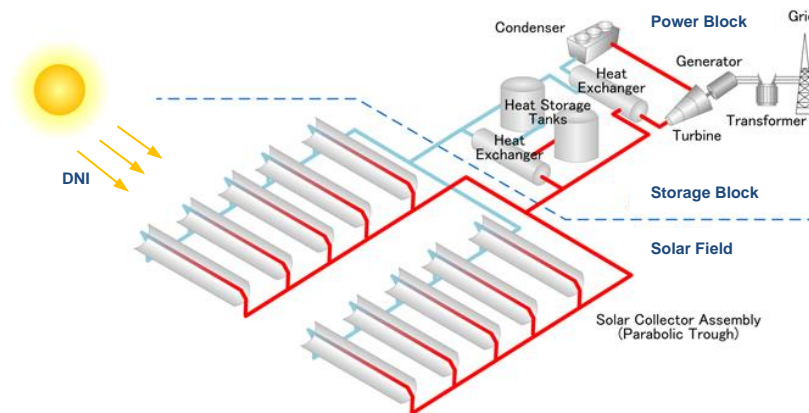


**Figure 4** Scheme of a PTC Solar Power Plant, with three integrated blocks: Solar Field, Thermal Storage and Power Block [12]

### Solar Field

The design of a solar field is commonly shaped by an extensive modular series of parallel collector rows. They are connected by hot and cold pipelines to the storage and power block. The format itself is designed to reduce losses and solar field costs by implementing pipelines as short as possible. The conventional orientation of the collector rows is north-south in order to maximize the annual output of the plant.

<sup>2</sup> Direct Normal Irradiance (DNI), i.e., the fraction of solar radiation which is not deviated by clouds, fumes or dust in the atmosphere and that reaches the Earth's surface as a parallel beams [12]

<sup>3</sup> Also known as Rankine Cycle

Figure 5 shows a large scale power plant project, *Noor<sup>4</sup> I* in Morocco, with an installed gross capacity of 160 MW<sub>el</sub> and 3 hours of thermal storage. *Andasol I* in Spain, the first European operational plant, has a designed gross capacity of 50 MW and 7.5 hours of thermal storage.



**Figure 5** Noor I Power Plant 160 MW, Ouarzazate Morocco (2016). The second phase Noor II has a capacity of 200 MW (2017) and Noor III of 150 MW with Solar Tower technology [13]

The total number of the rows is segmented into so-called loops, which define the size of the solar field. The required solar power is collected along its length to achieve operational temperatures at the end of the row.

The composition of a loop is based on a number of solar collector assemblies (SCA), which is the series of adjacent collectors driven by a single drive. Figure 6 exemplifies the loop subdivision within a solar field using HeliOTrough collectors. The number of units and distance per loop can vary depending on the implemented collector, yet the definitions remain general.

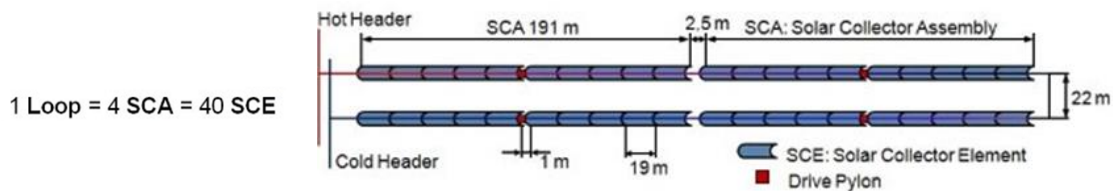


**Figure 6** HeliOTrough Loop segmentation and dimensions [14]

In literature, a single parabolic trough collector unit is also known as solar collector element (SCE). They are essential segments in a solar field, moreover their components, since they first

<sup>4</sup> Arabic for *glow, illumination*

collect and convert the input energy of the entire process. The total optical and thermal performance of a collector is characterized by the optical efficiency and the thermal losses of these components respectively [15]. Figure 7 presents a breakdown of the main elements at the example EuroTrough collector. Depending on their use, each of them fulfills a series of mechanical, physical and economical requirements. Specific collector designs differ in aspects such as aperture width, concentration ratio, reflector materials, support structure and receiver design [2].

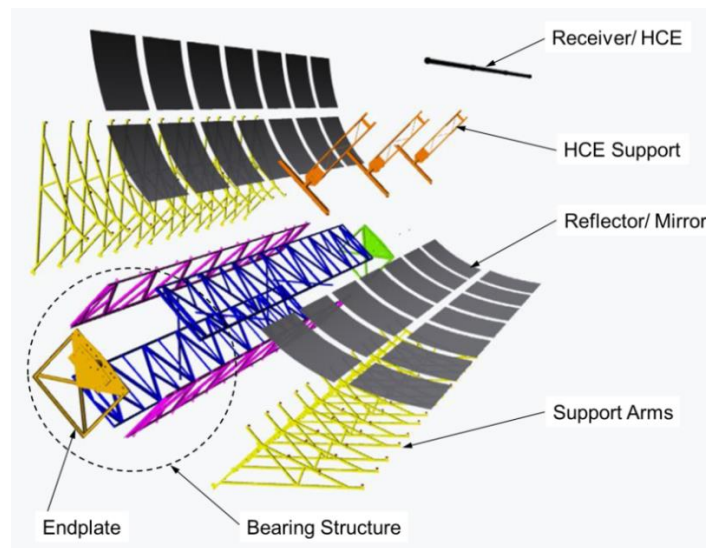


**Figure 7** Main components of a parabolic trough collector with EuroTrough collector as example [11]

The most relevant aspects considered in this thesis are summarized in Figure 8 in order to provide the reader with an overview of the components reviewed to categorize the different collector concepts and for the later analysis and their tasks along the energy conversion flow.

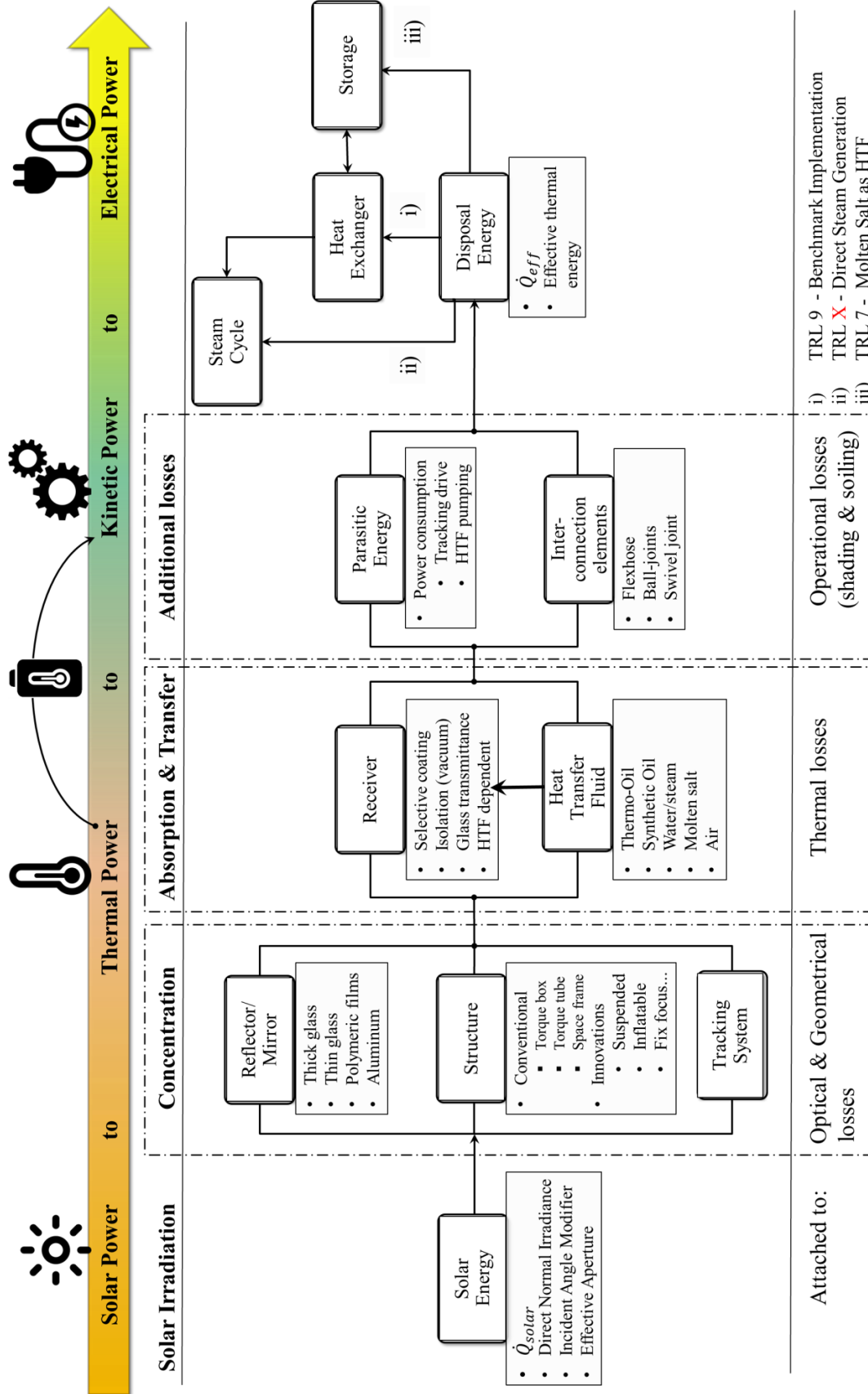


**Figure 8** Energy and components flow diagram in a parabolic trough solar field and three current applications: i) benchmark/conventional, ii) direct steam generation, iii) operation with molten salt as heat transfer fluid

## 2.1 Geometry and Concentration Ratio

Parabolic troughs concentrate the incident direct irradiance on its focal line. In a cross-section view, a symmetric parabola around its vertex is visible and the focus is reduced onto a point. An analytical representation of the parabola is given as follows:

$$y = \frac{1}{4f} x^2 \quad (1)$$

$f$ : focal length [m]

Moreover four important parameters characterize the collector's geometry: aperture width  $a$ , aperture length  $l$ , focal length  $f$  and rim angle  $\psi$ . These parameters are illustrated in Figure 9, where the length  $l$  is an unproblematic measure, included in the collector aperture area.

Another parameter is the concentration ratio  $C$ , which indicates the possible operating temperatures in a solar field. It is defined as the ratio of the radiant flux at the focal line ( $G_{im}$ ) to the direct irradiance on the collector's aperture ( $G_{b,ap}$ ). It is also simplified as the ratio of the projected collector aperture area to the projected receiver aperture area. The last description is commonly used and is distinguished as the geometrical concentration ratio  $C_g$ :

$$C_g = \frac{A_{ap,c}}{A_{ap,r}} = \frac{a \cdot l}{d_r \cdot l} = \frac{a}{d_r} \quad (2)$$

$A_{ap,c}$ : collector aperture area [m<sup>2</sup>]

$a$ : aperture width [m]

$A_{ap,r}$ : collector receiver area [m<sup>2</sup>]

$l$ : collector and receiver length roughly equal [m]

$d_r$ : receiver diameter [m]

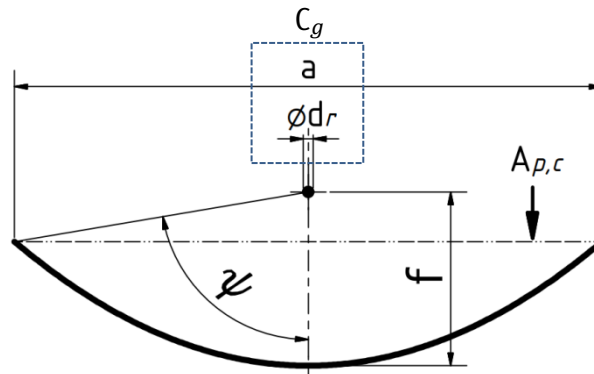


**Figure 9** Geometrical parameters and geometrical concentration ratio of a parabolic trough

Conventional parabolic troughs have a concentration ratio of about 82 suns. By now innovations reach a geometrical concentration ratio of 104 and intended 110. Higher concentration ratios mean a higher flux per length unit, reduction of receiver losses and also of the number heat collector elements.

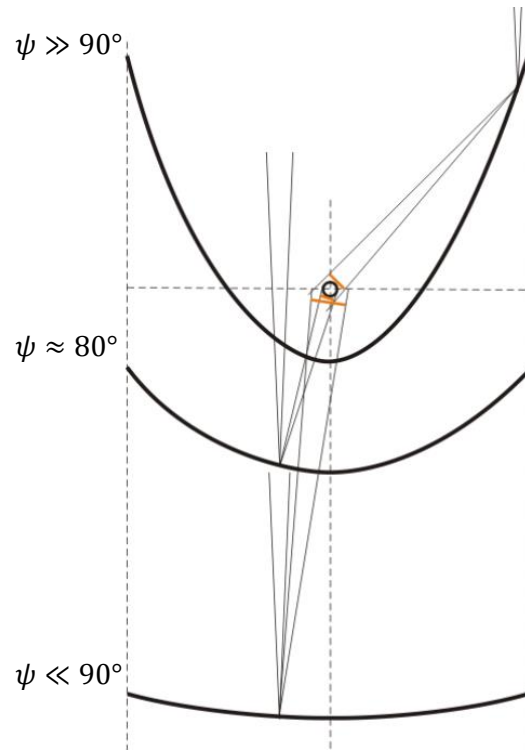


**Figure 10** Dependence of the focal spot size on the rim angle [16]

Another relevant parameter is the rim angle. Its value alone is sufficient to determine the shape of the cross-section of a collector. This means that parabolic troughs with the same rim angle are geometrically similar [16]. This parameter affects the concentration ratio and the irradiance on the absorber tubes, so it cannot be very small neither very large.

On the one hand, a very small mirror would be very narrow and not enough power would be projected into the receiver. On the other hand, a large rim angle would imply longer distances between the outer edges of the parabolic mirror, meaning a significant spread of the beam until the focal point, as shown in Figure 10. In this case the beam might not even reach the focal point, due to existing light deviations and slope errors on the mirrors. For these reasons large rim angles could mean an economic disadvantage if a part of the mirror surface, does not fulfill the required performance. In conventional parabolic troughs a rim angle of  $80^\circ$  is generally used.

## 2.2 Mirror Materials

The mirror composition and its reflective material are key elements for the optical performance of a parabolic trough. More than 90% of the incident solar radiation has to be concentrated on the absorber tube, requiring high specular reflectance and high geometrical precision. Silver and aluminum are commonly used due to their highly reflective properties. Their manufacturing and maintenance should contribute to an economically viable option, while offering long time durability in concerning resistance against UV-radiation, breakage, soiling and abrasion.

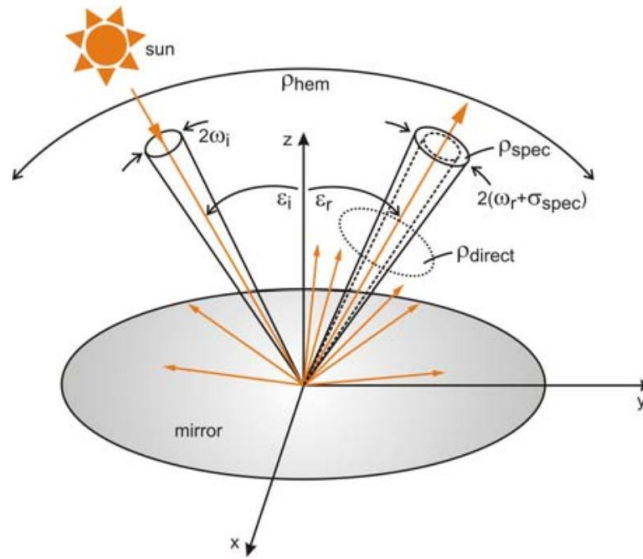


**Figure 11** Schematic representation of direct and diffuse reflection on a mirror surface [17]

The optical reflectance  $\rho$  of a surface is a parameter, indicating the amount of incident solar irradiation that is reflected by this surface. A distinction is made between two extreme types of reflection: the diffuse scattering reflection in the whole hemisphere  $\rho_{hem}$  and the specular reflection  $\rho_{spec}$ , both illustrated in Figure 11. The latter one obeys the law of reflection, according to which the incident angle  $\varepsilon_i$  equals the reflected angle  $\varepsilon_r$  of the light beam. Considering irregularities or slope errors of the mirror surface, a certain range of tolerance is defined for this parameter. It is measured of with specular reflectometers, which allows an angle of acceptance at 25 mrad and is shown by the offset half angle  $\sigma_{spec}$  in Figure 11.

In general, the reflectivity varies depending on the wavelength. It has to be specified for a given wavelength or a given wavelength range [16]. For CSP applications, the parameter values are therefore weighted with the solar spectrum, which result in the *solar weighted hemispherical*

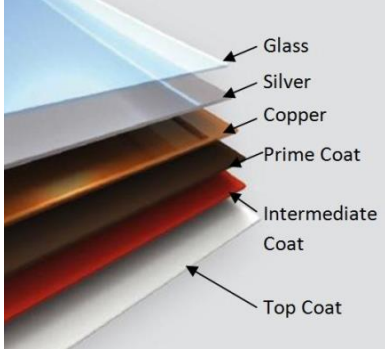
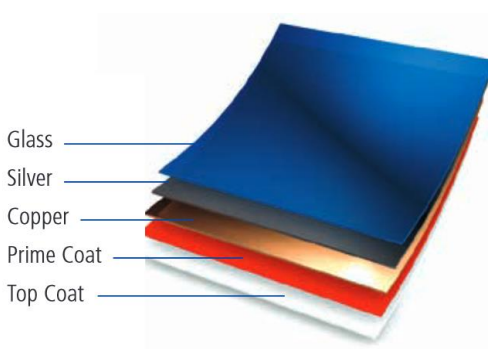
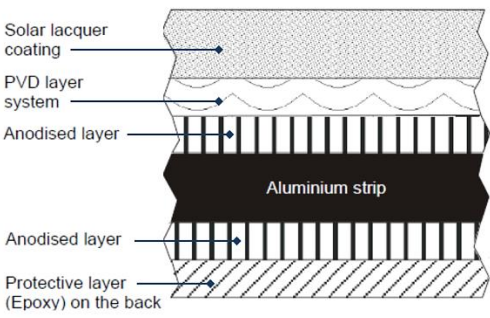
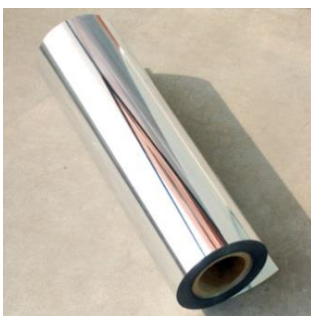
reflectance  $\rho_{SWH}$  and the solar weighted direct reflectance  $\rho_{SWD}$ . The latter one is of relevancy since it indicates the expected amount of sunlight that can hit the absorber [17]. Table 1 shows current reflector types enlightening their multi-layer structure.

First commercial collectors implemented **thick glass** mirror facets (4-5 mm) with a silvered back layer. In the glass the content of low iron increases the light transmission. Panels of that kind demonstrated their initial optical qualities after more than 15 years of operation with a solar weighted reflectance of 93.5% and a specular reflectance of 95.5%. The manufacturing of these facets has been enhanced and industrialized over the last 30 years with the increasing number of solar fields. Their specific price per square meter has dropped up to 44%, where current estimates are around 16 €/m<sup>2</sup> [18]. Measurement and practical experience have shown the superior quality of silvered glass mirror reflectors compared to alternative materials. The later presented category on conventional collectors shows a wide number of collector examples using thick glass mirror facets.

A different reflector option derives from the optimization of thick glass mirrors. **Thin glass** reflectors have demonstrated excellent optical qualities, durability, lightweight and cost reduction potential. The material offers a higher degree of flexibility, but it also remains a sensitive material towards breakage. Its use requires a rigid structural surface onto which it can be embedded, for instance, with a proper adhesive material. Because of their proven number of benefits these reflectors are been used in some of the innovative concepts (e.g. SL4600+, toughTrough and in fixed focus collectors). There are more ongoing investigations on ultra-thin flexible glass reflectors with a thickness of 100µm and the standard coating structure. The product is nevertheless not commercially available by now [18].

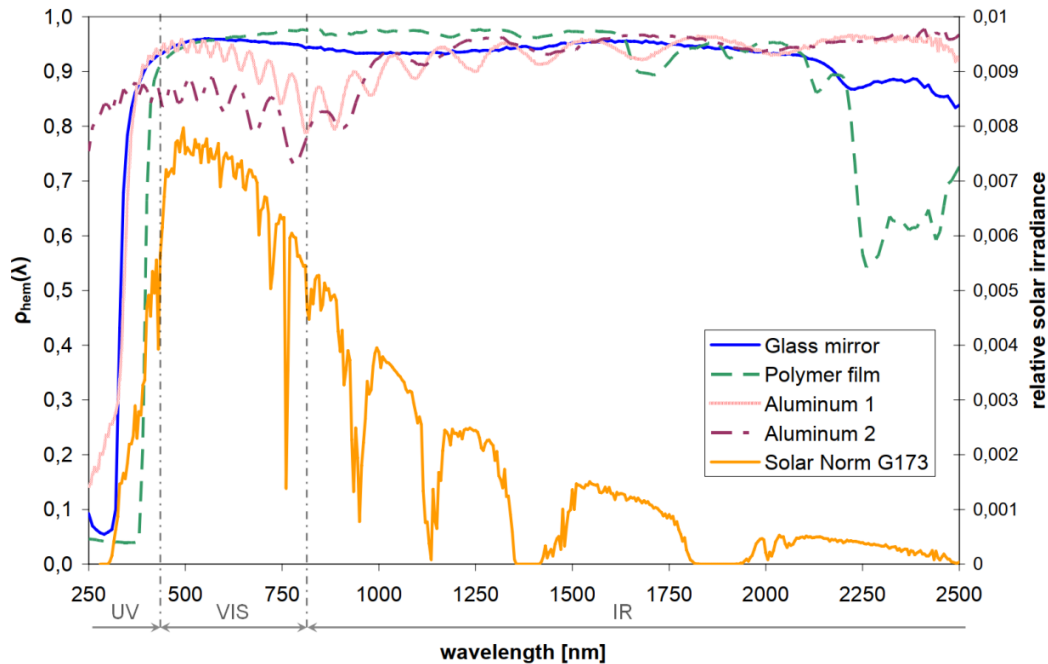
**Aluminum reflectors** are based on an aluminum substrate, commonly applying high-purity aluminum as the reflective layer followed by a protective top coat. The performance on reflectivity and durability has been too insufficient to get the breakthrough for large scale CSP application. They are nevertheless thanks to the low weight an economical alternative and still have optically improvement potential. Later studies have demonstrated an optimized layer system in comparison to commercially used reflectors. In this example the solar direct reflectance increased from 82.6% to 92.3% by using a reflective silver coating and silicon nitride (Si<sub>3</sub>N<sub>4</sub>) as the top layer [18].

**Table 1.** Overview on current reflector materials for parabolic trough collectors

Thick Glass (thickness 4-5mm)		Thin glass (thickness 1-2mm)	
 <p>a) [16]</p>		 <p>b) [19]</p>	
Solar weighted hemispherical reflectance	93.5%	Solar weighted hemispherical reflectance	93.0-96.0 %
Solar weighted direct reflectance	95.5%	Solar weighted direct reflectance	96.0%
Durability	Very good	Durability	Very good
Cost <sup>2</sup> (€/m <sup>2</sup> )	16 (36*)	Cost <sup>2</sup> (€/m <sup>2</sup> )	13 - 36
Issue: Breakage. Cost (earlier*), current price dropped to 44%		Issue: Breakage, Handling	
Aluminized reflector		Polymeric film reflector	
 <p>c) [18]</p>		 <p>d) [16]</p>	
Solar weighted hemispherical reflectance	86.0-90.0%	Solar weighted hemispherical reflectance <sup>1,4</sup>	92.5-94.0%
Solar weighted direct reflectance	79.0-92.3%	Solar weighted direct reflectance	87.4-95.0%
Durability	To be improved	Durability	To be improved
Cost <sup>2</sup> (€/m <sup>2</sup> )	<18	Cost <sup>2</sup> (€/m <sup>2</sup> )	9 - 13
Issue: Hemispherical and direct reflectance		Issue: Direct reflectance	
<sup>1</sup> S.Meyen [17]; <sup>2</sup> ASME-Journal of Solar Energy Engineering [20]; <sup>3</sup> ConSol Project [18]; <sup>4</sup> ReflechTech datasheet [21]			

Since the 1990s reflective **polymeric films** have been studied and optimized in terms of optical performance and longevity. This type of reflector gave an impulse to new collector concepts. They are described for the innovative collectors of Category B: Metal Structures & Sheet

Reflectors”. Polymeric films also have been compared to glass and aluminum reflectors. Results show that the smoothness of the surface is not sufficient to reach the values of glass reflectors in terms of specular reflection. In fact they show a beam deviation, 0.9 mrad in comparison to glass with less than 0.3 mrad [17]. This means that polymeric films are characterized by a wider beam deviation from the expected incident spot than glass mirrors. Figure 12 shows the hemispherical reflectance of different mirror materials.



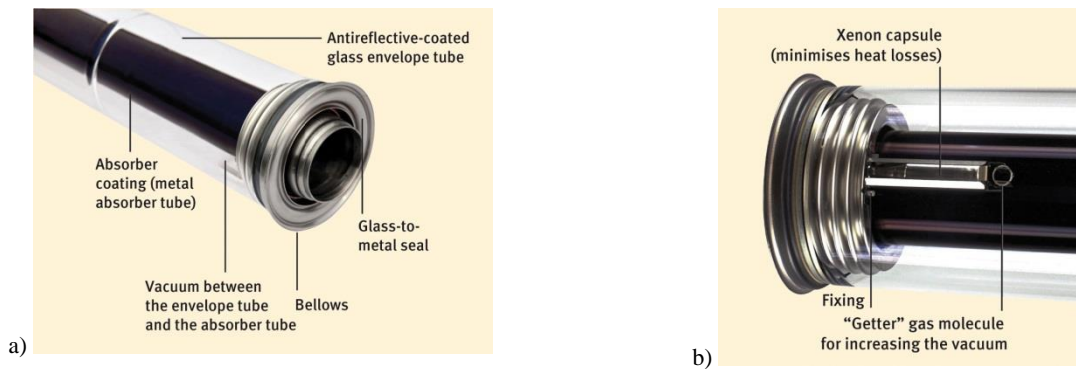
**Figure 12** Hemispherical reflectance spectra of different material samples according to standard ASTM G173-03 [17]

Figure 12 shows the wavelength ranges between 250-2500 nm containing the ultra violet, visual and near-infrared fractions of the spectrum. It also shows the solar weighted hemispherical reflectance value at each respective wavelength.

Even though aluminum coated and polymeric film reflectors have been implemented, their main challenge to overburden is that of longevity. Both are front surface reflectors, which cause a higher exposition of the reflective surfaces to the environment. From this follows a faster decrease of the specular direct reflectance of these materials [17].

### 2.3 Receivers

Receivers or absorber tubes have the task to convert the incident radiation into thermal energy and to transport it to the connecting pipelines between the solar field and the power block. The configuration of these components, Figure 13, defines the thermal performance of the collector, which also depends on its constructive suitability for a given heat transfer fluid. This also determines the operating temperatures at which the absorber tubes are used. The composition of the receiver is based on a vacuum isolated glass envelope with the absorber tube inside, made of stainless steel or carbon steel. It is sealed with bellows at each end, which also serve as mechanical compensators for the tubes' thermal expansion.



**Figure 13** a) Components of a receiver tube at the example of a PTR70 Schott receiver b) Integrated elements to enhance longevity and performance [source: Schott AG]

The main requirements for receivers are high absorption of the light and low emissivity of the thermal radiation. To achieve this, special treatments are essential for the single elements. The glass envelope is made of borosilicate, for instance, to attribute high transmittance  $\tau$  levels up to 96%. Receivers also require low reflectance  $\rho$  rates, for which an anti-reflective coating is applied.

The absorber tubes have a denominated selective coating, since optical behaviour parameters on the surface can be manipulated (or selected). In the case of absorber tubes, the absorptance  $\alpha$  must be high for one spectral range, namely the solar spectral range ( $0.25 \mu\text{m} \leq \lambda \leq 2.5 \mu\text{m}$ ), and its emittance  $\varepsilon$  must be low for another spectral range, namely the infrared range ( $3 \mu\text{m} \leq \lambda \leq 50 \mu\text{m}$ ) to reduce thermal radiation losses [16]. Figure 14 illustrates the layer structure on an absorber surface. The first layer is metallic and high reflective in the infrared range. It is

typically made of Molybdenum (Mo), Aluminum (Al) or Copper (Cu). The following layer consists of a Cermet<sup>5</sup> material, which is composed of a ceramic matrix and embedded metallic nano-particles, for instance Mo-Al<sub>2</sub>O<sub>3</sub> or Mo-Si<sub>2</sub>O [22]. On top the antireflection ceramic layer consists of oxides like Al<sub>2</sub>O<sub>3</sub> or Si<sub>2</sub>O.

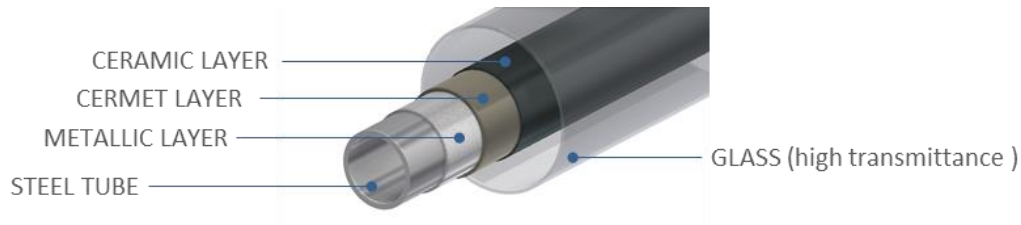


**Figure 14** Multi-layer coating of the absorber tube

Current receivers achieve absorptance values of the solar radiation between 0.95-0.96 and lower values of 0.09-0.10 in emissivity of the thermal radiation at 400°C. These results correspond to receivers dimensioned for thermo-oils. In the case of molten salt receivers surface emissivity values of 0.10 can be attained at operational temperatures of 600°C [23]. A selective coating is more difficult to design once temperatures rise, since there is a larger overlap between the thermal emission spectrum and the solar spectrum. An example curve for the reflectance of a selective coating is shown in Figure 15 at operational 700°C.

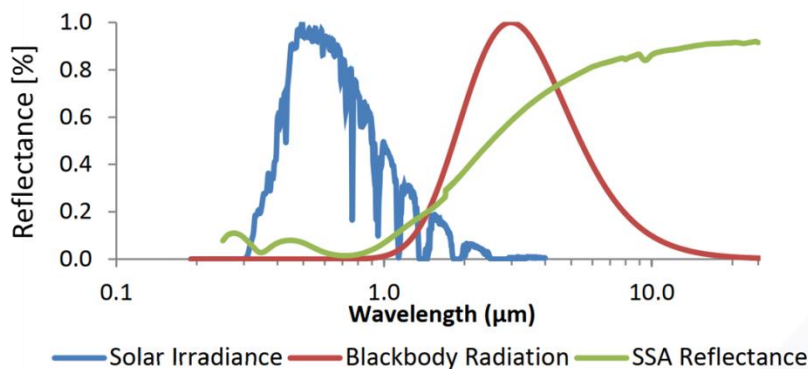


**Figure 15** Reflectance of a spectral selective coating, e.g. TaSi<sub>2</sub>, and spectral ranges of the solar radiation and the blackbody radiation at 700°C [24]

Absorber diameters vary between 70, 80 or 90 mm with a glass diameter of 115-125 mm. The diameter selection has an influence on the intercept factor  $\gamma$  and it is conditions the thermal

<sup>5</sup> *Cermet*: name derived from the materials composition ceramic and metal

losses of the system. The intercept factor is the ratio of the reflected radiation to the reflected radiation hitting the absorber. A big diameter can increase the intercept factor, but it possesses at the same time a larger surface area. This would subsequently increase thermal losses at high temperatures. That is why smaller diameters have an advantage regarding thermal performance.

In the majority of collector concepts the receiver is a movable component through the entire assembly, not only while it is tracking the sun, but also due to the thermal expansion it experiences between standby and operational state. A rough calculation of the length difference by thermal expansion is around  $\Delta L_{th} = 0.65$  m per each  $L = 100$  m receiver tubes, at an outlet operational temperature of  $560^\circ\text{C}$ <sup>6</sup> with molten salt as heat transfer fluid. The expansion coefficient of the stainless steel tubes is  $\alpha_{St} = 0,012$  mm/m·K [25].

$$\Delta L_{th} = L \cdot \alpha_{St} \cdot \Delta T \quad (3)$$

$\Delta L_{th}$ : thermal length expansion difference [mm]       $\alpha_{St}$ : expansion coefficient [mm/m K]  
 $L$ : receiver length [m]       $\Delta T$ : temperature difference [K]

A further receiver concept was developed for air as heat transfer fluid as an innovative approach and it is implemented in the Airlight collector with an inner diameter of 140 mm.

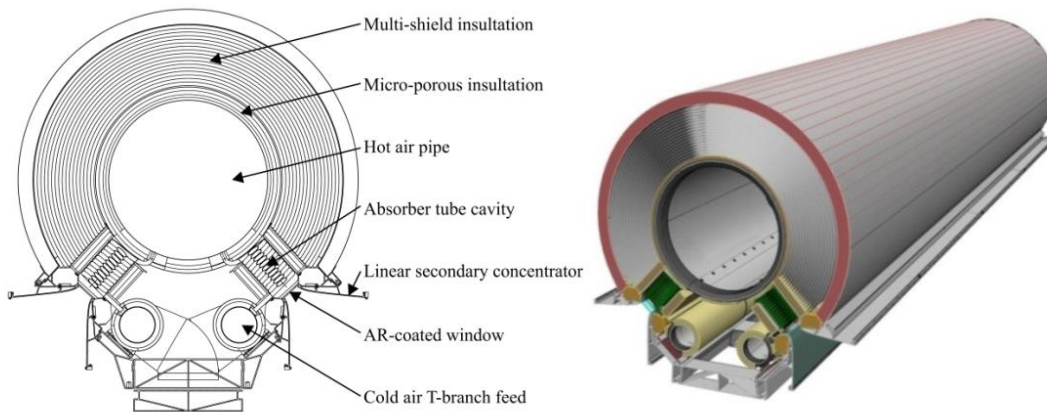


**Figure 16** Receiver for air as heat transfer fluid implemented used in the Airlight collector [26]

The receiver tubes together with the specific heat transfer fluid are the main drivers that determine the thermal performance of a collector. In the next section relevant fluids are presented. Then a more detailed behaviour of the thermal losses in section 2.5.2 is treated.

<sup>6</sup> A rough calculation using thermos-oil as HTF at  $400^\circ\text{C}$  is a  $\Delta L_{th} = 0,5$  m per each  $L = 100$ m

## 2.4 Heat Transfer Fluid

The heat transfer fluid (HTF) is the fluid circulating between the solar field cycle and the power block cycle. Its main task is to accumulate the thermal energy from the solar field and transport it to the storage block or power block. The type of HTF determines the operational temperature range of the solar field and so the maximum power cycle efficiency that can be obtained [20]. On the one hand the operational temperatures are limited by the freezing and decomposition temperature of the medium. On the other hand the maximum theoretical efficiency of the power cycle can be described with the Carnot-efficiency theorem, given as:

$$\eta_{Carnot} = 1 - \frac{T_L}{T_H} \quad (4)$$

$T_H$ :	highest temperature of the thermodynamic cycle [K]
$T_L$ :	lowest temperature of the thermodynamic cycle [K]
$\eta_{Carnot}$ :	Carnot efficiency [-]

This way, when the highest temperature of the thermodynamic cycle increases, a higher heat-to-work energy conversion can be reached. Therefore thermal stability for a HTF is a significant criterion that should be fulfilled. Other requirements on HTFs are listed in Table 2.

First power plants at Solar Electric Generating Systems (SEGS) used **mineral oil** as HTF in the solar field and simultaneously as storage fluid. Due to the high flammability of this medium, it was substituted by organic oils enabling a higher thermal stability. Currently organic **thermo-oils**, a compound of biphenyl ( $C_{12}H_{10}$ ) and diphenyl-oxide ( $C_{12}H_{10}O$ ), are the most frequented HTFs with over 25 years of experience. They satisfy the majority of the aspects listed in Table 2, starting with a low freezing temperature at about  $12^\circ\text{C}$ , a high heat capacity and maximal operating temperatures at  $400^\circ\text{C}$  [16]. However, for higher temperatures than that, thermal cracking starts to occur, which deteriorates the oil composition. Therefore and because of aging periodical replacement is necessary [27]. Thermo-oils are available in large amounts, but at the expense of high costs. They are also deficient in flammability and environmentally more harmful than other possible media. Current synthetic oils remain under research to improve the thermal stability at higher temperatures and for more affordable prices.

**Table 2.** Heat transfer fluid requirements [16]

HTF Requirement	Motive
High evaporation temperature	The HTF must be liquid and operated under manageable pressure. The HTF cannot evaporate at the high temperatures in the solar field.
Low freezing temperature	No freezing protection measures are necessary, if temperatures in the solar field drop.
Thermal stability	The HTF needs to withstand operation temperatures and avoid thermal cracking. Operating temperatures are constrained to this requirement.
High heat capacity	To favor the storage and transportation of high amounts of thermal energy
Low viscosity	Reduces important pumping energy
Low investment cost & Availability	Cost savings of the final LCOE and of logistic efforts
Environmental compatibility	Common responsibility
Low inflammability & Low risk of explosion	Reduction of operational fire hazards

Other media are **molten salts**, which are salt mixtures heated up to their liquid temperature. They have succeeded in CSP as storage medium, due to their low price and good thermodynamic properties, which enhance some of the technical advantages compared to thermal oils (see Table 3). This HTF, aside of being accessible and available has high thermal stability, high density, good thermal/electric conductivity and relative low viscosity [28]. They can operate at 550°C with a thermal stability up to 600°C, for instance, with *Solar Salts* composed of a binary salt mixture containing 60% sodium nitrate (NaNO<sub>3</sub>) and 40% potassium nitrate (KNO<sub>3</sub>). Its volumetric heat capacity is reasonable and its vapour pressure is very low, allowing storage under atmospheric pressure and eliminating the cost of thick walls for the storage tank [29]. Corrosion resistant materials should be considered, as molten salt tanks are prone to rusting.

The use of molten salts as heat transfer fluid suggests a direct storage system as an alternative power plant design concept, making heat exchangers are negligible; see Figure 17. This design could reduce the expenses on thermal storage costs by 65% and increase, not only the storage  $\Delta T$  up to 2.5 times, but also the steam cycle efficiency to  $\geq 40\%$  [30].

**Table 3.** Characteristics of nitrate/nitrite salts and Therminol VP-1 [29]

Property		Solar Salt	Hitec	Hitec XL	Therminol VP-1
<b>Composition (weight percentage)</b>					
Salt <sup>1</sup>	NaNO <sub>3</sub>	60%	7%	15%	
	KNO <sub>3</sub>	40%	53%	43%	
	NaNO <sub>2</sub>		40%		
	Ca(NO <sub>3</sub> ) <sub>2</sub>			42%	
Organic Compound <sup>2</sup>	C <sub>12</sub> H <sub>10</sub> O				73.5%
	C <sub>12</sub> H <sub>10</sub> O				26.5%
<b>Operating temperatures</b>					
Liquidus temperature [ °C]		227 <sup>3</sup>	141 <sup>5</sup>	140 <sup>5</sup>	12 <sup>2,4</sup>
Upper temperature [ °C]		593 <sup>4</sup> -600 <sup>1</sup>	454 <sup>5</sup> -538 <sup>4</sup>	460 <sup>5</sup> -500 <sup>4,1</sup>	400 <sup>2,4</sup>
<b>Chemical properties at 400 °C<sup>6</sup></b>					
Viscosity ( $\eta$ ) [mPas]		1.773	1.710	n/a	0.149
Heat conductivity ( $\lambda$ ) [W/m/K]		0.511	0.330	n/a	0.076
Heat capacity ( $c$ ) [J/kg/K]		1516	1562	1304	2635
Density ( $\rho$ ) [kg/m <sup>3</sup> ]		1834	1790	1903	694
Volumetric heat capacity ( $s$ ) [kJ/m <sup>3</sup> /K]		2780	2796	2482	1829
<b>Economical parameters<sup>7</sup></b>					
Nominal cost [\$/kg]		0.49	0.93	1.19	2.2

<sup>1</sup>(Kelly 2007) <sup>2</sup>(Solutia Inc 2012) <sup>3</sup>(Kramer 1980) <sup>4</sup>(Raade 2011b) <sup>5</sup>(Bradshaw 1990) <sup>6</sup>(Steag 2012) <sup>7</sup>(Kearney 2003)

A long-term concept of using molten salts has been demonstrated on a 5 MW<sub>el</sub> solar plant by Archimede Solar Energy at Priolo Gargallo, Sicily. A further large commercial power plant has not been deployed up to date since some disadvantages of molten salts could be considered a risk. Above all, the high freezing temperatures of the fluid could affect key components like receivers, pipelines, valves and pumps by salt solidification. Daily drainage concepts of the fluid

[31], recirculation of the fluid [30] or heat trace systems in the receivers are current technical options to maintain the fluid above the freezing temperature.

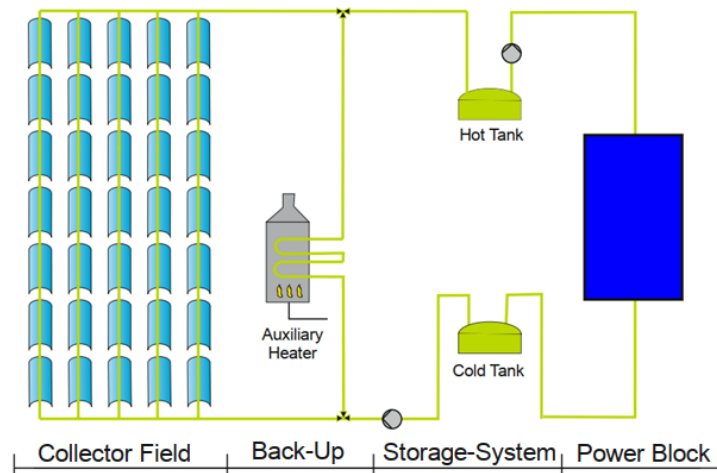


**Figure 17** Direct storage system cycle overview using molten salts. The solar field cycle and the steam generation cycle are decoupled [32]

Special receivers with improved selective coatings have been developed to avoid higher thermal losses at higher temperatures. Frequent breakdowns of interconnecting elements, like flexible hoses and ball-joints between the collectors and the solar field piping, are a big problem, caused when operating with molten salts. The state of the art collectors using this fluid are limited to only a few.

The great advantage of molten salts is the cost efficient use of storable thermal energy. Therefore, current solar research investigates the implementation of molten salts in the solar field and storage block in one cycle.

Another accessible heat transfer fluid is **water/steam**. The cycle of implementation is called *direct steam generation* (DSG). It is composed of a single cycle, where the HTF of the solar field is the same circulating in the Rankine cycle. Demineralized **water** is heated in to steam and again to water in the same cycle. DSG still remains under research, though the working principle was demonstrated at the *Plataforma Solar de Almeria* on the DISS project at 100 bar steam pressure and temperatures of 500°C [33].

## 2.5 Collector Efficiency

In this section the relevancy of the above presented components regarding the collectors' performance is highlighted. At first a general overview of the parameters that influence the collectors' and the solar fields' performance is shown in Figure 18.

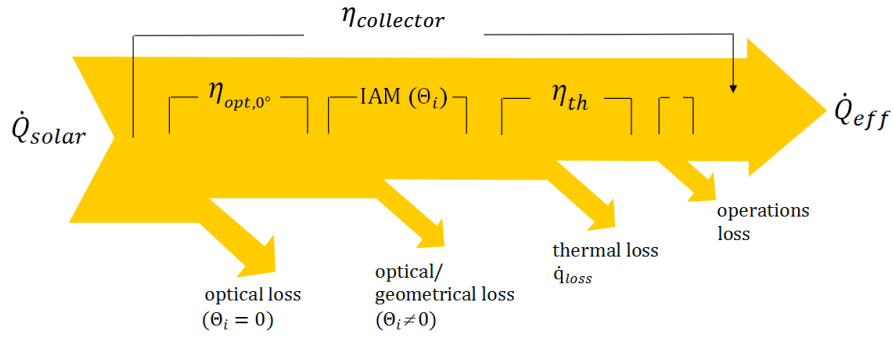


**Figure 18** Calculation of the effective thermal energy in a PTC

Parabolic troughs only use a fraction of the incident solar energy for heat production because of energy losses during the solar-to-heat conversion as expressed with Eq.(5) [34]. Here the collector efficiency can be firstly introduced as the ratio between the gained to the effective thermal power as in Eq. (6), derived from the general collectors' efficiency equation [35]:

$$\dot{Q}_{eff} = \dot{Q}_{solar} - \dot{Q}_{loss} \quad (5)$$

$$\eta_{col} = \frac{\dot{Q}_{eff}}{A_{eff} \cdot DNI} = \eta_{opt,0^\circ} - c_1 \frac{(T_m - T_{amb})}{DNI} - c_2 \frac{(T_m - T_{amb})^2}{DNI} \quad (6)$$

$\dot{Q}_{solar}$ :	concentrated solar energy [W]	$DNI$ :	direct normal irradiance [ $W/m^2$ ]
$\dot{Q}_{loss}$ :	thermal losses [W]	$\eta_{opt,0^\circ}$ :	peak optical efficiency [-]
$\dot{Q}_{eff}$ :	effective thermal energy [W]	$c_1, c_2$ :	linear, quadratic loss coefficient [ $W/m^2K$ ], [ $W/m^2K^2$ ]
$\eta_{col}$ :	collector efficiency [-]	$T_m$ :	mean temperature [ $^\circ C$ ]
$A_{eff}$ :	effective aperture area [ $m^2$ ]	$T_{amb}$ :	ambient temperature [ $^\circ C$ ]

Additional parameters for a given collector have to be specified to describe its effective values. Especially parameters regarding receiver losses and optical losses, which are empirically estimated [34]. An example of a collector's (type LS-2) efficiency curve is shown in Figure 19.

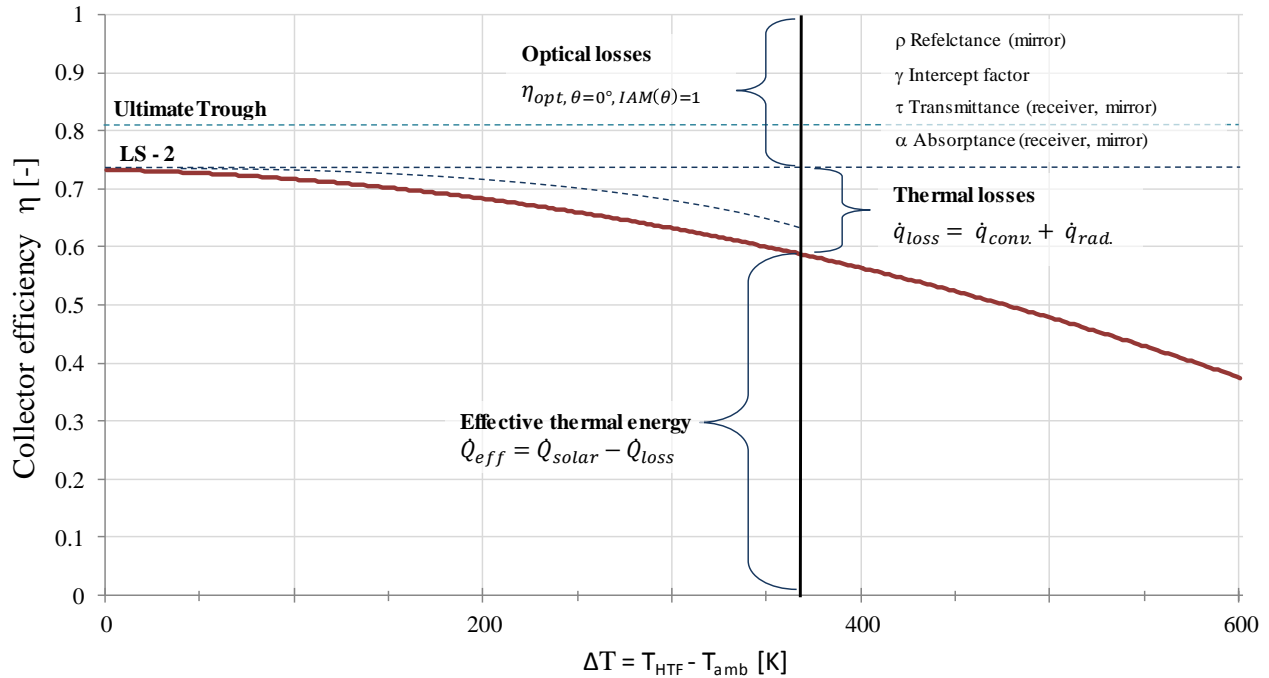


**Figure 19** Collector efficiency curve at the example of an LS-2 collector with empirical parameter values and DNI= 800 W/m<sup>2</sup>.

The graphic describes the composition of the effective thermal energy and the types of losses that constrain the system. It also shows that the collector's efficiency significantly drops, merely due to thermal losses as  $\Delta T$  increases. The optical losses fraction also remains theoretically constant assuming ideal operational losses, by means of perfectly clean mirrors, no shades on the aperture and no end losses. This diagram is a model based on previous results to highlight the parameters and the general behaviour curve of a parabolic trough collector. In real operations an LS-2 collector can operate up to 300°C with mineral oil as heat transfer fluid. The introduced parameters in Figure 19 are next further explained.

### 2.5.1 Optical Losses

#### Peak optical efficiency

Optical losses occur even at optimal direct normal irradiance. This happens when the sun is perpendicular with respect to the collecting surface, or in other words, when the incidence angle is  $\theta_i = 0^\circ$ . These losses have to do with the optical properties of the mirrors and receivers: the total reflectance  $\rho_{\text{tot}}$ , the absorptance  $\alpha$  behavior, the transmittance  $\tau$  of the glass materials and finally the qualitative inaccuracies of the mirrors. The last causes optical deviations, which influence the intercept factor  $\gamma$  of the collector-to-receiver light beam concentration. According to the definition, that the maximal collector's efficiency is constrained by the maximal (peak) optical efficiency [36]:

$$\eta_{\text{opt},0^\circ} = \rho_{\text{tot}} \cdot \gamma \cdot \tau \cdot \alpha \quad (7)$$

$\eta_{\text{opt},0^\circ}$ :	peak optical efficiency [-]	$\tau$ :	transmittance [-]
$\rho_{\text{tot}}$ :	total specular reflectance [-]	$\alpha$ :	absorptance [-]
$\gamma$ :	intercept factor [-]		

State of the art collectors for electricity production possess a peak optical efficiency of 78% to 82%. This value can be identify in a graphical representation of a collector's efficiency, if no thermal losses are considered, for instance, when  $\Delta T = 0$  K. In Figure 19 a peak optical efficiency for the LS-2 at 0.73 can be read and for the UltimateTrough at 0.82.

#### Incident angle modifier $\text{IAM}(\theta_i)$ and cosine losses $\cos(\theta_i)$

For a following observation on the optical parameters, an incidence angle  $\theta_i \neq 0^\circ$  is assumed. So the sun is not perpendicular to the aperture area. Figure 20 shows this scenario for an East-West-oriented parabolic trough with the tracking angle  $\rho \neq 0^\circ$  as well. As the sun position varies from east to west each day and the tracking angle over the seasons, a parameter called Incident Angle Modifier  $\text{IAM}(\theta_i)$  is describes the angular dependent loss mechanisms. Correlations of the incident angle modifier are usually based on measurement campaigns for each specific collector [34].



- $\eta_{endloss}$ : Refers to the reflected light beam losses at each collector end that do not hit the receivers due to the sun inclination. On one end the fraction is reflected out of the receivers range and on the other end a part of the receiver remains untouched by the rays. In between adjacent modules the end losses retained, since the next collector uses the reflected light of the previous one.
- $\eta_{clean}$ : Refers to the degree of cleanness of the mirrors and receivers, for instance, from dust, soiling or humidity.

### 2.5.2 Thermal Losses

In an operational solar field, heat losses occur in the receivers and the heat transfer fluid pipes. These losses depend on the temperature difference between the heat transfer fluid and the surrounding. The thermal balance on a receiver is delimited by a glass envelope to the air. The heat on this surface gradually decreases in form of convection and radiation losses. This specific receiver's heat losses can be expressed as followed:

$$\dot{q}_{loss} = \dot{q}_{conv \rightarrow air} + \dot{q}_{rad \rightarrow sky} \quad (9)$$

- $\dot{q}_{loss}$ : specific thermal losses [W/m]  
 $\dot{q}_{conv \rightarrow air}$ : thermal losses due convection [W/m]  
 $\dot{q}_{rad \rightarrow sky}$ : thermal losses due radiation [W/m]

**Figure 21** shows a one dimensional receiver heat balance including conductive, convective and radiative transfers. Values are usually expressed in relation to the receiver's length in  $W/m_{receiver}$ . Conductive losses are neglected in Eq. (9) since this type of losses merely occurs in the heat transfer fluid transport pipes [34].

Figure 22 shows the heat losses grow more exponentially the greater the temperature difference. The reason is the radiation losses that increment the losses to the forth power of the temperature difference value. Convective and conductive losses grow in proportion to  $\Delta T$ . For this study an approximation of the thermal losses can be written as followed:

$$\dot{Q}_{loss} = \dot{q}_{loss}(\bar{T}_{HTF}) \cdot l_{rec} \tag{10}$$

$\dot{Q}_{loss}$ : thermal losses [W]

$\dot{q}_{loss}(\bar{T}_{HTF})$ : specific thermal receiver losses in dependence to the mean operational temperatures [W/m]

$l_{rec}$ : receiver length [m]

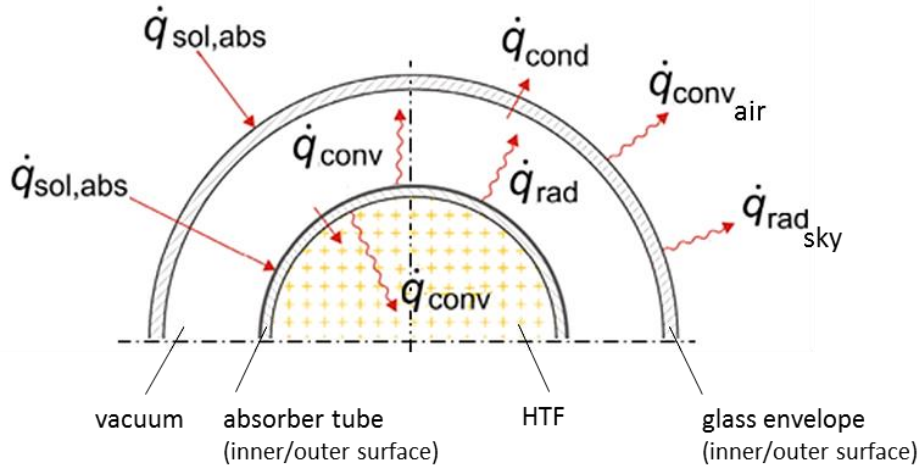


Figure 21 A one-dimensional heat balance on a receiver cross-section; adapted from [34]

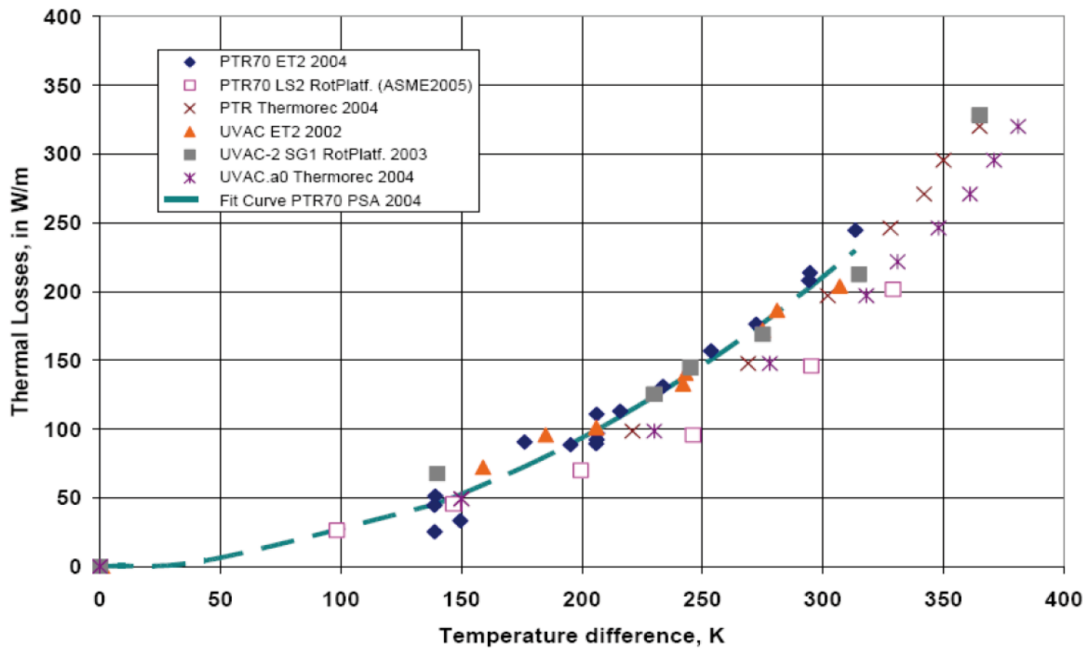


Figure 22 Heat loss measurements for different receiver types [37]

In the graphic different receiver types were measured to demonstrate their thermal behaviour. Comparing this with Figure 19 a correlation between the receiver losses and the collector's

efficiency can be seen. The trivial statement is that higher operating temperatures increase losses, hence also the collector's performance.

### 2.5.3 Parasitic Energy Losses in the Solar Field

Another type of loss is the parasitic energy consumption, which appears at the power plant level. These losses constitute the required electrical power to operate the plant. Normally this electricity is rather provided by the thermal plant itself or by the grid-network, when the plant is offline [34]. The majority of this power is consumed by the pumping of the heat transfer fluid through the extensive collector rows or through the storage tanks and also by the tracking drives of the collectors. A percentage of the parasitic consumptions is also attributed to further electrical components, valves, ventilators, adding other drives and pumps in the BOP (Balance of plant). The parasitic energy consumption amounts around 6-8% of the generated power or about 2% of the input power [38]. The average operating efficiency of parabolic trough plants ranges from 9% to 14% [39]

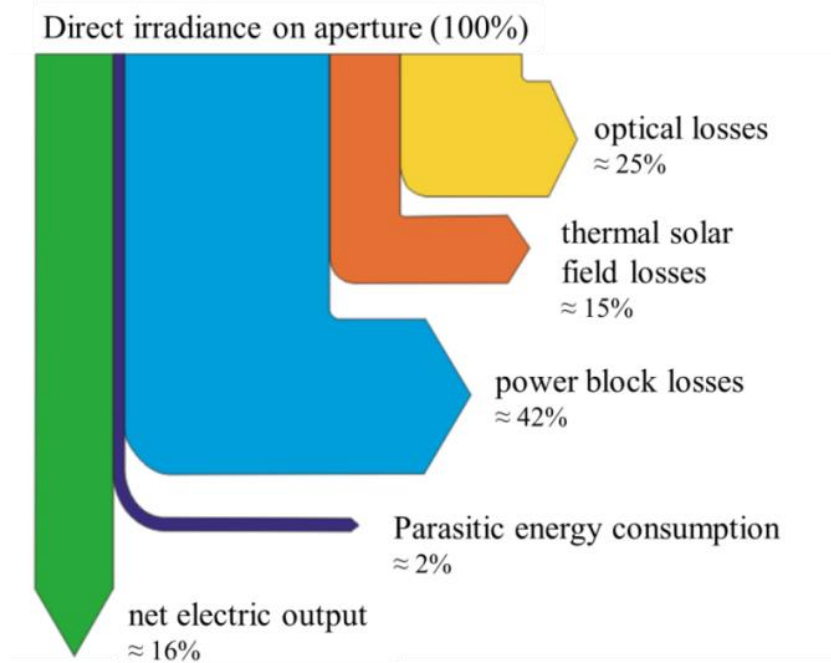


**Figure 23** Estimated energetic flow in a parabolic trough power plant [38]

### 3. Parabolic Trough Collector Concepts

The chapter presents a selection of information to highlight the characteristics of various collectors, some that have been implemented in solar power plants and others that comprehend innovative approaches to enhance the current performance or application. Mainly aspects which define the optical and thermal efficiency are included, as a transition to the analytic section in Chapter 4.

First a categorization of the collectors was required as preparation for the comparative analysis. Following aspects were considered: bearing structure, reflector type and structure materials. The purpose of it is to identify similar aspects of the manufacturing, the assembly, working mechanism and also that of the optical and thermal properties. There are together 34 collectors reviewed in Annex B and sorted in their respective categories as shown in Figure 24.

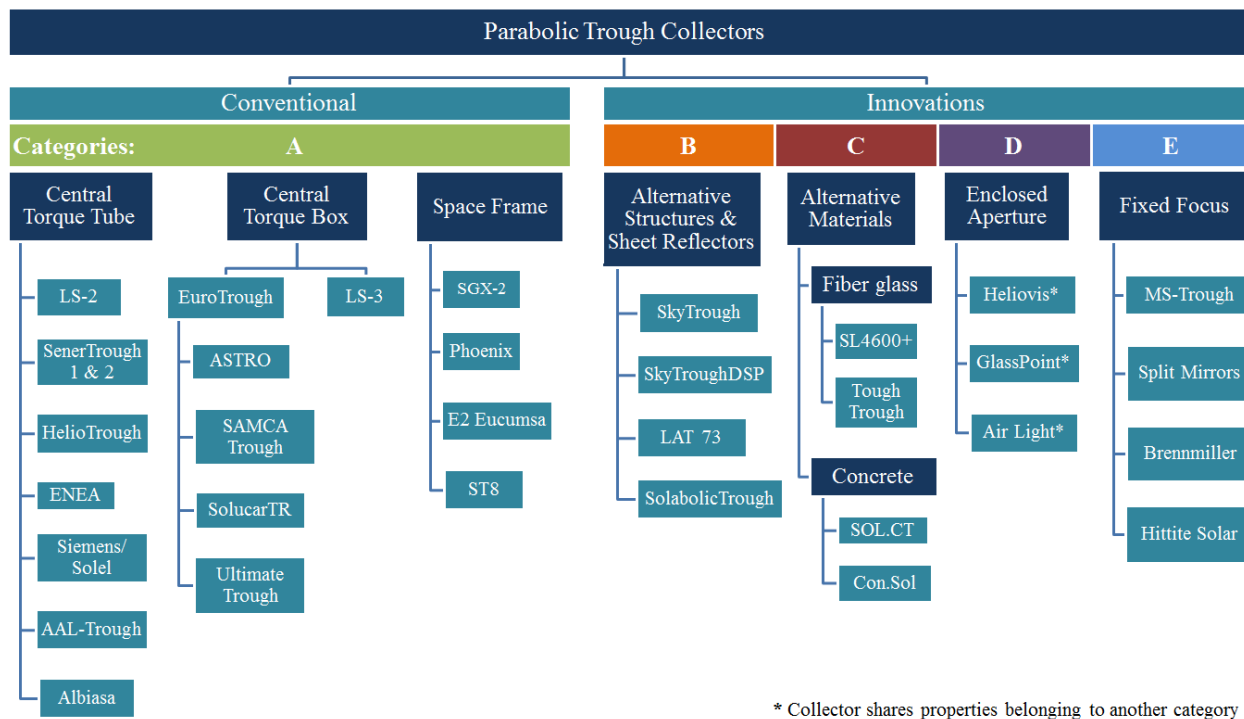


**Figure 24** Genealogy of selected parabolic trough collectors categorized into the main conventional and innovative concepts with a further subdivision according to their prevalent feature (see Annex B)

The collectors are divided into conventional and innovative concepts. Innovative concepts of parabolic trough collectors are understood according to Pitz-Paal et. al (2005) [1]. Innovative concepts will:

- i. *“Increase the power generation efficiency, mainly through increasing operating temperatures*
- ii. *Reduce solar field costs by minimising components’ costs and optimising optical design*
- iii. *Reduce operational consumption of water and parasitic power.”- EASAC, 2011 [40]*

Conventional collector concepts are classified in Category A and further subdivided by their main body structure, namely: the central torque tube, central torque box and space frame. These structures are the main support of the reflectors and are the torque transmission mechanism along the collector solar collector assembly.

Furthermore innovations are classified in:

- Category B for *Alternative Structures and Sheet Reflectors*
- Category C for *Alternative Materials e.g. Sandwich Composites and Concrete Structures*
- Category D for *Enclosed Aperture Collectors*
- Category E for *Fix Focus Collectors*

Additionally a category of historical collectors is included to emphasize the development of the design’s structures and geometries.

### 3.1 Category: Historical Collectors

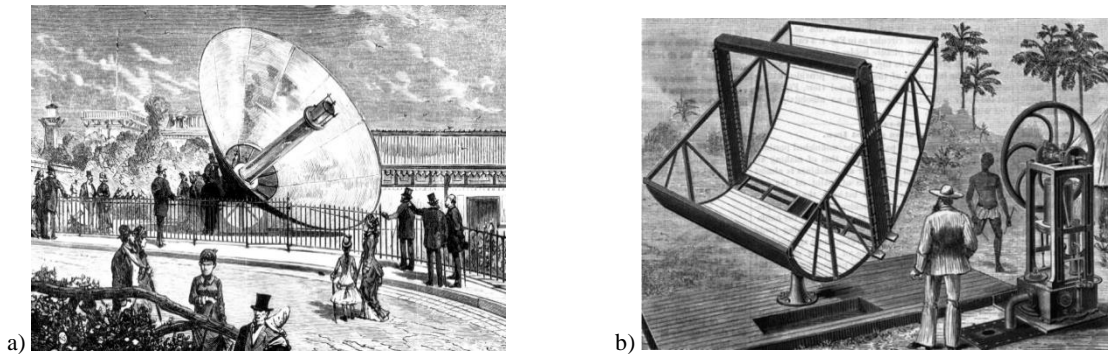


**Figure 25** a) Augustine Mouchout's sun power engine with axis tracking system and truncated concentrator cone. b) John Ericsson's schematic parabolic trough collector with a steam engine and a regulating device (flywheel) for energy storage [41]

Using the solar power as an energy source was not an enigma back in the 19<sup>th</sup> century. In fact a group of inventors believed that the sun had the potential to replace coal power. The way of implementation rather meant a technical challenge.

Pioneers of the field like John Ericsson (1803-1889), Augustin Mouchout (1825-1912) and Frank Shuman (1862-1918) shared the notion that one day coal deposits would be lacking easy access at someday. They recognized the need to use another, abundant source of energy. For this reason first concepts were developed for the production of steam by concentrated solar radiation, leading to the construction of the first reflectors, receivers, geometries, tracking systems and plans for new fields of application.

In 1907 Dr. Wilhelm Maier and Adolf Remshardt patented a device for the general use of sun's heat for steam generation in Germany. In 1912 Frank Shuman & Charles Vernon Boys invented the *Sun Boiler* and set an important milestone in the history of CSP.

A first solar field was deployed in 1913 to generate steam for a low pressure engine to pump water from the Neil River to irrigate a cotton plantation (see Figure 26). The power output at the low pressure steam engine was around 45kW enabling the pumping of around 23 m<sup>3</sup> of water per minute. The configuration of the plant was composed of five rows of collectors of each 61 m long and 4 m aperture with a 6 m wide space gap between the rows. In total the operating aperture area of the solar field was around 1200 m<sup>2</sup>. A rough calculation estimates a 41% to 46% peak optical efficiency of those collectors.

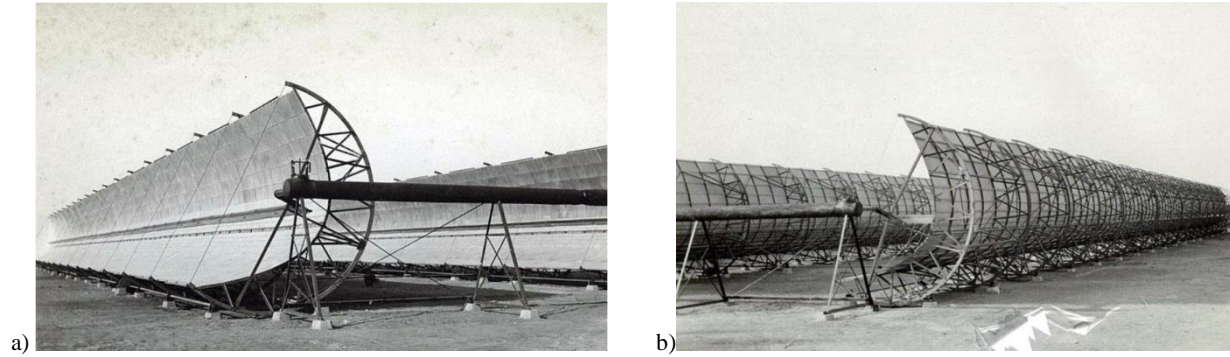


**Figure 26a)** Front sight **b)** back sight of a collector row at the Solar Engine One power plant in Al Meadi, Egypt 1912 [41]

The solar field's format possessed similarities to current operating plants. It showed the collectors in rows with the pipeline distribution and connections to the main steam pipe. The collector's structure was made out of iron frames with a lead coating which were connected to one another and geared, by means of central rack and cog wheels to the engine at ground level [42]. The boiler (in analogy to the current absorber tubes) was coated with a dull black paint or treated with a chemical process (e.g. the treatment of lead with sulphureted hydrogen) followed by a coating of varnish or enamel to reduce the loss of heat by conduction and convection [42].

At that time terms like automation, efficiency optimization, auxiliary storage tanks and mirror shapes, were already topics with a future vision. Shuman considered also an application of the technology to generate electricity at large scale between the tropics of Cancer and Capricorn (i.e. solar belt), yet limitations were significant. Even though the technology was already proven, the plant operated only for one year (1914) and none of its kind was built in the world until the late 1980s. The First World War led to the dismantling of the plant to supply the metal for Britain's munitions industry. Later the industry, still focused on fossil resources, gave no chance to the still ineffective and expensive solar technology.

### 3.2 Category A: Conventional Collectors

Parabolic trough collectors within this category follow the same concept defined by their components. They determine the common design and functionality while tracing the sun. Their specific elements and mechanisms are for example

- (1) Silvered glass reflector facets, about 4 to 5 mm thickness, with a specular reflectance of 93.5% and more than 15 years durability.



**Figure 27** Reflector facets [43]

- (2) Vacuum insulated receivers, with stainless steel tubes and respective selective coating, are usually of a maximum length of 4 m. Modern receivers are suitable for other heat transfer fluids at higher temperatures and pressures.
- (3) Heat transfer fluid and operating temperatures ranging up to 300°C with mineral oil and 400°C with silicon and synthetic oil. Further adaptation of some collectors for steam can reach up to 500°C (at high pressures ~100 bar) and others with nitrate molten salts up to 550°C.
- (4) Hydraulic or geared drive system with a tracking axis below the vertex of the parabolic cross-section. The rotary axis is built coaxial to the centre of mass axis as an optimisation, to reduce the loads on the drives.
- (5) Flexible interconnection elements such as ball-joints or flex-hoses. These elements suffer from frequent breakdowns during operation and tend to have low resistance against high pressure.

- (6) Central torque unit, from which further arms extend to support the mirrors and the heat collector elements supports (HCE) in the case of torque box and tubes. Other alternative or well optimized structures like space frame came to use to minimize the assembly costs, achieve lightweight structures with standardized frame components.



**Figure 28** From left to right: double torque box, torque box, torque tube, space frame [44]

- (7) Assembly jigs, which are usually installed on-site rather in the open sky or in an assembly hall. With the jigs the accurate mounting of the central body and the arms is achieved up to a structure tolerance of 0.5 mm. An assembly without costly jigs is suggested for space frame structures while for other types like the UltimateTrough an automatic assembly line is proposed.

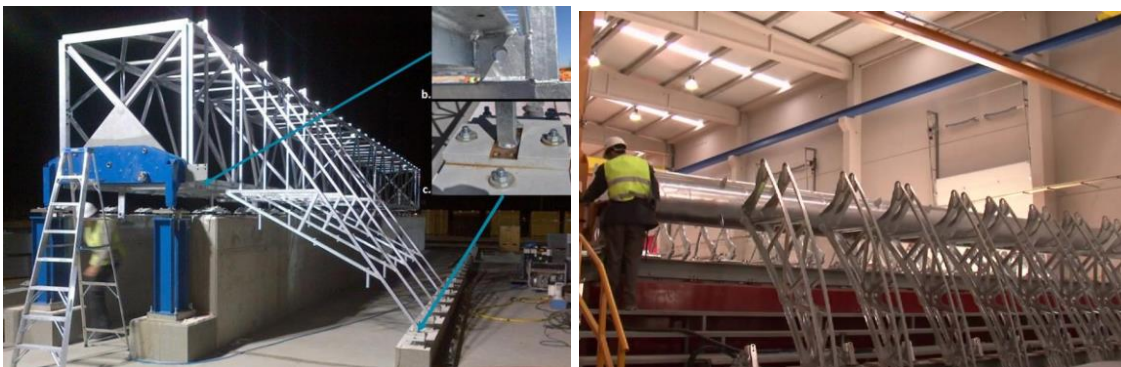


**Figure 29** (left) assembly jig of a torque box structure [45], (right) assembly jig of a torque tube structure [46]

- (8) Hydraulic or geared drive system with a tracking axis below the vertex of the parabolic cross-section, with optimized properties by placing the tracking axis on the centre of mass axis.

- (9) Flexible interconnection elements such as ball-joints or flex-hoses. These elements suffer from frequent breakdowns during operation and tend to have low resistance against high pressure.

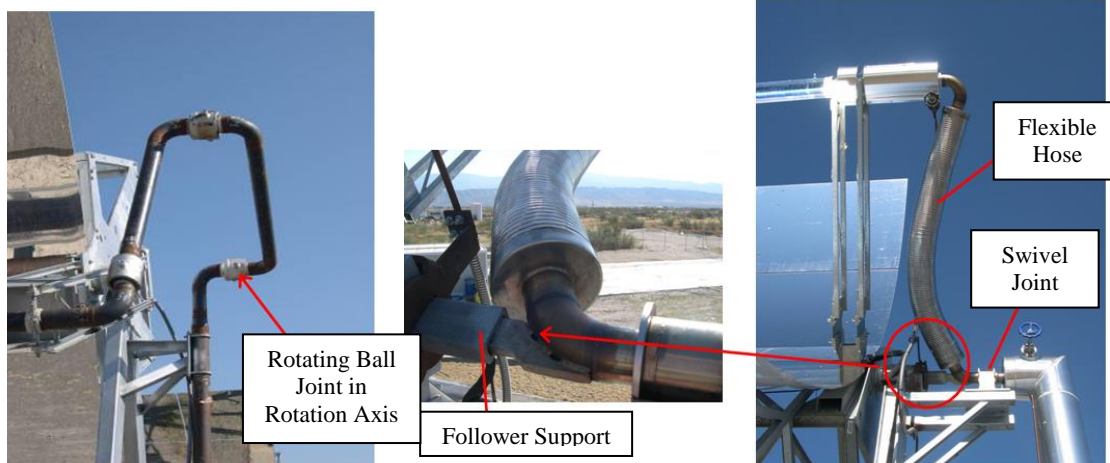


**Figure 30** Flexible interconnection elements [43]

The successful deployment of solar fields using several of these concepts for energy production established the basic standards for modern solar power plants in the global market, making them indispensable for the study. Within the category technological advances aiming the cost reduction are observed, for example the standardization of components, simpler assembly structures, manufacturing methods and logistics. A baseline for a solar field cost is drawn by the EuroTrough collector with a total of 230 €/m<sup>2</sup> in the example of 50MW Andasol and similar solar power plants. Elements included in the cost estimation are later specified.

Solar field efficiency and economic feasibility calculation models conclude that higher concentration ratios can lead to a significant reduction of element square meter. The scaling effect of the collector's aperture can, for example, reduce the total area of the solar field, thus reducing elements like pipelines, receiver tubes, mirrors, pylons and drives among other elements. The efforts to reach these aims are presented in the description of the concepts of this class. It is important to keep in mind that larger apertures are subject to stricter requirements in accuracy and robustness of their structure. Figure 31 shows a timeline with an overview of the collectors and their respective modules dimensions.

CATEGORY A: Conventional Parabolic Trough Concepts

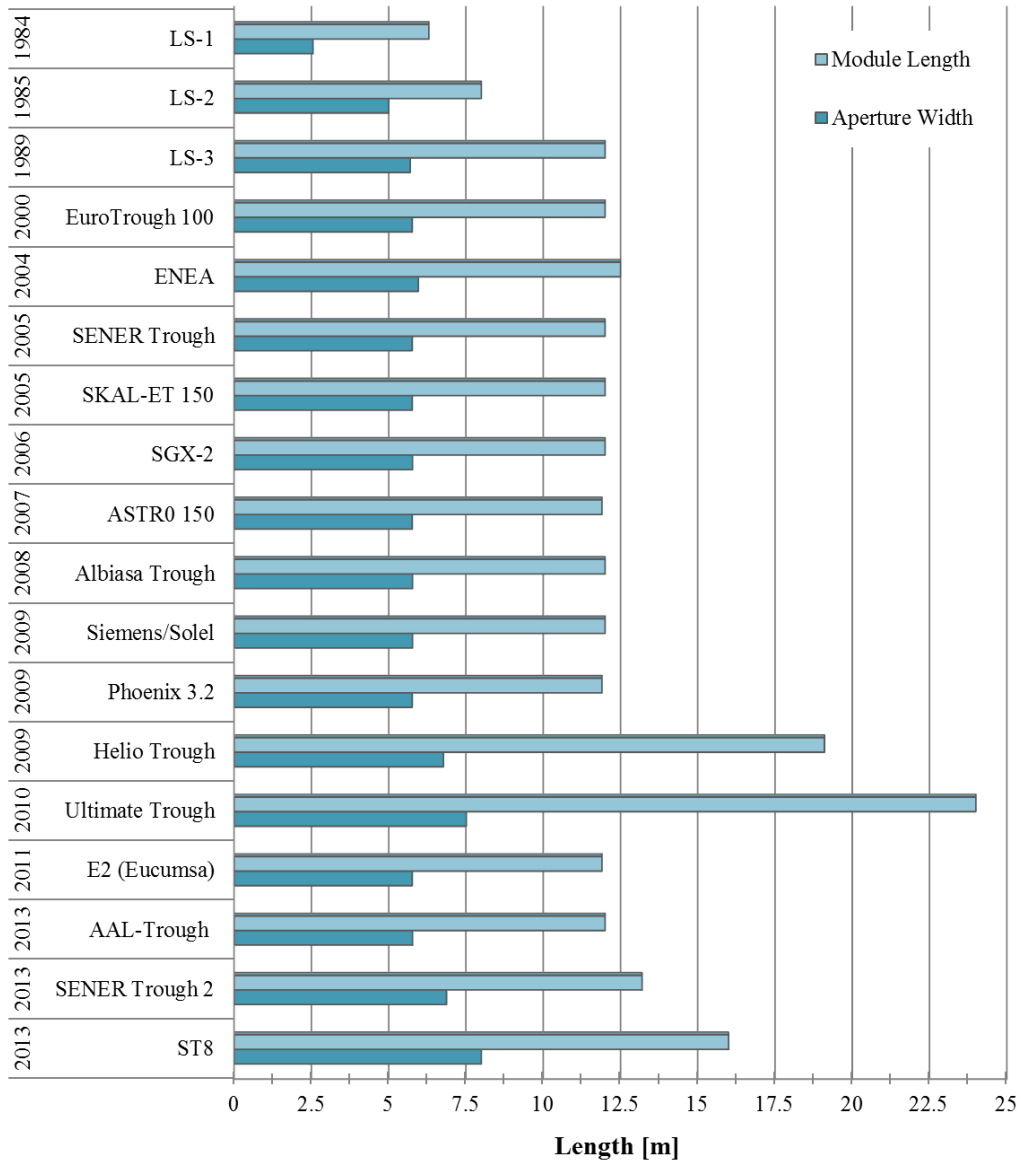


Figure 31 Time line conventional collectors and module's dimensions

### 3.3 Category B: Metal Structures & Sheet Reflectors

In category B there are concepts derived from the structural advances of conventional collectors. Included are collectors with space frames and an alternative metallic structure that seek to lighten the weight and reduce the elements per square meter. These collectors aim for a significant costs reduction per module without adjudicating the characteristic performance.

More important than the structural implementation of metals such as aluminum, is the reflector material that replaces the conventional thick glass panels. Three types of products are shown in the included concepts, among them polymeric reflective films and coated aluminum sheets (see also Chapter 2.2 Mirror Materials). Each of these has not only different optical properties, but also other needs of maintenance, assembly and durability properties. Glass mirrors make around 13% of the costs of a solar field and weight around  $10 \text{ kg/m}^2$ , e.g. RP2 Flabeg type facet. Aluminum reflectors, e.g. ALMIRR, can weigh  $4.8 \text{ kg/m}^2$  with 4 mm thickness and similar to polymeric films, which are in nominal thickness 0.1 mm, attached to an aluminum sheet surface.

Thanks to the standardization of the profiled tubes and connection nodes, the installation of these collectors does not require assembly jigs. Their structure also allows a more efficient assembly in terms of workmanship (cranes, men power...), reducing the installation expenses.

Collectors in these category target higher concentration ratios to up to 104 in the example of the Large Aperture Trough by enlarging the aperture's width. The suitability for molten salt as heat transfer fluid is also present in the case of the SkyFuelDSP. With regard to the structure both apply aluminum tube space frames.

A further innovative approach is targeted by the Solabolic Trough, with aluminum sheet reflectors mounted by tension cables in the structure. The concept was inspired on hanging bridges as for example the Golden Gate in San Francisco, USA. Two segments of a module were prototyped and showed some structural challenges. These limitations currently impeded a large scale deployment of the collector<sup>7</sup>. Therefore the concept is excluded from the evaluation and analysis.

---

<sup>7</sup> See Annex B

### 3.4 Category C: Non-Metallic Materials

This category presents parabolic trough collectors implementing (i) composite sandwich structures and (ii) high performance concrete materials. While the first subdivision (i) is more focused on the parabolic aperture structure, the concepts with concrete suggest an overall casting of the main body and the support structures.

A different line of manufacturing, transport and assembly process is demanded for these collectors. The use of alternative materials aims a breakthrough in costs reduction with concrete as a cost efficient and worldwide accessible material. Furthermore the enhancement of the geometric parabolic accuracy and resistance towards strong winds should also be favored with the composite materials. In both cases a significant weight reduction can be achieved and Table 4 sums up the density values of the here alluded materials.

**Table 4.** Densities and Young's moduli of diverse materials [18]

Material	density [kg/m <sup>3</sup> ]	Young's modulus [GPa]
Steel	7850	210
Aluminum	2710	70
Sandwich Composite (et. Schapitz 2011):		
i.    Fiberglass	1460	25.25
ii.   Foam	25	1.7
iii.  Thin glass	2500	70
Ultra-High Performance Concrete- (UHPC) e.g. Nanodur®, Ductal®	~2510	0.045 - 0.053

#### (i) Fiberglass sandwich composite structures

The first subdivision includes the Solarlite SL4600+ and the Tough Trough collector. In general the elements are constituted of a three layered composite. The outer layer is a mat of fiber glass and resin, which encloses an inner core usually of Polystyrene (PS) or injectable Polyurethane (PU) foam, see Figure 32. In both cases the structure results in an increased bending stiffness, where epoxy resin is utilized in the case of a PU core.

In addition to the higher stiffness, the production of sandwich composites has the advantage that the mirror material is incorporated directly in the manufacturing process. For this purpose an

adhesive technology is applied. Furthermore, the reverse side of the composite is equipped with a UV-stable protection to avoid the material's degradation.

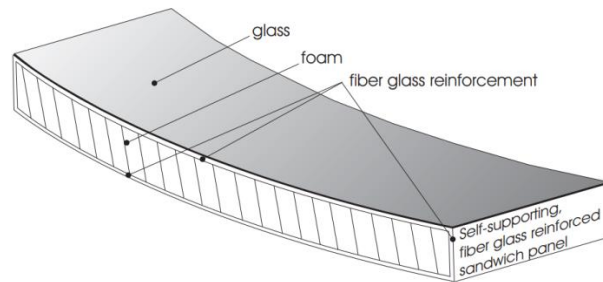


**Figure 32** Self-supporting fiber glass reinforced sandwich structure [47]

### (ii) High performance fiber reinforced concrete

This subdivision is represented by two examples, namely the SOL.CT and the ConSol collectors. The Airlight collector corresponds also to a further concept with this properties section, but it is sorted in 3.5 Category D: Enclosed Aperture Collectors due to its prevalent characteristic of an enclosed aperture.

Ultra-high performance concrete (UHPC) is commercially used for architecture and civil infrastructures, which require great durability and tensile strength. A composition example of an UHPC is shown in Table 5. For the application on parabolic trough confectioning specific machinery is needed, e.g. mixture machines for concrete processing, transportation cranes and molding elements. Due to the intended apertures and large size elements a production hall is required, which should also be big enough to enable the storage of the pieces while hardening.

**Table 5.** Example mixture of an UHPC composition [48]

Material	Amount (kg/m <sup>3</sup> (lb/yd <sup>3</sup> ))	Percent by Weight
Portland Cement	712 (1,200)	28.5
Fine Sand	1020 (1,720)	40.8
Silica Fume	231 (390)	9.3
Ground Quartz	211 (355)	8.4
Superplasticizer	30.7 (51.8)	1.2
Accelerator	30.0 (50.5)	1.2
Steel Fibers	156 (263)	6.2
Water	109 (184)	4.4

1 kg/m<sup>3</sup> = 1.686 lb/yd<sup>3</sup>

RDM = relative dynamic modulus (see p. 134)

### 3.5 Category D: Enclosed Aperture Collectors

The collectors of this category are necessarily differentiated from the conventional ones, since they include a type of translucent cover above the collecting area in their structure. Different configurations and materials like polymeric membranes or glass types have been developed for these collectors as an adaptation to certain regions of the world. More likely environments of implementation are strong winds, high rate of humidity and heavy air due to dust, sand or pollution. These conditions mean exhausting maintenance work of the collector's components and a significant drop of the performance due soiling layers in the reflectors and absorber tubes. Moreover resources like water could be less accessible in such an environment, for instance in a desert region in the Middle East. In fact these collectors could not be considered a technology of application, if it was not for their adapted solutions to the environment.

They also give an alternative perspective on the implementation of technology and contemplate the use of heat transfer fluids like air, steam and oil for different industrial processes that propose a significant saving of CO<sub>2</sub> emissions.



**Figure 33** Enclosed collector concepts. (left) HelioTube (by Heliervis AG), (center) Airlight (by R. Presley), (right) Glasspoint

It can be observed that none of the collectors follow a specific design, but rather overflow to new approaches in order to adapt them to the enclosed aperture. The main curiosity of the concept focusses on the optical performance, since placing a layer in front of the collecting area cause additional optical effects. A general assumption on these collectors is based on a lower optical efficiency in comparison to the conventional collectors. The reflectance, transmittance and absorbance that are attached to the covering materials, can be the main reasons, as described for the maximal optical efficiency in Eq.(7).

### 3.6 Category E: Fixed Focus

In a fix focus collector the main characteristic is featured by the stationary focal axis along the module, which implies alternative structures to those conventionally applied. In general a fix focus collector has the purpose to place the receivers on the focal axis and coaxially to it, the rotary axis of the parabolic concentrators.

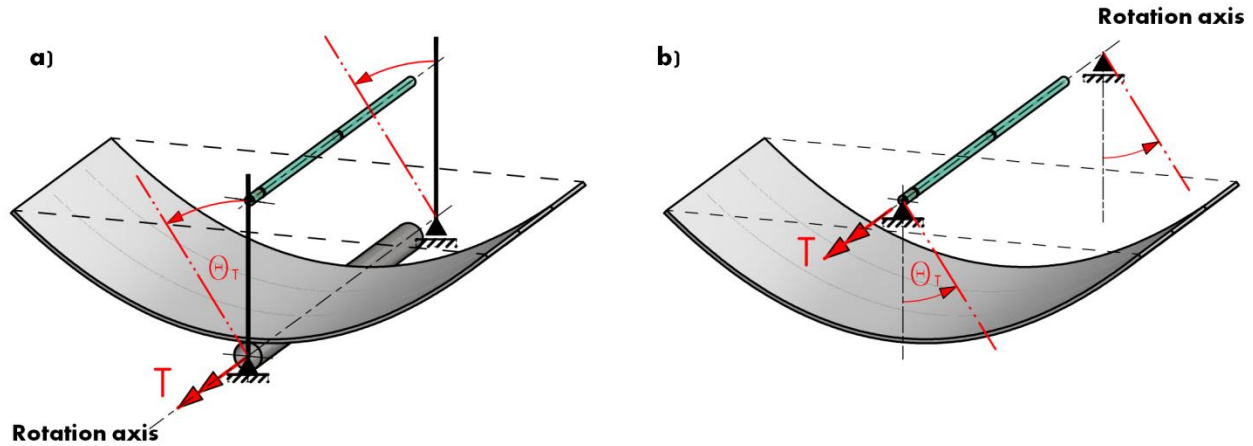


**Figure 34 a) Conventional version:** The torque axis is placed at the torque unit of the collector (e.g. torque tube), which implies the movement of the receiver while tracking the sun. **b) Fixed focus:** The rotational axis coincides with the focal line of the parabola where the receivers are placed. In this case the reflector surface is the movable element.  $T$  stands for the torque and  $\theta_T$  for the torque angle from the middle plane as reference.

Collectors out of this category usually have their rotary axis at the vertex of the parabola structure or slightly below, making the absorber tube to rotate together with the whole concentrator, as schematized in Figure 34a). For this reason, flexible connections are required in those collectors between the modules and the main pipelines, which comprehend on standard elements like ball joints or swivel joints.

A fixed focus collector instead, can eliminate these components since no movement influences the absorber tubes and 'non-flexible' elements can be used at the end of their solar collector assembly, by means of direct welded or flanged piping connections. This specifically targets the elimination of parts that present frequent breakdowns in solar power plants, which are in addition not only costly in acquisition, but also in maintenance. The capital costs of these components are

estimated at 8%<sup>8</sup> of the total share in a conventional solar field, including: material, assembly and installation cost [49]. One last aspect to remark on these elements is that they have a significant influence on the performance of the solar field. In operation the gaskets of the ball-joints exhaust with time, thus causing temperature and pressures drop, thus increasing thermal and parasitic losses. In the worst case, a failure of a joint could lead to important flammable leakages causing fire hazards<sup>9</sup>.

The movability of the absorber tube has been one limitation for the use of molten salts as heat transfer fluid and also for direct steam generation, due to the high operational temperatures and process pressure. Therefore, this concept offers the potential to increase the solar field's efficiency, while reducing, first solar field components per square meter and second, reducing operations and maintenance (O&M) costs.

In conventional collectors an optimized solution to alleviate the stress requirements on components like bearings on the pylons and drive units, is that of placing the collector's center of mass on the rotary axis (e.g. UltimateTrough, HelioTrough). Since the rotary axis of a fix focus is constrained to the focal line, the concept requires a meticulous mass distribution of the components in order to achieve this particular coaxial alignment. Figure 35 shows two case sketches regarding the center of mass on a fixed focus collector.

The center of gravity at the estimate position can be influenced by the parabolic geometry for example with the variation of the rim angle. In this case a rim angle of less than 90° ( $\Psi < 90^\circ$ ) is exemplified, not meaning the restriction for  $\Psi \geq 90^\circ$ .

For situation in Figure 35a) the torque load  $M_t$  around the axis is the force  $F_G$  at distance  $a$ :

$$M_t = F_G \cdot a \quad (10)$$

In order to relocate the center of mass at the focal point  $S_f$  of the collector additional masses can be included. In Figure 35b) as an example the mass  $M$  can be implemented to achieve this balance around  $S_f$ :

---

<sup>8</sup> Case study for an EuroTrough

<sup>9</sup> Fire accident at Andasol Solar Power Plant on 15<sup>th</sup> December 2009

$$\sum M_{S_f} = 0 \rightarrow 0 = F_G \cdot a - F_M \cdot b + \sum_i M_{t_i} \quad (11)$$

In practice all elements need to be taken into account by means of possible heat collector element supports or torque units (etc.), which is expressed by the term  $\sum_i M_{t_i}$  on last equation.

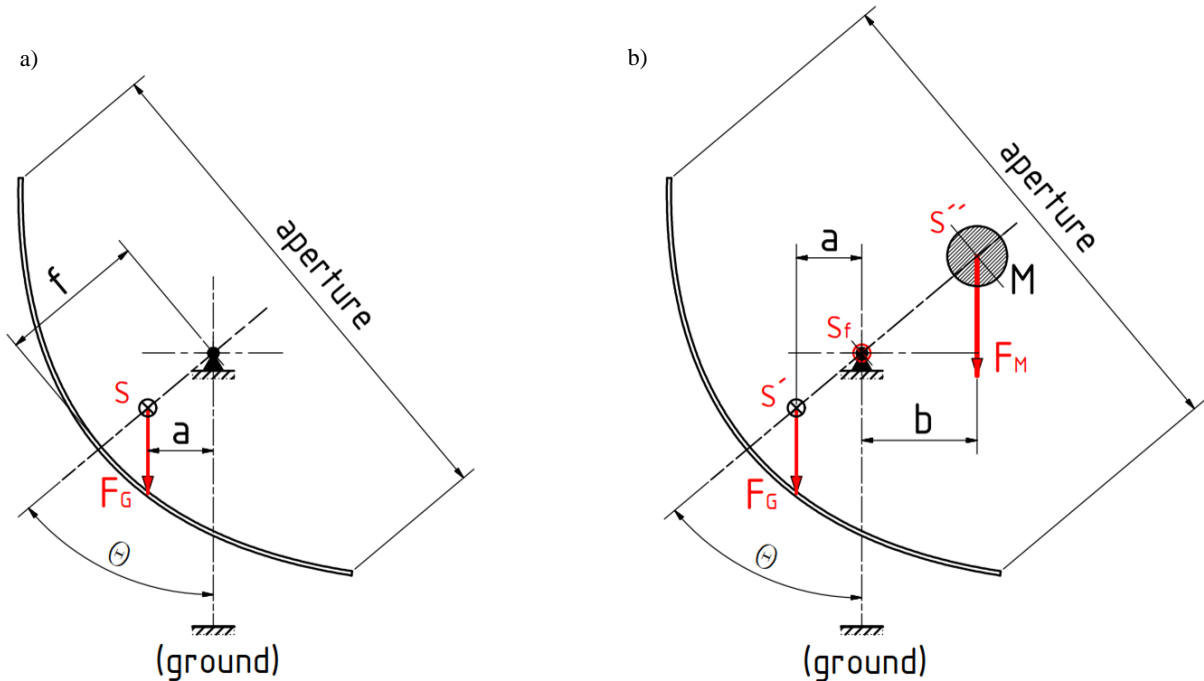


**Figure 35** Mass distribution in a parabolic trough with the rotation axis at focal length  $f$  from its vertex. **a)** The parabola's centre of gravity  $F_G$  at point  $S$  alone represents a torque load that can only be compensated by rigid bearings and counter load of the drive unit. **b)** The centre of mass at the focus  $S_f$  can be in balance by adding a mass  $M$  with a centre of gravity  $S''$  that equalizes the load of  $F_G$  at now named  $S'$ . The parabolic trough will be balanced around the mass point for any value of  $\theta$ .

Following this thought also elements like holding structures and drive mechanisms are more likely to be adapted to the designed. The concept needs special bearings enabling the support of the collector's structure as well as a continuous connection between the receivers along the solar collector assembly.

### **3.7 Technical Overview**

The following tables sum up the researched collector concepts of this thesis. Annex B offers a complementary and more detailed overview on materials, structures and special features of each collector. Moreover a pictorially exposition of these aspects can be seen, as well as further information about the manufacturers and projects of implementation.

Table 6, Table 7 and Table 8 compare the composition of the bearing structure, the type of reflector, receivers and to geometrical and dimensional properties. The heat transfer fluid for which each collector is suitable is contained and the abbreviations are to be understood as follows:

- “TO” for “Thermo-Oil” includes mineral, synthetic and silicone oils
- “MS” for “Molten Salt”
- “HS” for “Heated Steam” meaning demineralized water as high-pressure steam

**Table 6.** Overview of Category A: Conventional Parabolic Trough Collectors

Category / Collector	Bearing Structure			Module			Geometric			Optical			Reference		
	Aperture Width [m]	Module Length [m]	Module Gross Aperture Area [m <sup>2</sup> ]	SCA Length [m]	Rim Angle [°]	Focal Length [m]	Geometric Concentration ratio [-]	Peak Optical Efficiency [-]	Absorber Tube- $\varnothing$ [mm]	Heat Transfer Fluid	Reference				
LS-1	torque tube	2.55	6.3	16.1	50.2	-	0.94	61	71	40	SEGS I-II				
LS-2	torque tube	5.00	8.0	40.0	47	80	1.49	71	76	70	SEGS I-VII				
LS-3	V-truss framework	5.70	12.0	68.4	99	80	1.71	82	74	70	SEGS VII-IX				
EuroTrough [SKAL-EIT100/150]	torque box	5.76	12.0	69.1	100/150	80	1.71	82	75	70	SEGS V/ Kuraymat/ Andasol				
ASTRO 150	torque box; no weldings	5.76	11.9	68.5	-	-	-	-	-	-	Solnova, Spain/ North-Africa				
Phoenix 3.2	aluminum space frame w/steel torque arms	5.76	11.9	68.5	-	-	-	-	-	-	Solnova				
Eucumsa (E2.7)	steel space frame as Phoenix design	5.76	11.9	68.5	125	-	-	-	-	-	Solana, Arizona/ South Africa				
Space Tube ST8.2	space frame	8.00	16.0	128.0	-	-	-	-	-	-	SolarTAC, CampoSol				
ENEA	torque tube	5.96	12.5	74.5	100	~77	1.8	75-80	-	-	Archimede Power Plan				
SGX-2	aluminium space frame	5.77	12.0	69.2	150	-	-	82	-	70	Saguaro, Nevada Solar 1				
SENER Trough	torque tube, stamped cantilever arms	5.76	12.0	69.1	150	80	1.7	82	-	70	Extresol, Spain				
SENER Trough 2	torque tube, stamped cantilever arms	6.87	13.2	90.7	-	-	-	86	-	80	Valle 2, Cádiz, Spain				
Hello Trough	torque tube	6.77	19.1	129.3	191	90	1.71	76	81	90	Test Loop SEGS Blythe, USA				
Ultimate Trough	torque box	7.51	24.0	180.2	247	90	1.95	94	82	80	Harper Lake, USA/ Saudi Arabia, Duba				
Solel/ Siemens	torque tube	5.77	12.0	-	99	-	-	-	-	-	Lebrija, Spain				

**Table 7.** Overview of Category B: Alternative Structures & Sheet Reflectors and Category C: Alternative Materials

Category / Collector	Category B - Alternative Structures & Sheet Reflectors										Category C - Alternative Materials				
	Bearing Structure	Aperture Width [m]	Module Length [m]	Module Gross Aperture Area [m <sup>2</sup> ]	Modules per SCA [#]	SCA Length [m]	Rim Angle [°]	Focal Length [m]	Geometric Concentration ratio [-]	Reflector Type	Peak Optical Efficiency [-]	Absorber Tube-Ø [mm]	Heat Transfer Fluid	Reference	
Category B - Alternative Structures & Sheet Reflectors	SkyTrough	aluminium space frame	6.00	13.9	83.4	8	115	82.5	1.71	75	polymeric film (ReflechTech)	76	80	TO	Demonstration, SEGS II
	SkyTrough DSP	aluminium space frame	7.00	17.7	124.2	8	148	82.5	2.00	87.5	polymeric film (ReflechTech)	75	80	MS, TO	Chabei, China
	LAT 73 - Large Aperture Trough	aluminium space frame	7.30	12.0	87.6	16	192	84.8	2.00	104	polymeric film (3M 1100)	77	70	TO	Dagett, SEGS I
	Solabolic Trough	torque box, profiled arms	5.77	12.5	68.1	12	150	~82.0	1.70	72	aluminium sheet	-	80	TO	Segment Prototype
Category C - Alternative Materials	Solarite SL 4600+	torque tube, sandwich composite panels	4.6	12	55.2	10	120	87.6	1.2	66	laminated thin glass	75	70	HS	Kanchanaburi, Thailand
	Tough Trough	torque tube, sandwich composite panels	-	-	-	4	-	-	-	-	taminated thin glass	-	-	TO	Prototype, Mecklenburg-Vorpomern, DE
	SOLCT	concrete	2 / 6 / 9	12	72.0	4	-	-	1.8/2.2	-	cold bent thin glass	-	-	TO	None; demonstration planned for 2019
	ConSol	concrete	5.77	12	69.2	12	144	80.0	1.71	82	toated aluminium	67	70	TO	Demonstration, Germany

**Table 8.** Overview of Category D: Enclosed Aperture and Category E: Fix Focus of different Parabolic Trough Collector

Category / Collector	Category D - Enclosed Aperture										Category E - Fix Focus				
	Bearing Structure	Aperture Width [m]	Module Length [m]	Module Gross Aperture Area [m <sup>2</sup> ]	SCA Length [m]	Rim Angle [°]	Focal Length [m]	Geometric Concentration ratio [-]	Reflector Type	Peak Optical Efficiency [-]	Absorber Tube-Ø [mm]	Heat Transfer Fluid	Reference		
Category D - Enclosed Aperture	<b>Airlight</b>	fibre reinforced concrete and inflatable polymeric membrane	9.70	212	2,056.4	1	212	73.5	3.25	70	polymeric film	61	140	Air	Ait Baha Pilot Plant, Morocco
	<b>GlassPoint</b>	cabled suspended mirrors, fixed receiver	7.64	8	61.1	12	180	88.8	1.95	109	coated aluminium	0.68	70	HS	Berry Petroleum, MIRAHAH, Oman, Kuwait, California
	<b>Heliovis</b>	inflatable polymeric membrane tube, with metal frames	8.00	220	1,760.0	1	220	67.4	3	80	polymeric film	0.71	80	TO & HS	Mercajucar, Spain
Category E - Fix Focus	<b>Hittite Solar</b>	space frame and semi-circular structure supported on ground	6	12	72	6	72	-	-	75	thick glass	-	80	HS	Demonstration SCA
	<b>Brenmiller</b>	double torque tube, circular frame and profiles	-	-	-	-	-	-	-	-	thick glass	-	-	TO	Demonstration SCA
	<b>Split Mirrors</b>	truss frame, fibre glass and resin, foam	6	12	72	12	144	-	0.98 (mean)	86	embedded thin glass	75	70	TO & MS	None
	<b>MS-Trough</b>	double torque tube, thin sandwich composite	7.8 / 6 prototype	12	94	66	800 / 1000	-	1.2 (mean)	110	embedded thin glass	78	70	MS	Prototype (1:4), Tabernas, Spain

## 4. Value Analysis and Evaluation

### 4.1 Comparison Criteria

With the definition of the state of the art on different parabolic trough collectors and their relevant components, a value analysis is intended with a comparative character. As seen in Table 6, Table 7 and Table 8, a variety of parameter combinations form the basis for the analysis.

The main interest is to identify those collectors with the potential to have a competitive performance for the large scale solar field deployment for electrical power generation. In the Chapter 2 the collector performance drivers were exposed, as well as the roles of selected components like concentration factor, geometry, mirrors, receivers and heat transfer fluids. The categories in Chapter 3 enable some generalizations to facilitate the study of structure materials, manufacturing and the cost of their introduction.

In the following subsections the collectors are compared on specific criteria, which are derived on the basis of the study's objectives. The definition of these criteria is based on a techno-economic perspective.

#### 4.1.1 Optical Performance

The optical performance is influenced by the type of reflector and structural geometric accuracy. The investigated parameters of comparison are: mirror material, peak optical efficiency, IAM, end losses and shading.

##### Reflector Type

A previous study for the characterization of the optical properties of reflector materials for concentrating solar power technology measured the specular reflectance  $\rho_{spec}$  and the surface's degradation rate among others. Using these results, it is possible to rank the reflector types according to the beam deviation of the reflected incident solar rays. The importance of the concentration of the light in a minor area (i.e. focus) is that of the interception accuracy at the focal point. The greater the beams diversion, the greater are the optical losses caused by the material or its surface.

Thick & thin glass, polymeric films and sputtered aluminum reflectors, are the state of the art. Results of the aforementioned study are presented in Figure 36. The images show the measured specular beam profile and demonstrate the marginal size of specular beam diversion of all samples [17]. Even though thin glass mirrors were not measured similar results to Figure 36a are assumed, due to the similar architecture and materials of thick glass.

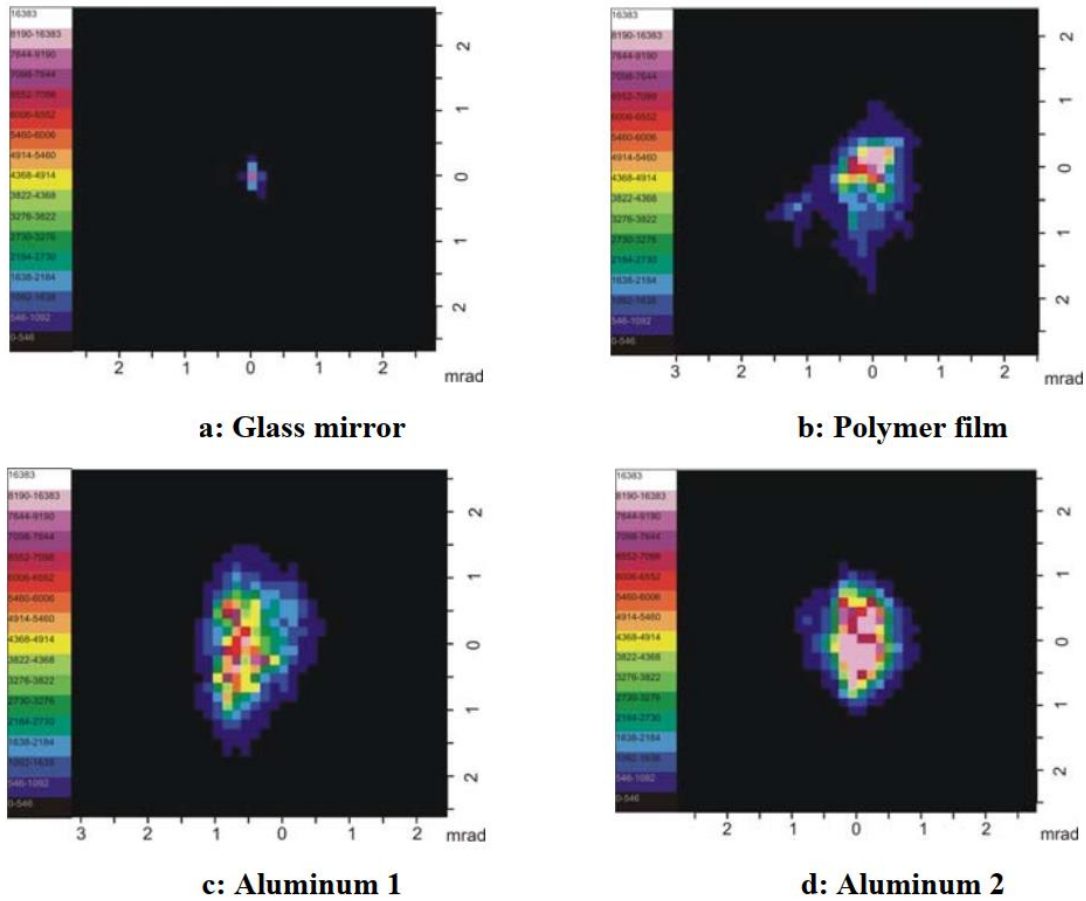


**Figure 36** Images of specular beam diversion of different material samples. Profile in the range of 3-4 standard deviations respectively  $\sigma_{spec}$  in both directions to zero [17]

Furthermore degradation rates are higher in first surface mirrors, which is the case for polymeric films and aluminum. For the analysis the reflector ranking is shown Table 9.

**Table 9.** Ranking of reflector types for large scale application of parabolic troughs

Thin glass	Thick glass	Polymeric film	Aluminum Sheet
i	ii	iii	iv

### Peak optical efficiency

In most of the commercial collectors the peak optical efficiency is explicitly given. An estimation approach can be applied for others. Considering equation Eq. (6) only the absorbed thermal output  $\dot{Q}_{abs}$  and the dimensions of the effective aperture area are required to determine the peak optical efficiency:

$$\eta_{opt,peak} = \frac{\dot{Q}_{abs}}{A_{eff} \cdot DNI} \quad (12)$$

$\eta_{opt,peak}$ : peak optical efficiency [-]                       $A_{eff}$ : effective aperture area [m<sup>2</sup>]  
 $\dot{Q}_{abs}$ : absorbed thermal energy [W]                      DNI: direct normal irradiance [W/m<sup>2</sup>]

The DNI is considered at a value of 800 W/m<sup>2</sup>. Table 10 shows the values for each collector. In some cases the estimation was accomplished by using Eq. (12).

**Table 10.** Peak optical efficiency of different parabolic trough collectors

Category/ Collector		$\eta_{opt,peak}$	Category/ Collector		$\eta_{opt,peak}$
A	UltimateTrough	0.80 <sup>1</sup>	D	Airlight	N.A
B	SkyTrough	0.76 <sup>2</sup>		GlassPoint	0.68 <sup>7</sup>
	SkyTroughDSP	0.75 <sup>3</sup>		Heliovis	0.71 <sup>8</sup>
C	LAT73	0.77 <sup>4</sup>	E	Hittite Solar	N.A <sup>*</sup>
	SL4600	0.75 <sup>5</sup>		Brenmiller	N.A <sup>*</sup>
	Tough Trough	N.A <sup>*</sup>		Split Mirrors	0.75 <sup>9</sup>
	Sol.CT	N.A <sup>*</sup>		MS-Trough	0.78 <sup>10</sup>
	ConSol	0.67 <sup>6</sup>			

Sources Table 10: [9]<sup>1</sup>, [50]<sup>2</sup>, [51]<sup>3</sup>, [52]<sup>4</sup>, [18]<sup>5</sup>, [18]<sup>6</sup>, [53]<sup>7</sup>, [54]<sup>8</sup>, [47]<sup>9</sup>, [55]<sup>10</sup>

Among the collector types, the peak optical efficiency ranges between 80.1% attributed to the UltimateTrough [9] and 61% as estimated for the Airlight collector. In the case of the MS-Trough (78%) [55] and Split Mirrors (75%) [47], both innovations are reported on the basis of numerical results as an estimation for real scale modules. Other collectors present no access on this parameter, and neither an estimation chance. The influence of this parameter can be seen once comparing the overall performance in the coming sections.

### Incidence Angle Modifier - IAM

This parameter is collector specific, defined by the structure, mirror errors and reflectivity, as well as by the geometry, including end losses. Considering the incidence angle of the solar rays the natural cosine losses are also calculated within the modifier factor. Figure 37 shows the behaviour of this factor at different incident angles for two different collector types. Table 11 contains the respective correlation factors, for instance,  $b_1$  and  $b_2$ .

**Table 11.** Incidence Angle Modifier at the example of an EuroTrough and SkyFuel collector [56] [57]

$IAM(\theta) = 1 + \frac{b_1 \cdot \theta^2}{\cos(\theta)} + \frac{b_2 \cdot \theta}{\cos(\theta)}$		$K = IAM(\theta) \cdot \cos(\theta)$
factor	$b_1$	$b_2$
EuroTrough*	$-2.8596921 \cdot 10^{-5}$	$-5.25097 \cdot 10^{-4}$
SkyFuel	-0.1227	0.0278

\*computing the units for  $\cos(\theta)$  [deg] and  $\theta$  [rad]

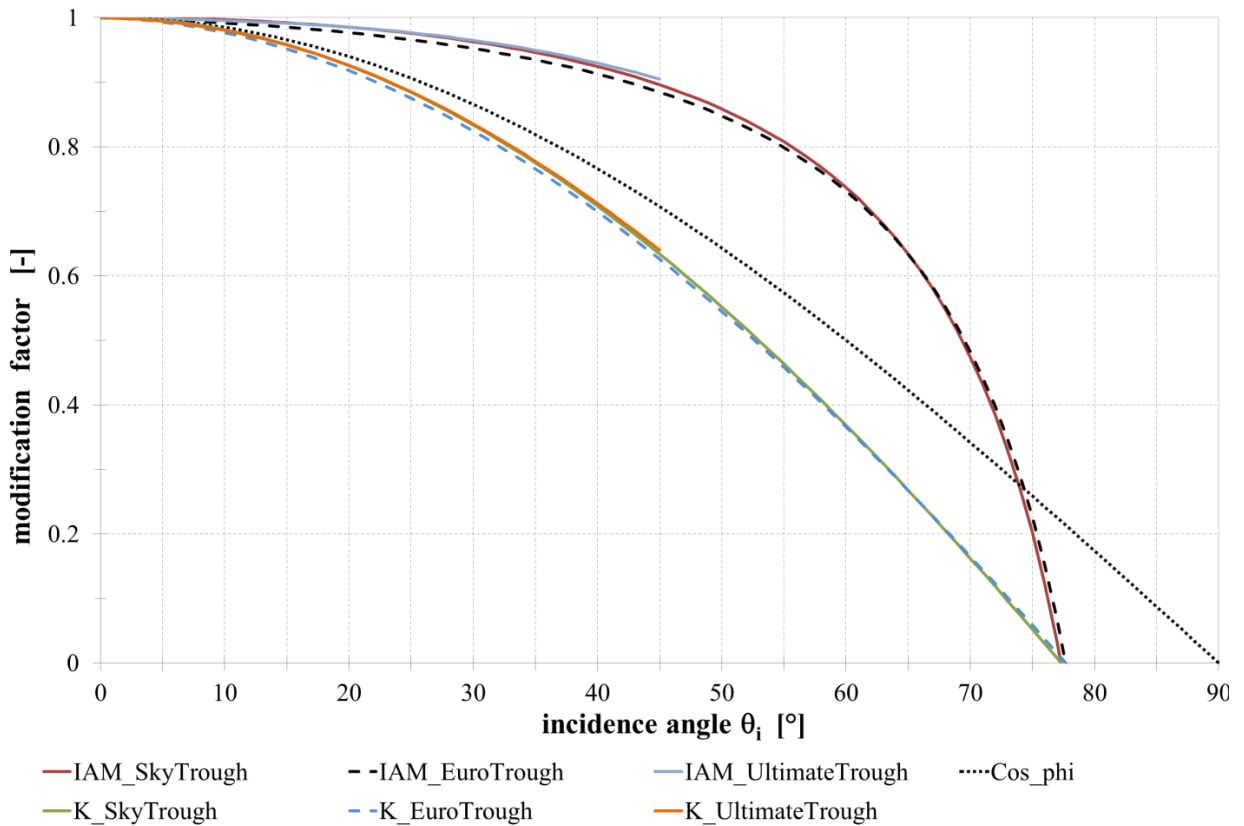


**Figure 37** Incidence Angle Modifier curves with and without cosine losses

IAM correlations are collector specific and determined after measurement campaigns of the operational modules. This detail constrains the comparison to present the IAM behaviour of each

collector, due to accessibility of information. This factor will be equally considered at  $\theta = 0^\circ$  and subsequently  $IAM(\theta) = 1$ , to simplify the later performance estimation of all collectors.

For conventional structurally similar collectors the tendency of this factor curve seems to be similar as could be appreciated in Figure 37. Once comparing a conventional collector with glass facets against a collector with polymeric film reflectors (considered an innovation), the similarity is remarkable. It is also seen that the largest fraction of losses is based on the cosine losses, which affect all collectors.

### End losses

These factors are normally included in the IAM. They are nevertheless geometrical parameters that can be estimated and exposed with a comparative character. A simplified equation in dependence of the specific SCA collector length  $l_{col}$  and the focal length  $f$  can be expressed as follows [57]:

$$\eta_{end} = 1 - \frac{2 \cdot f \cdot \tan(\theta_i)}{l_{col}} \quad (13)$$

$\eta_{end}$ : end losses efficiency [-]

$l_{col}$ : collector length [m]

$f$ : focal length [m]

$\theta_i$ : incidence angle [rad]

Results on Figure 38 show greater losses for instance on the GlassPoint collector as a consequence of the lower length (8 m) and a greater focal length (1.95 m). On the other hand the MS-Trough and the Split Mirror collectors both with 12 m module length, have lower losses because of their reduced mean focal length: 0.98 m for the Split Mirror and 1.2 m for the MS-Trough.

Since the relevant range of the solar incident angle for parabolic trough applications is between  $0^\circ$  and  $60^\circ$ , the losses in all collectors suppose a small fraction in comparison to the above presented cosine losses and IAM [2].

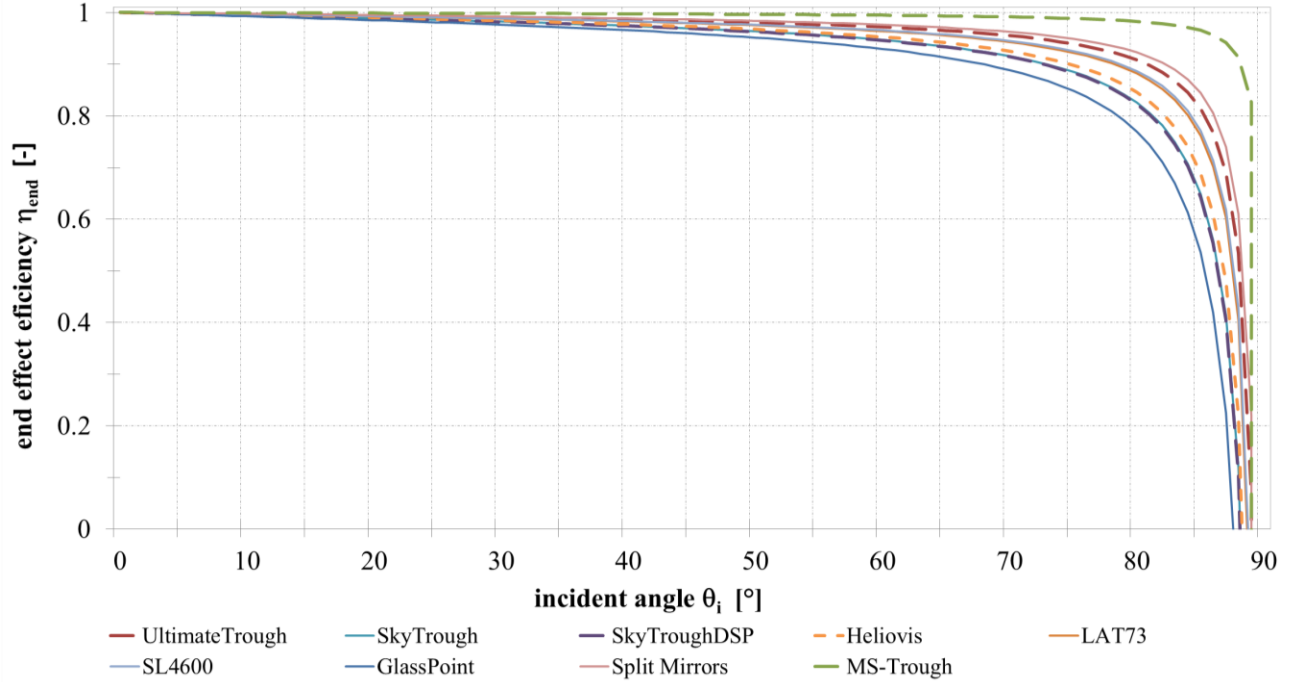


**Figure 38** End losses curves of different collectors neglecting the spacing between the modules of a solar collector assembly

## Shading

The argumentation for the shading efficiency does not defer from that. The shade losses are strongly depended on the construction format of the collector rows. To minimize these kind of losses the distance between the rows is more or less 3 times the collector aperture width or  $d_{row} = 3 \cdot a_{col}$ . For a total estimation of the solar field shade losses, it is necessary to fix the number of rows contained in it. To enable a comparison an equal number of collector rows is given for each collector, namely at  $n_{row}=12$ . Figure 39 show the results using Eq. (14) [34].

$$\eta_{shade} = 1 - \frac{n_{row}-1}{n_{row}} \cdot \frac{a_{col}-d_{row} \cdot \cos(\rho)}{a_{col}} \quad (14)$$

$\eta_{shade}$ :	shade loss efficiency factor [-]	$a_{col}$ :	collector aperture width [m]
$n_{row}$ :	number of rows [-]	$d_{row}$ :	distance between rows [m]
$\rho$ :	tracking angle [rad]		

For the GlassPoint collector the computed dimensions represent an entire glass house module. Since the collectors are compactly built, shade losses start appearing at  $\rho=49^\circ$  and increase linearly. The represented shade losses do not include the shadings caused by elements above the

aperture of the collectors, as it is the case on the GlassPoint (due to the glasshouse structure) and Heliovis collectors (due to the receiver's support and main circular support structure). All other collectors following the three times aperture value for the row distance, do not show significant losses until  $\rho=71^\circ$ , which is above the relevant range of  $60^\circ$ .

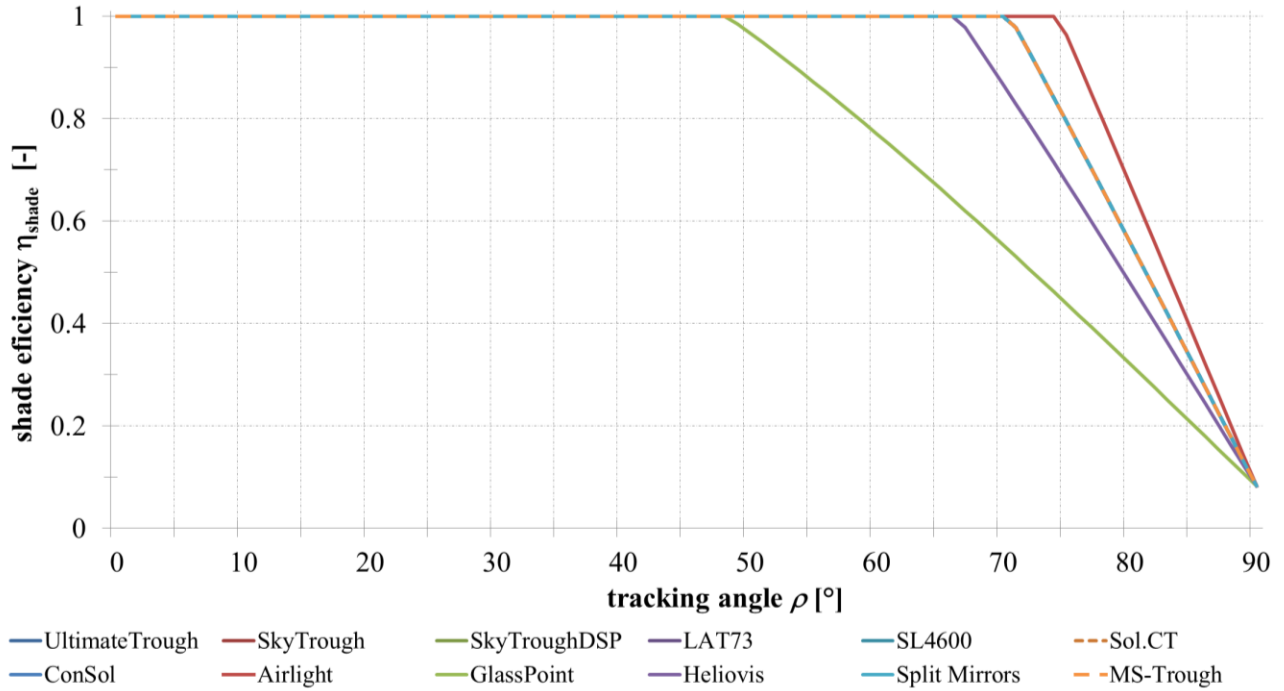
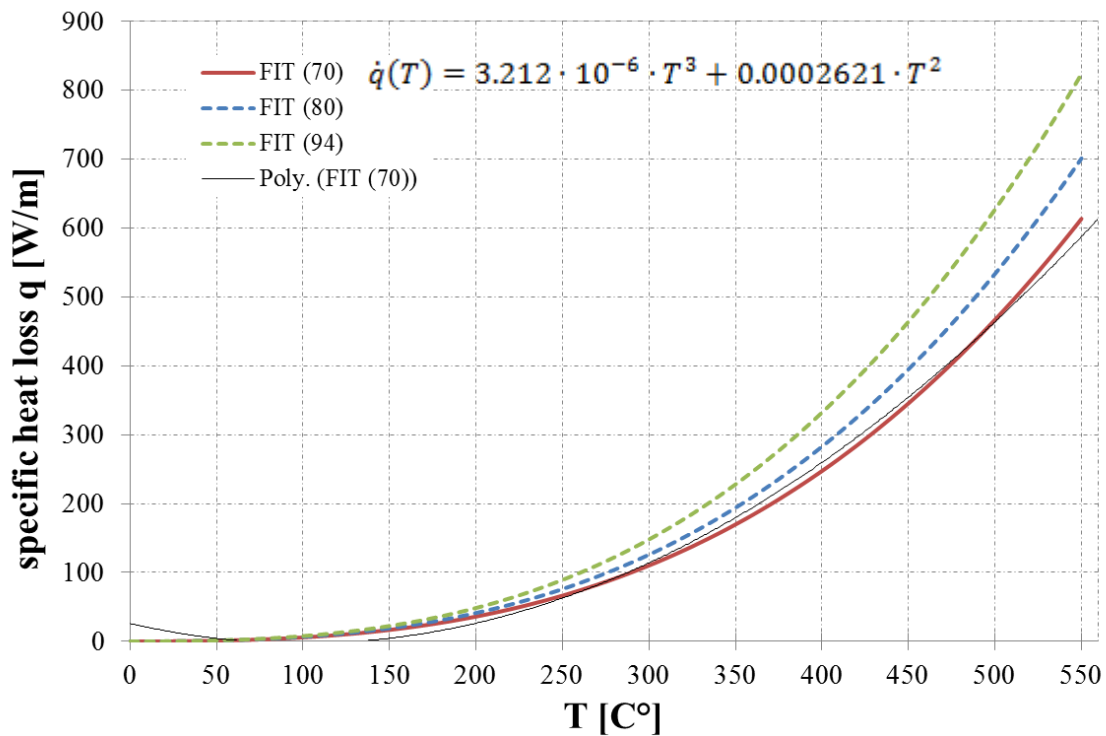


Figure 39 Shade losses of different parabolic trough collectors

### 4.1.2 Thermal Performance

To describe the thermal performance it is important to take elements like the receivers and the streaming fluid of the solar field into account. Also operational parameters like the volumetric flow, mass flow and the pressure of the cycle are relevant to get at operational temperatures. As summed up before, there are suitable receiver types, for thermo-oils, pressurized steam and molten salts; (see Table 6 to Table 8). Assumptions are made for the theoretical comparison of the thermal aspects, because the operating temperatures and specific heat capacity factors vary according to the fluid and concentration ratio of the collectors.

First a comparison of all evaluable collectors using the same heat transfer fluid is made, in this case thermo-oil of type VP-1. Secondly the suitable collectors for molten salts are differed from those suitable only for thermo-oil. In both scenarios a global assumption is made for the receiver specific heat losses  $\dot{q}$  in W/m.



**Figure 40** PTR70 specific heat loss curve fit with a polynomial of 3<sup>rd</sup> order (red) and 2<sup>nd</sup> (black). A 1.14 factor defines the  $\varnothing 80\text{mm}$  loss curve and 1.34 respectively for  $\varnothing 94\text{mm}$ .

Figure 40 shows the heat losses of a PTR70 ( $\varnothing 70$  mm) receiver tube for thermo-oil used to operate at  $T=400^\circ\text{C}$ . The loss values are taken from the product data sheet and interpolated with a 3rd order polynomial. As the diameter tube varies from each collector, a further factor is introduced accordingly to simulate the losses at higher temperatures e.g. for  $T=550^\circ\text{C}$  for molten salts. By this factor the percentual additional loss caused by larger receiver diameter is taken into account, implying a larger receiver surface. It is estimated for a diameter  $\varnothing 80$  mm that receiver losses will at least be increased by a factor of 1.14 ( $80/70$ ), while for  $\varnothing 90$  mm by a factor of 1.34 ( $94/70$ ) as the ratio of the diameters is calculated.

### Scenario 1: Length estimation

To introduce the influence of the concentration ratio on the thermal power output, the operation of all collectors with the same fluid is assumed. The thermo-oil VP-1 is a suitable choice for this scenario, because thermo-oil is the benchmark for PTC power plants and the receiver losses (above) can be described. Furthermore it is presumed that the collectors are operated at the same mass flow  $\dot{m}$  to achieve operational temperatures from the inlet ( $T_{in} = 290^\circ\text{C}$ ) to the outlet ( $T_{out} = 400^\circ\text{C}$ ). The output thermal power per loop is estimated from a 30 MW solar field composed of 40 EuroTrough loops in Kuraymat, Egypt. For each loop an estimate of  $2.0 \text{ MW}_{th}$  (thermal output) results in a mass flow of  $\dot{m} = 7.5 \frac{\text{kg}}{\text{s}}$ , according to  $\dot{Q} = \dot{m} \cdot c_p \cdot \Delta T$  and considering a mean heat capacity factor of  $c_p = 2.44 \frac{\text{kJ}}{\text{kg}\cdot\text{K}}$ .

Under these conditions, it is up to find the respective collector length, for which  $\dot{Q}_{abs}$  is equal to  $2.0 \text{ MW}_{th}$ . The following equation shows the approach:

$$\dot{Q}_{eff} = \dot{m}_{HTF} \cdot c_p \cdot (T_{out} - T_{in}) = \dot{Q}_{solar} - \dot{Q}_{loss} \quad (15)$$

$\dot{Q}_{eff}$ :	effective thermal energy [W]	$\dot{m}_{HTF}$ :	heat transfer fluid mass flow [kg/s]
$\dot{Q}_{solar}$ :	incident solar energy [W]	$c_p$ :	specific heat capacity factor [J/kg·K]
$\dot{Q}_{loss}$ :	thermal losses [W]	$T_{in}, T_{out}$ :	collector inlet and outlet temperature [K]

The output temperature is most important. Therefore an iterative equation is introduced:  $T_{out}$  is calculated after each receiver meter described as  $T_{i+1}(l)$ , until  $T_{i+1}(l) = 400^\circ\text{C}$ . Considering

Eq. (5) for  $\dot{Q}_{solar}$  and Eq. (10) for  $\dot{Q}_{loss}$  the results are suited to each collector property and the temperature can be written dependant on the length as follows:

$$T_{i+1}(l) = l \cdot \left[ \frac{DNI \cdot a_p \cdot \eta_{opt,peak} - \dot{q}(T_i)}{\dot{m}_{HTF} \cdot c_p} \right] + T_i ; \quad 290^\circ C \leq T_i(l) \leq 400^\circ C \quad (16)$$

$T_{i+1}$ :	outlet temperature [ $^\circ C$ ]	DNI:	direct normal irradiance [ $W/m^2$ ]
$T_i$ :	inlet temperature [ $^\circ C$ ]	$a_p$ :	aperture width [kg/s]
$l$ :	length [m]	$\dot{q}(T_i)$ :	specific heat receiver losses [ $W/m$ ]

For this calculation, the results vary according to the collector aperture width  $a_p$  (i.e. geometry), the peak optical efficiency  $\eta_{opt,peak}$  (i.e. optical performance) and the specific thermal losses  $\dot{q}(T_i)$ , which depend on the receiver's diameter. For the proposed scenario the collectors are considered to be under the same irradiation of  $DNI=800 W/m^2$ .

**Table 12.** Required PTC aperture length to reach operational temperature of thermo-oil  $T=400^\circ C$ .

Collector	MS-Trough	UltimateTrough	Heliovis	LAT73	SkyTroughDSP	GlassPoint	Split Mirrors	SkyTrough	EuroTrough	ConSol	SL4600+	
<b>Required length</b>	$l_{col, 2.0 MW}$ [m]	425	435	459	461	498	501	574	578	606	683	771
<b>%- difference to the shortest length</b>	$\Delta l_{col,MIN}$ [%]	-	2%	8%	8%	17%	18%	35%	36%	43%	61%	81%

Table 12 sums up the results of the simulation and Figure 41 gives a graphical representation. They show that the MS-Trough and the UltimateTrough have the shortest and similar required lengths with a 10 m difference to each other. The difference of 346 m between the MS-Trough and the SL4600+ is much greater. This example emphasizes the potential of larger aperture widths, or rather aperture areas to gain more thermal power, assuming a good optical efficiency. From an economic point of view, shorter collectors require less specific elements, as for example receivers and drives, and thus reducing thermal losses and structural material. The large apertures and their high concentration ratio to the receiver are certainly favourable. The MS-Trough with 7.8 m aperture has 4% more collecting area than the UltimateTrough with 7.51 m aperture.

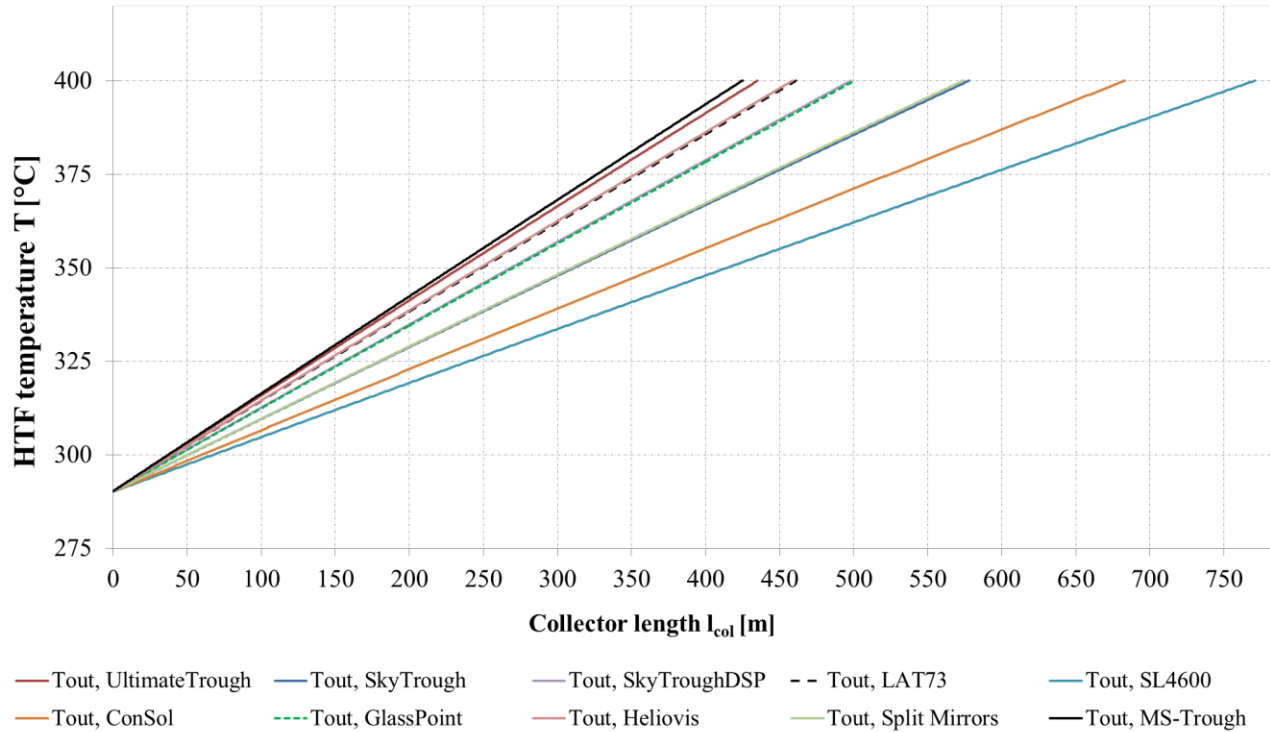


**Figure 41** Required collector length of different PTC to achieve operational temperatures with VP-1

In PTC power plants a modular structure is applied, with rows in different formats, also called loops. This scenario is based on a theoretical frame, to expose the potential of each collector once set under the same operational and fluid media conditions, to show the relevant parameters influence the required deployment of the collectors.

### Scenario 2.1: Thermal power & performance with VP-1

Approaching a more practical scenario, the length parameter is now defined, by the length of the respective collector loop. The collectors are further considered with thermo-oil as HTF, but also the ones for molten salt operation are differentiated and separately compared. This scenario aims not only to describe the performance at optimal conditions, but also to simulate the respective loop thermal power gain and losses at operational design mass flow. Last not least, the study aims to demonstrate the improvement potential of a power plant under the use of molten salts (vs. Thermo-Oils) as HTF.

The analysis is considered at optimal conditions for incident angle  $\theta_i=0^\circ$ , for which the cosine losses and IAM take the value of 1<sup>10</sup>. For the cleanliness factor, brand new installed reflectors are assumed ( $\eta_{clean}=1$ ) at a normal irradiance of 800 W/m<sup>2</sup>. According to Eq. (8) the solar thermal energy is computed as follows:

$$\dot{Q}_{solar} = A_{eff} \cdot DNI \cdot \eta_{opt,0^\circ} \cap [IAM(0^\circ), \cos(0^\circ), \eta_{shad}, \eta_{endloss}, \eta_{clean} = 1] \quad (17)$$

$\dot{Q}_{solar}$ :	solar thermal energy [W]	$\cos(\theta)$ :	cosine losses [-]
$A_{eff}$ :	effective aperture area [m <sup>2</sup> ]	$\eta_{shad}$ :	shade loss efficiency factor [-]
DNI:	direct normal irradiance [W/m <sup>2</sup> ]	$\eta_{endloss}$ :	end loss efficiency factor [-]
$\eta_{opt,0^\circ}$ :	peak optical efficiency [-]	$\eta_{clean}$ :	cleanness efficiency factor [-]
IAM:	incidence angle modifier [-]		

And for the thermal losses in analogy to Eq. (10), where  $x$  is the loop length [34]:

$$\dot{Q}_{loss} = \int q(\bar{T}) dx \quad (18)$$

$\dot{Q}_{loss}$ :	thermal losses [W]	$\bar{T}$ :	mean temperature [K]
$q(\bar{T})$ :	specific heat collector losses [W/m]	$x$ :	length [m]

To find out the performance at  $\Delta T$  between the atmospheric and heat transfer fluid temperatures, Eq. (6) can be solved as followed:

$$\eta_{col} = \eta_{opt} - \frac{\dot{Q}_{loss}(\Delta T)}{DNI \cdot A_{eff}} \quad (19)$$

$\eta_{col}$ :	collector efficiency [-]	$\Delta T$ :	loop inlet/outlet temperature difference [K]
$\eta_{opt}$ :	optical efficiency [-]	DNI:	direct normal irradiance [W/m <sup>2</sup> ]
$\dot{Q}_{loss}$ :	thermal losses [W]	$A_{eff}$ :	effective aperture area [m <sup>2</sup> ]

To facilitate the comparison from a global point of view, three collectors have been adapted for the study.

- **GlassPoint:** The collector is specifically used for process heat generation with steam, more precisely for enhanced oil recovery (EOR). An operational assumption with thermo-oil as heat transfer fluid is set for this scenario.

<sup>10</sup> Driven by the IAM and cosine losses, End losses and shadings are equal to 1

- **SL4600:** Its main operational purpose is direct steam generation (DSG). Same assumption is met as the previous collector.
- **MS-Trough:** The collector is specifically designed to operate with the denser molten salt medium in comparison to oil, which is the reason for its 800 m to 1000 m continuous solar collector assembly length. The pressure drop in a collector loop of these dimensions represents an unrealistic implementation at approximately 20 bar<sup>11</sup>. The loop length is therefore established at 600 m for oil operations.

Figure 42 exposes the performance curve of the collector concepts, with their respective receiver diameter.

On one hand, it is important to highlight, that the computed receiver losses are based on laboratory environment measurements by the receiver's manufacturer. In practical cases, the thermal conductive and radiation losses are greater than considered. The trend of the collector performance remains nevertheless describable, since the thermal losses are rather depended from the receiver and not from the collector concept itself. On the other hand optical properties are considered accordingly to realistic inputs. At operational temperature  $T_{SF,out}=400^{\circ}\text{C}$  the thermal efficiency can be determined, as well as the amount of thermal losses in relation to the gained thermal power.

Table 13 sums up the computed parameters as well as the results for the respective collectors. The UltimateTrough yields the best thermal performance at operational temperatures ( $T=400^{\circ}\text{C}$ ) with 76% followed by the MS-Trough with 75%. Heliomis (68%), GlassPoint (65%) and ConSol (63%) have the lowest thermal performance of this case.

Adding up the respective thermal losses of each collector and calculating the thermal gain, it is possible to estimate a factor, which describes the efficiency of the loop. The MS-Trough loses 3.6% for each  $\text{MW}_{th}$ , while GlassPoint 4.2%, the UltimateTrough 4.9%, and the SL4600+ 6.5%. The conclusion: The smaller the loss per gained  $\text{MW}_{th}$  power, the more effective is the use of the thermal energy.

---

<sup>11</sup> See case in section 4.1.3 Parasitic Consumption (Table 15).

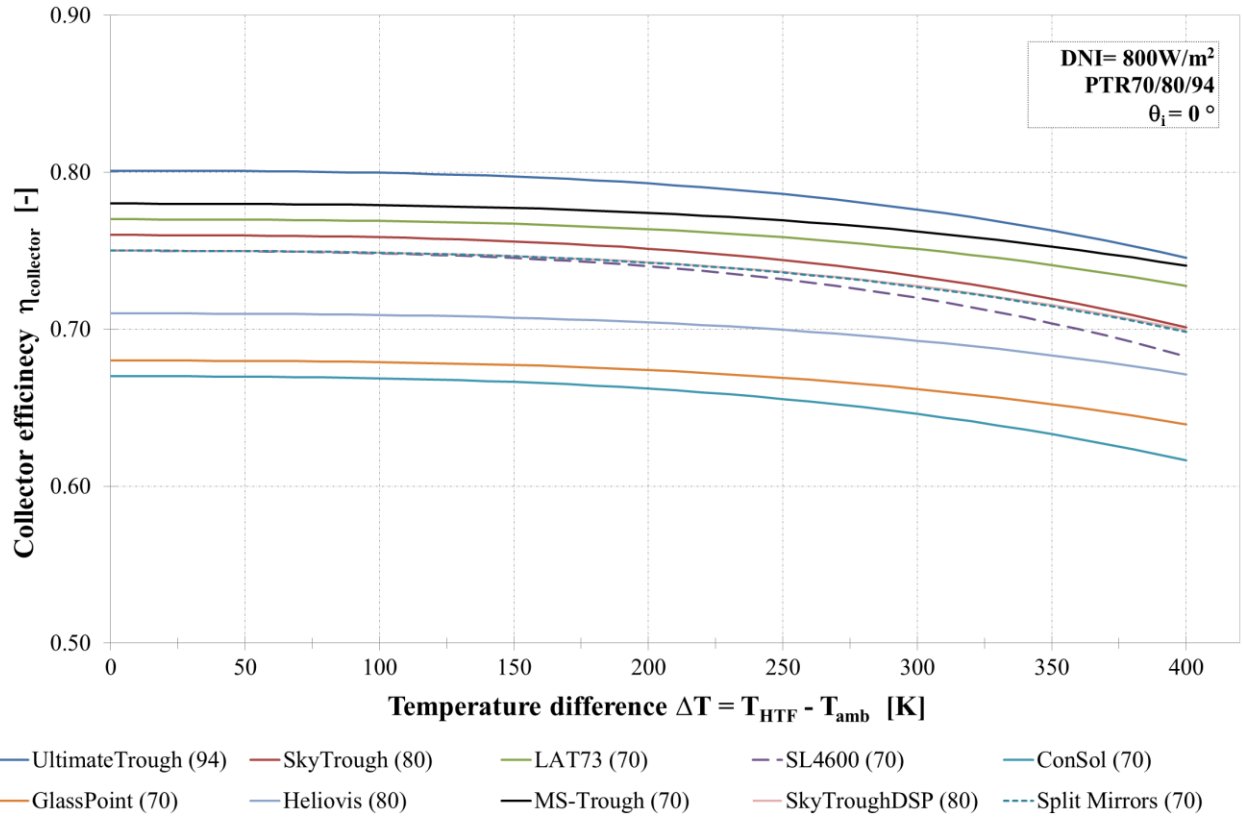


Figure 42 Performance comparison of different PTC loops with Thermo-Oil as HTF

Table 13. Simulation results of different PTC loops and relevant parameters for the computation with Thermo-Oil as HTF

Collector with VP-1 as HTF			<div style="display: flex; justify-content: space-around; font-size: small;"> <span>Euro Trough</span> <span>Ultimate Trough</span> <span>SkyTrough</span> <span>SkyTrough DSP</span> <span>LAT73</span> <span>SL4600</span> <span>ConSol</span> <span>GlassPoint</span> <span>Heliovis</span> <span>Split Mirrors</span> <span>MS-Trough (600)</span> </div>										
			600	960	460	592	576	720	576	360	440	576	600
<b>a<sub>col</sub></b>	Aperture width	m	5.77	7.51	6.00	7.00	7.30	4.60	5.77	7.64	8.00	6.00	7.80
<b>L<sub>Loop</sub></b>	Loop length	m	600	960	460	592	576	720	576	360	440	576	600
<b>Ød<sub>abs</sub></b>	Absorber diameter	m	0.07	0.094	0.08	0.08	0.07	0.07	0.07	0.07	0.07	0.08	0.07
<b>η<sub>optical</sub></b>	peak optical efficiency	-	0.75	0.801	0.76	0.75	0.77	0.75	0.67	0.68	0.71	0.75	0.78
<b>m<sub>Design</sub></b>	Mass flow at Loop design	kg/s	7.62	16.40	5.90	8.86	9.30	6.97	6.30	5.35	6.80	7.40	10.50
<b>Q<sub>loss</sub></b>	Thermal Loss per Loop	MW <sub>th</sub>	0.10	0.22	0.09	0.11	0.15	0.12	0.10	0.06	0.08	0.10	0.10
<b>Q<sub>solar</sub></b>	Solar Thermal Power	MW <sub>th</sub>	2.04	4.40	1.58	2.38	2.50	1.87	1.69	1.44	1.82	1.99	2.82
<b>Q<sub>eff</sub></b>	Effective Thermal Energy	MW <sub>th</sub>	1.94	4.18	1.49	2.26	2.34	1.75	1.59	1.38	1.74	1.89	2.72
<b>Q<sub>loss</sub> ÷ Q<sub>solar</sub></b>	Losses for each MW thermal power	%	4.9%	4.9%	5.6%	4.8%	6.0%	6.5%	5.7%	4.2%	4.4%	4.9%	3.6%
<b>η<sub>th</sub></b>	Thermal Efficiency	-	0.74	0.76	0.72	0.72	0.73	0.70	0.63	0.65	0.68	0.72	0.75
<b>η<sub>global</sub></b>	Global Efficiency (Carnot factor = 0.52)	%	0.38	0.40	0.37	0.37	0.38	0.37	0.33	0.34	0.35	0.37	0.39

### Thermal scenario 2.2: Thermal power & performance with Molten Salt

This scenario only deals with collectors designed for operation with molten salts. The comparison follows the same format as in “Thermal scenario 2.1”, yet considering operational solar field outlet temperatures at  $T_{SF,out}=550^{\circ}\text{C}$ . Two collectors are adapted for the comparison as follows:

- **UltimateTrough:** Operational conditions for Molten Salt have been simulated in a previous study to optimize its performance. The computed parameters are based on them, regarding the receiver diameter to  $\varnothing 70\text{mm}$  and subsequently the optical efficiency of 75.5% [9].
- **MS-Trough:** Once operating with salt the previous modification for “thermal scenario 2.1” is no longer required. The collector length is at 800 m as designed.

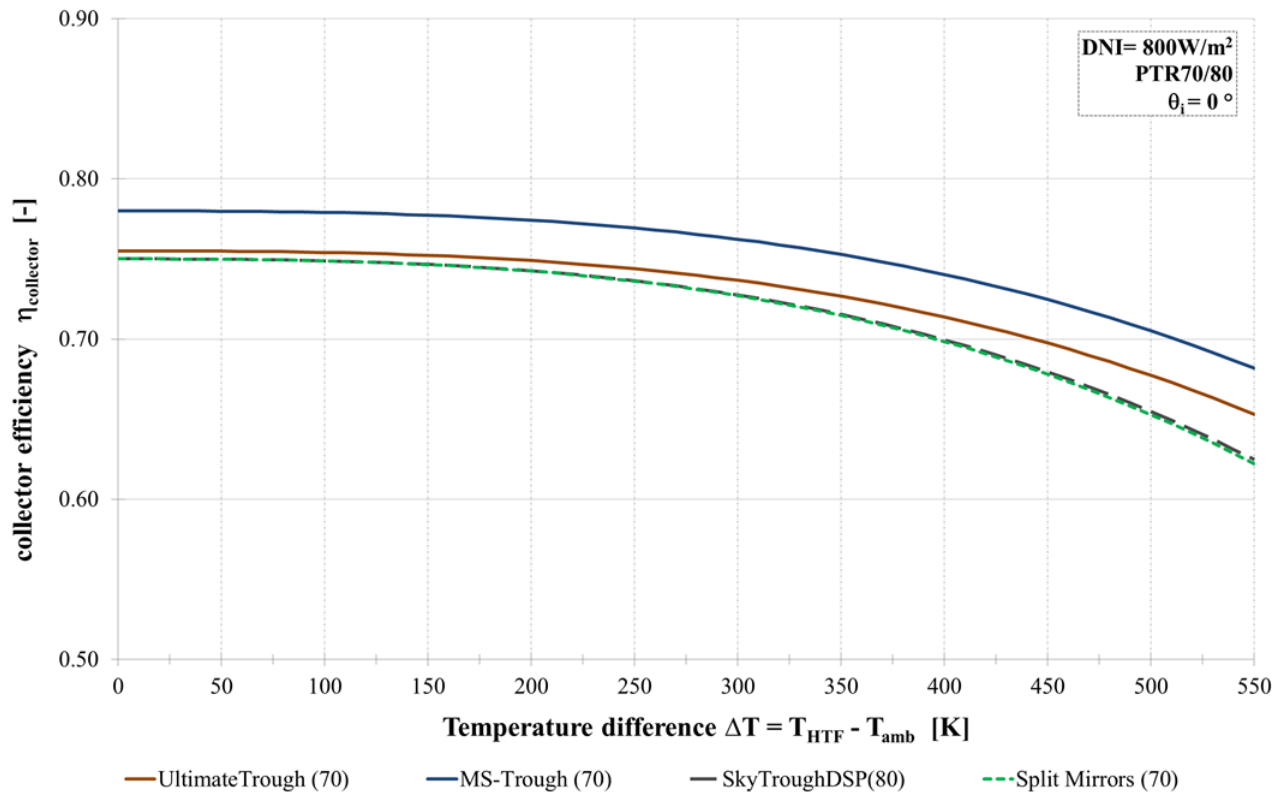


**Figure 43** Performance comparison of different PTC loops with Molten Salt as HTF

Figure 43 shows the collector performance curves of the four collectors. The parameters show a higher overall performance of the MS-Trough collector with an optical efficiency difference of

3.2% higher than the UltimateTrough and 3.8% to the SkyFuelDSP and Split Mirrors. In the thermal performance at 550°C, the MS-Trough shows also higher results than the UltimateTrough, SkyFuelDSP and Split Mirrors by 4.3%, 5.8% and 7.4% respectively.

The computed parameters and the thermal power values are shown in Table 14. The UltimateTrough has a higher thermal power output compared to the other collectors. Yet it shows a 7.4% portion of losses related to the gained thermal power. The SkyFuelDSP lost 9.4% and the Split Mirrors 9.6%. The difference between the MS-Trough and the UltimateTrough is marked by only a 0.5%.

**Table 14.** Simulation results of different parabolic trough collector loops and relevant parameters for the computation with Molten Salt as heat transfer fluid

Collector with Molten Salt as HTF						
		Ultimate Trough	SkyTrough DSP	Split Mirrors	MS-Trough (800)	
$a_{col}$	Aperture width	m	7.51	7.00	6.00	7.80
$L_{Loop}$	Loop length	m	960	592	576	800
$\varnothing d_{abs}$	Absorber diameter	m	0.07	0.08	0.07	0.07
$\eta_{optical}$	peak optical efficiency	-	0.76	0.75	0.75	0.78
$\dot{m}_{Design}$	Mass flow at Loop design	kg/s	10.30	5.78	4.80	9.25
$Q_{loss}$	Thermal Loss per Loop	MW <sub>th</sub>	0.30	0.21	0.18	0.25
$Q_{solar}$	Solar Thermal Power	MW <sub>th</sub>	4.06	2.28	1.89	3.64
$Q_{eff}$	Effective Thermal Energy	MW <sub>th</sub>	3.76	2.06	1.71	3.39
$Q_{loss} \div Q_{solar}$	Losses for each MW thermal power	%	7.4%	9.4%	9.6%	6.9%
$\eta_{th}$	Thermal Efficiency	-	0.70	0.69	0.68	0.73
$\eta_{global}$	Global Efficiency (Carnot factor = 0.61)		0.43	0.42	0.42	0.44

The optical efficiency seems to be decisive on the results for molten salts, but also for thermo-oils, where the UltimateTrough outperformed the other collectors. There are only few collectors suited for molten salts applications, but they come to a competitive thermal efficiency ranging of 73% and 69% at 550°C.

### 4.1.3 Parasitic Consumption

Departing from the previous scenarios for the thermal performance estimation 2.1 and 2.2, it is possible to study the electric parasitic consumption. Here only the electric consumption by the heat transfer fluid pump in the solar field is calculated. The aim is to find out, if there is an effect of this criterion, when thermo-oils or molten salts are applied as heat transfer fluid.

Other power consumers like ventilators, valves and BOP pumps for instance, are not included. The power for tracking and control can be considered constant over the day. Thus, fixed aperture area specific base load values are considered such as 0.25-0.3 W/m<sup>2</sup> [34].

The electric consumption of the heat transfer fluid pumps ranges between 0.8 and 0.9<sup>12</sup> and it can be estimated in dependence of the following parameters [34]:

$$P_{HTF} = \frac{\dot{V}_{HTF} \cdot \Delta p_{HTF}}{\eta_{pump}} \quad (20)$$

$P_{HTF}$ : electric power consumption [W]                       $\Delta p_{HTF}$ : pressure loss of the solar field [bar]  
 $\dot{V}_{HTF}$ : volumetric flow of heat transfer fluid [m<sup>3</sup>/h]                       $\eta_{pump}$ : pump efficiency [-]

Considering as well the mean density of the fluid, the volumetric flow is written also as follows:

$$\dot{V} = \frac{\dot{m}_{Design}}{\rho_{mean}} = \frac{\dot{Q}_{SF}}{\rho_{mean} \cdot c_p \cdot \Delta T_{HTF}} \quad (21)$$

$\dot{V}$ : volumetric flow [m<sup>3</sup>/h]                       $\dot{Q}_{SF}$ : thermal energy from solar field [W]  
 $\dot{m}_{Design}$ : mass flow at design [kg/s]                       $c_p$ : heat capacity factor [J/kg·K]  
 $\rho_{mean}$ : mean density [kg/m<sup>3</sup>]                       $\Delta T_{HTF}$ : inlet and outlet temperature difference [K]

For the example only the pressure drop over the loop will be simulated, which decreases over the receivers, cross-over pipelines, ball-joints and 90° elbows, until the pipelines to the hot head. Since the simulation for each collector requires a certain study on how the loop is deployed and on the number of interconnection elements, a common design is considered as shown in the Figure 44. A EuroTrough loop is set as standard case and only those collectors following this format are evaluated under these conditions, namely the: UltimateTrough, SkyFuel, SkyFuelDSP, LAT73, SL4600+ and ConSol collectors.

---

<sup>12</sup> Depends on supplier

GlassPoint, Heliomis, Split Mirrors and MS-Trough implement their specific format. In all of them, elements like ball joints are due to their concept design not required.

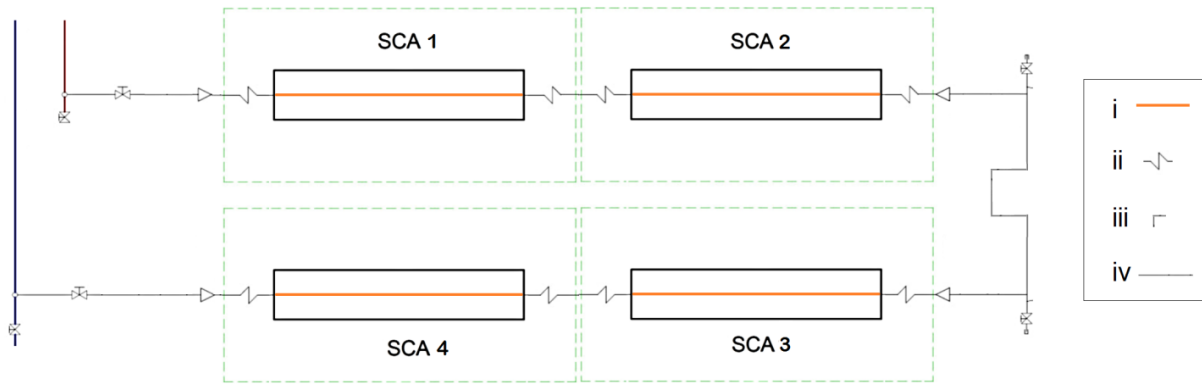


**Figure 44** Scheme of a conventional loop. (i) Receiver piping, (ii) cross-over piping with ball-joints, (iii) 90°-elbows and (iv)

In the scheme straight tubes as (i) and (iv) are differentiated since they normally differ in diameter and material. Number (ii) considers the cross-over pipes between solar collector assemblies, for instance, as previously illustrated in Figure 30. This section is composed of a combination of straight tubes, ball-joints and 90° elbows. As the turbulent streaming flows through this straight tubes and obstacles, the pump has to compensate the caused pressure drop  $\Delta p$  at the expense of the parasitic electric consumption. The total pressure drop of the loop is here defined as:

$$\Delta p = \Delta p_{receiver} + \Delta p_{crossover} + \Delta p_{obstacle} \quad (22)$$

$\Delta p$ : overall pressure drop [bar]                       $\Delta p_{crossover}$ : pressure drop in the crossover-sections [bar]  
 $\Delta p_{receiver}$ : pressure drop in the receivers [bar]                       $\Delta p_{obstacle}$ : pressure drop in ball-joints or elbows [bar]

Where the pressure drops due to the straight receiver tubes (i)  $\Delta p_{receiver}$  is given as:

$$\Delta p_{receiver} = \lambda \cdot \frac{8 \cdot L \cdot \dot{m}^2}{d^5 \cdot \pi^2 \cdot \rho} \quad (23)$$

$\lambda$ : friction coefficient, turbulent stream [-]                       $d$ : tube's inner diameter [m]  
 $L$ : tube's length [m]                       $\rho$ : mean density of the fluid [kg/m<sup>3</sup>]  
 $\dot{m}$ : mass flow at design [kg/s]

Here  $\lambda = 0.015$  is the friction coefficient for a turbulent stream,  $L$  the total receiver length and  $d$  the receiver inner tube diameter. Also due to the aforementioned obstacles (ii) and (iii) the following equation is valid for a single obstacle:

$$\Delta p_{obstacle} = \frac{\xi_{90^\circ} \cdot 8 \cdot \dot{m}^2}{d^4 \cdot \pi^2 \cdot \rho} \quad (*13) \quad (24)$$

Here  $\xi_{90^\circ} = 0.35$  is the pressure loss coefficient and  $d$  the inner tube diameter of the cross-over pipeline. For the study pressure losses at the ball joint are assumed as equal as the  $90^\circ$  elbows to apply this equation.

For the situation of the elements in (iii), the Eq. (23) and Eq. (24) need to be added. The length  $L$  and the inner diameter  $d$  are now those of the cross-over pipes:

$$\Delta p_{crossover} + \Delta p_{obstacle} = \left( n \cdot \xi_{90^\circ} + \frac{\lambda \cdot L}{d} \right) \frac{8 \cdot \dot{m}^2}{d^4 \cdot \pi^2 \cdot \rho} \quad (*13) \quad (25)$$

The  $n$  corresponds to the number of ball-joints and  $90^\circ$  elbows. The value of  $\lambda$  is generalized for the cases.

Finally it is necessary to convert the thermal-to-electric power gained by the simulated loops to estimate the parasitic consumption in relation to the produced power. Here the effective thermal output  $\dot{Q}_{eff}$  is multiplied by the efficiency factor of the solar power plant  $\eta_{SP}$  given between 0.36 and 0.38:

$$P_{el} = \dot{Q}_{eff} \cdot \eta_{SP} \quad (26)$$

$P_{el}$ : thermal-to-electric power [ $W_{el}$ ]

$\eta_{SP}$ : solar field's efficiency [-]

$\dot{Q}_{eff}$ : effective thermal energy [ $W_{th}$ ]

The portion of electric power for self-consumption of the plant can be described as follows:

$$P_{parasitic} = \frac{P_{HTF}}{P_{el}} \quad (27)$$

$P_{parasitic}$ : parasitic power consumption [%]

$P_{HTF}$ : parasitic power consumption of the heat transfer fluid's pump [ $W_{el}$ ]

$P_{el}$ : thermal-to-electric power [ $W_{el}$ ]

\*13 For Eq.(24).-Eq.(25) same units and descriptions are use as in Eq.(22). - Eq.(23)

## Results

The results on Table 15 describe the scenario for the parasitic consumption of the heat transfer fluid pump. Since the collectors are evaluated at design mass flow, higher mass flow also results in higher pump parasitic consumption  $P_{HTF}$ . This scenario is highly variable, as real power plants count with a designed pressure drop of about 10 bar to 14 bar, which in operation may be influenced by the design of the piping's and interconnection elements. Also the length of the collector influences significantly the value for the pressure drop on the receiver  $\Delta p_{receiver}$  significantly. This can be seen in the case of SkyFuel ( $L_{loop}=460$  m) vs. the LAT73 ( $L_{loop}=576$  m) or even the UltimateTrough ( $L_{loop}=960$  m).

The assumed length modification of 600 m instead of 800 m for the MS-Trough exemplifies this behaviour, which results in an increased pressure drop from 8.4 bar to 19.9 bar (42% difference) on the straight receiver tubes by just varying the length of the receiver tube. A possible alternative to reduce the pressure drop are also tubes with greater diameters, as can be seen from Eq.(23) to Eq.(25).

**Table 15.** Parasitic power consumption due to the HTF pump of the solar field with Thermo-Oil as HTF

			Euro Trough	Ultimate Trough	SkyTrough	SkyTrough DSP	LAT73	SLA600	ConSol	GlassPoint	Heliovis	Split Mirrors	MS-Trough (800)	MS-Trough (600)	
<b>Pressure Drop with VP-1 as HTF</b>															
$\Delta p_{receiver}$	Pressure drop on receiver tubes	bar	4.4	6.9	1.0	2.9	6.3	4.4	2.9	1.3	1.3	4.0	8.4	19.9	
$\Delta p_{crossover} + \Delta p_{obstacles}$	Pressure loss on crossover pipes and obstacles	bar	3.4	2.9	0.9	2.2	5.2	2.7	2.3	0.3	0.4	0.7	0.2	0.4	
$\Sigma \Delta p$	Total preassure loss per loop	bar	7.8	9.9	1.9	5.1	11.5	7.2	5.2	1.6	1.7	4.7	8.6	20.3	
<b>Parasitic Consumption</b>															
$P_{HTF}$	Electric power consumption of the HTF pump	kW <sub>el</sub>	9.8	26.4	1.9	7.3	17.4	8.2	5.3	1.4	1.9	5.7	14.8	46.3	
$P_{el}$	Thermal-to-electric power	MW <sub>el</sub>	0.70	1.51	0.54	0.81	0.84	0.63	0.57	0.50	0.63	0.68	0.98	1.27	
$P_{parasitic}$	Parasitic Power consumption due to HTF pumping	%	1.4%	1.8%	0.3%	0.9%	2.1%	1.3%	0.9%	0.3%	0.3%	0.8%	1.5%	3.7%	

In the case of the MS-Trough, GlassPoint and Split Mirrors, the absence of ball joints rectifies lead to lower pressure losses ranging from 0.7 and 0.2 bar. Compared to that, other collectors show a pressure drop between 5.2 and 0.9, for the computed loop conditions.

For the scenario with molten salts as heat transfer fluid Table 16 shows the results. The SkyTroughDSP and the Split Mirrors collectors require the lowest mass flow as presented in Table 14. These collectors have also the shortest collector loops compared to the UltimateTrough and the MS-Trough, which is the main reason for their low parasitic consumption. All four collectors represent s an evident enhancement on the pressure losses, and subsequently on the parasitic consumption. The main reason for this is the implementation of molten salts as compared in Figure 45.

**Table 16.** Parasitic power consumption due to the HTF pump of the solar field with molten salt as HTF

			Ultimate Trough	SkyTrough DSP	Split Mirrors	MS-Trough (800)
<b>Pressure Drop with Molten Salt as HTF</b>						
$\Delta p_{\text{receiver}}$	Pressure drop on receiver tubes	bar	5.4	0.5	0.7	3.6
$\Delta p_{\text{crossover}} + \Delta p_{\text{obstacles}}$	Pressure loss on cross-over pipes and obstacles	bar	2.7	0.4	0.1	0.1
$\Sigma \Delta p$	Total preassure loss per loop	bar	8.1	1.4	0.8	3.7
<b>Parasitic Consumption</b>						
$P_{\text{HTF}}$	Electric power consumption of the HTF pump	kW <sub>el</sub>	5.7	0.5	0.2	2.4
$P_{\text{el}}$	Thermal-to-electric power	MW <sub>el</sub>	1.35	0.74	0.62	1.22
$P_{\text{parasitic}}$	Parastic Power consumption due to HTF pumping	%	0.42%	0.06%	0.03%	0.19%

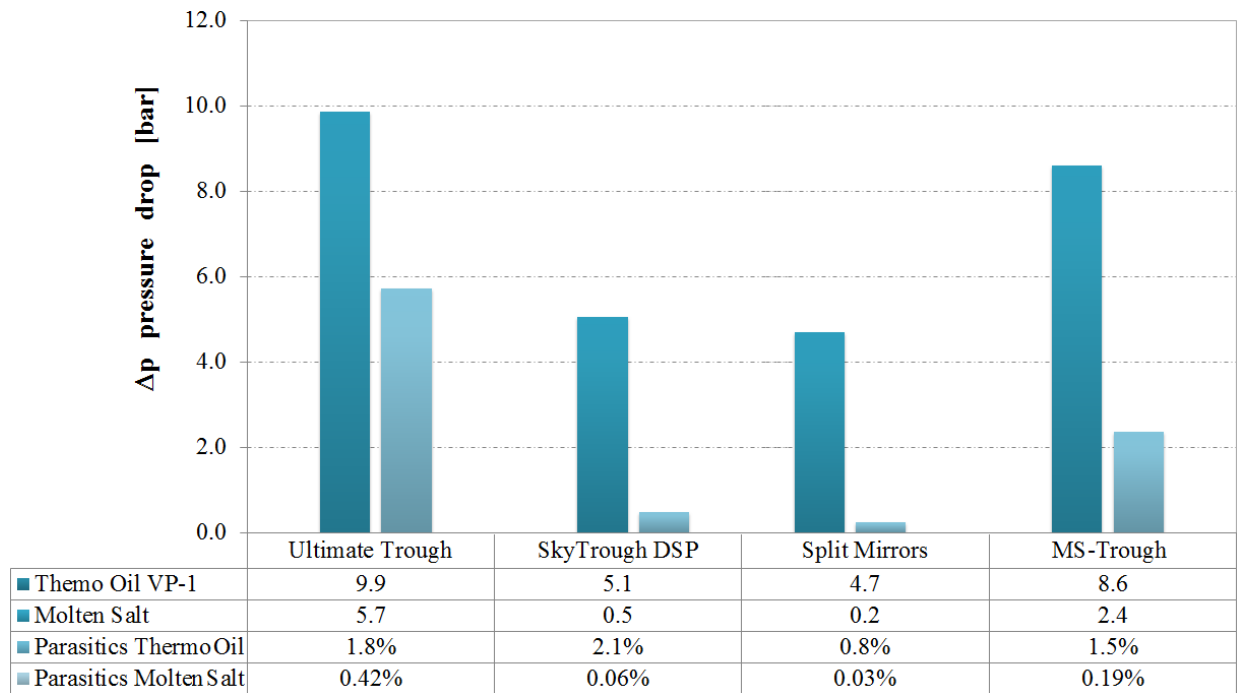


**Figure 45** Pressure drop and parasitic consumption of different PTC loops with Thermo-Oil (VP-1) VS. Molten Salt as HTF

#### 4.1.4 Global Efficiency by Heat Transfer Fluid

The analysis on the heat transfer fluid is not only necessary to underline the potential of molten salts vs. thermo-oil collectors to enhance the solar power plant's performance, but also to point out technical challenges. Thermo-oils are state of the art, for which 38% efficiency of the power block can currently be attained. A conversion efficiency to up to 43.3% is achievable with the implementation of molten salts as heat transfer fluid [9].

As the UltimateTrough and the MS-Trough were the collectors outperforming the others in both scenarios, only these are chosen for the following example. To characterize the global (or maximal theoretical thermal-to-mechanical) efficiency, the Carnot efficiency  $\eta_{carnot}$  is necessary to introduce. This theorem derived from the second law of thermodynamics, describes the rate of thermal energy that can theoretically maximal be converted into work (see Eq.(4)).

$$\eta_{global} = \eta_{carnot} \cdot \eta_{col} \quad (28)$$

$\eta_{global}$ : global efficiency of power plant [-]                       $\eta_{col}$ : collector efficiency [-]  
 $\eta_{carnot}$ : Carnot efficiency [-]

The study now allocates in the power block, where the highest temperature of the cycle is defined by the thermal exchange from the solar field. For both thermo-oil and molten salt an ideal thermal exchange from the solar field to the power block is assumed. Therefore the respective operational temperatures  $T_{high}$  of the fluid are considered, which are for thermo-oils 400°C (673K) and for molten salt 550°C (823K)<sup>14</sup>. In both cases the lowest temperature  $T_L$  of the Rankine cycle at 50°C (323K) is supposed [34].

**Table 17.** Collector efficiencies with Thermo-Oil and Molten Salt as heat transfer fluid

Collector	$\eta_{col}$	$\eta_{carnot}$	$\eta_{global}$	HTF	$T_{high}$
UltimateTrough	74.6%	52.0%	38.8%	Thermo-Oil	400 °C
	65.3%	60.8%	39.7%	Molten Salt	550 °C
MS-Trough	74.0%	52.0%	38.5%	Thermo-Oil	673 K
	68.2%	60.8%	41.4%	Molten Salt	823 K

<sup>14</sup> A thermal stability for molten salts at 565°C has been demonstrated [28]

Table 17 contains the results that characterize the global efficiency of the power plant. The MS-Trough with 41.4% reaches a greater outcome once operating with molten salts in comparison to the UltimateTrough with 39.7%, by a difference of 1.7%. These values are in fact a demonstration of the improvement of the global efficiency with molten vs. thermo-oils, where the highest global efficiency is achieved by the UltimateTrough with 38.8%. To complement the overview of this study Figure 46 shows the different curves.

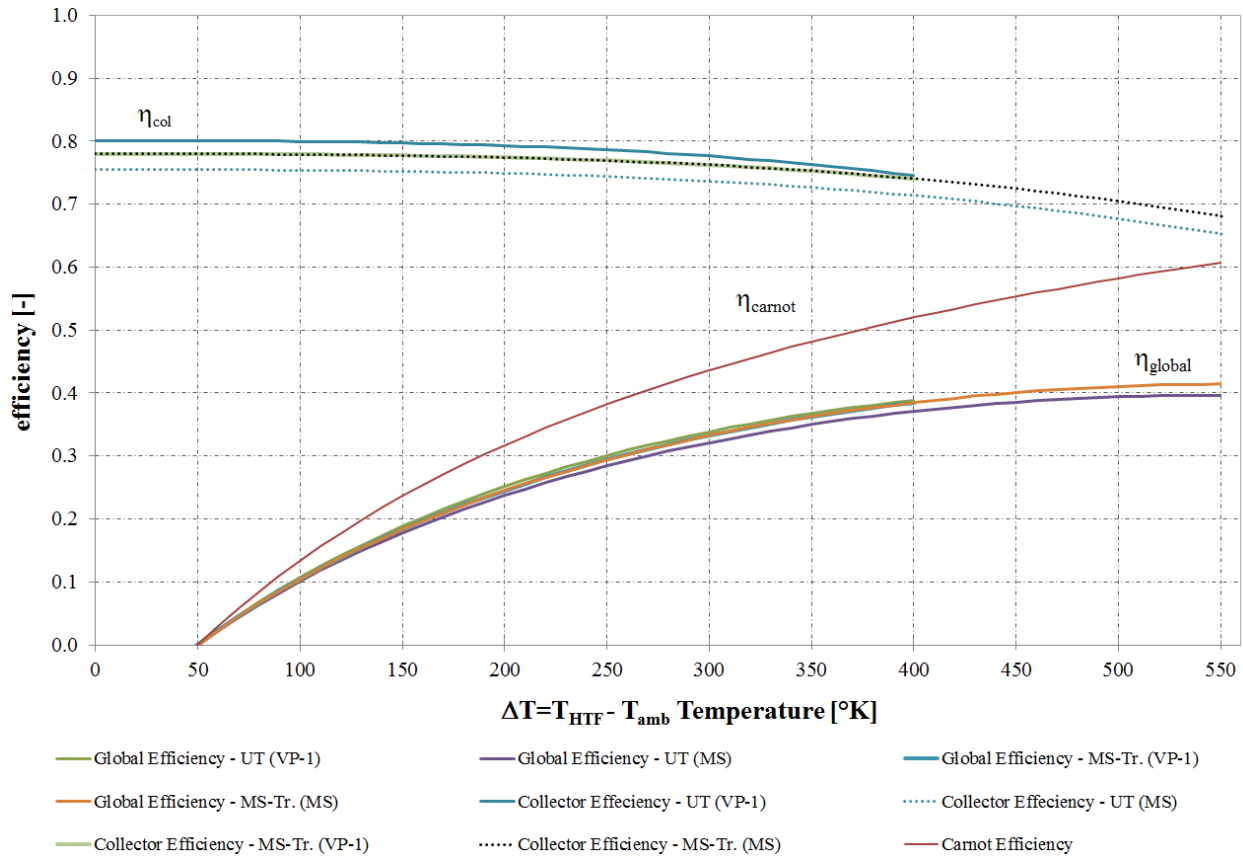


**Figure 46** Global conversion efficiency at the example of the UltimateTrough and MS-Trough with Thermo-Oil and Molten Salt

The collector efficiency curves are taken from the thermal scenarios 2.1 and 2.2 as mentioned before and global efficiency is estimated according to Eq. (31).

Looking at these results, molten salts have the potential to improve the overall performance of the power plant. There are still more aspects, supporting, but also limiting its application. The state of the art solar salt 60%  $\text{NaNO}_3$  + 40%  $\text{KNO}_3$  has a freezing temperature at  $223^\circ\text{C}$  and a solar field freeze protection temperature at  $272^\circ\text{C}$ . Compared to that, thermo-oils remain in a liquid state to up to  $12^\circ\text{C}$  and require a solar field freeze protection at  $62^\circ\text{C}$  [9].

Molten salt solar fields require a constant higher thermal state to avoid the solidification of the salt in the pipelines, including receivers and cross-over elements. Thus the requirements on the piping material, isolation material and antifreeze heating system are also higher and therefore higher in cost. The piping needs to be first made of stainless steel as a corrosion resistant material and secondly, it should be fully equipped, for instance, with induction heaters trough the kilometers of piping on the solar field. Also the heating of movable components i.e. ball-joints or swivel joints, comprehend on a cost intensive character. (This will be discussed in the next section).

It represents indeed a high risk to implement molten salt as heat transfer fluid in the solar field for which the reliability of the fluid has been proven, yet not as satisfactory as thermo-oil<sup>15</sup>. Although experiments have demonstrated the feasibility of a melting reaction system through induction, in case the salt solidifies<sup>16</sup>. Furthermore adapted solar field formats are suited to prevent this from happening with new operating strategies for molten salt [31].

---

<sup>15</sup> See Archimede Solar Energy

<sup>16</sup> See Novatec Puerto Errado demonstration for Linear Fresnel collectors

### 4.1.5 Costs Scenario

In a parabolic trough power plant the capital cost of the solar field amounts about 31% with a 7.5 hours storage system that adds further 11% to the total costs as described for the Andasol plant in Spain. In the solar field the costs of the heat transfer fluid (approx. 5% to 8%) are excluded, yet it is included in the storage block [8]. This means that the parabolic trough collectors and the supplementary operational equipment (e.g. drives, pylons, electric components, inter loop piping...), plus the header piping, among others, are carriers of one third of the costs of the solar plant.

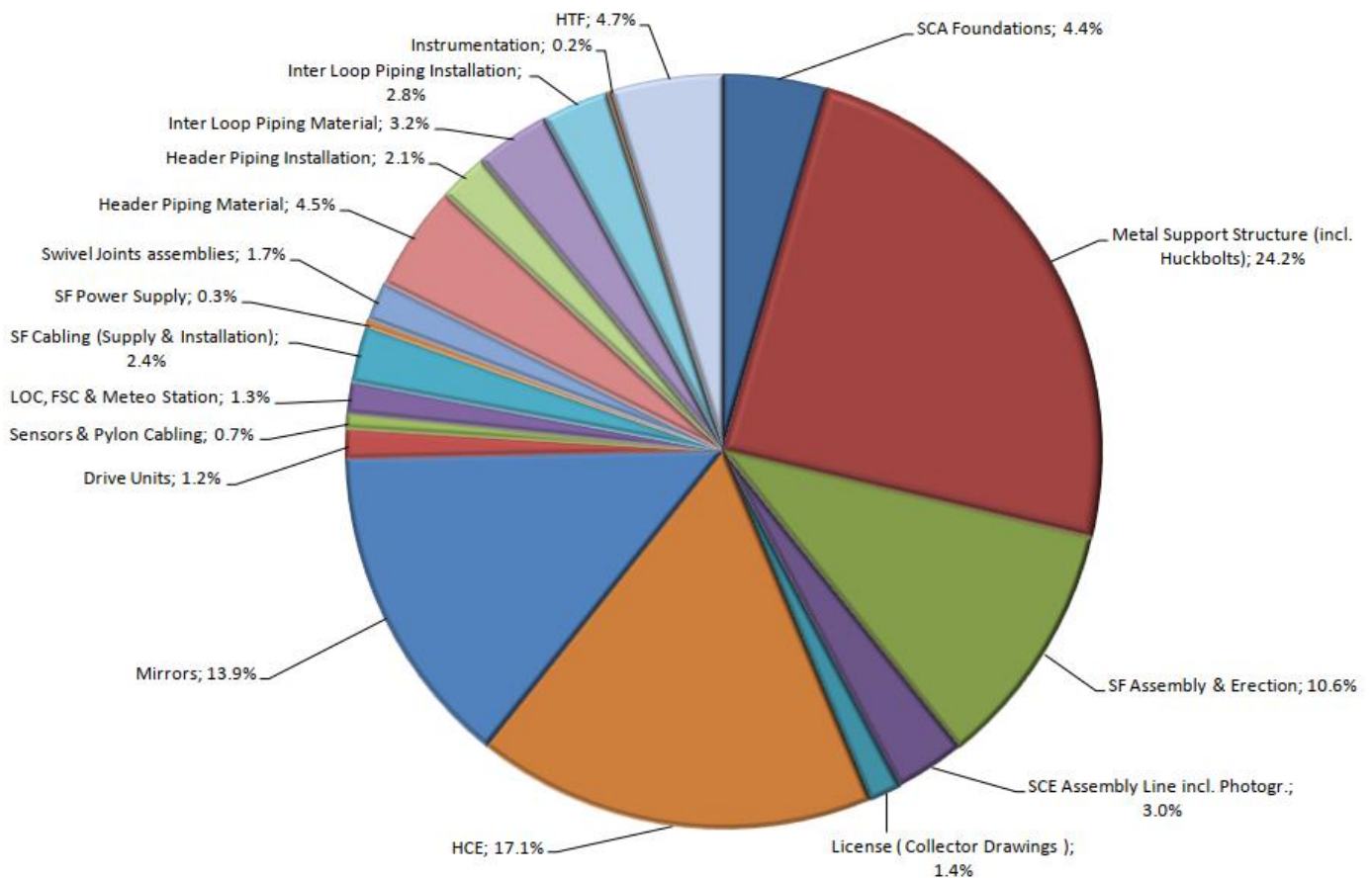


Figure 47 Solar Field cost of Andasol I (50 MW) power plant with EuroTrough collectors [49]

The graphic refers to the construction of Andasol 1 and represents the percentage of all components of the total construction costs. As can be seen in Figure 47, the collector costs are implicit, but with a breakdown of the single elements such as mirrors, heat collector elements

and metal support structure. Even the assembly line and photogrammetry verification are included.

On a solar field with molten salts as heat transfer fluid other requirements are established, for example, the use of additional extensive heat tracing systems and other materials (e.g. stainless steel piping for corrosion resistance). This causes an increase of the solar field costs, but on the other hand significant reductions on the storage and adjacent blocks. The application of the same transfer fluid in the solar field and storage system enables a more effective use of the higher temperature difference between the two tanks, increasing the capacity of their given volume [9].

**Table 18.** Case study of thermo-oil vs. molten salt power plant with EuroTrough (ET) and UltimateTrough (UT) collectors [9]

Case ID		ET 50MWe VP-1 at 393°C Daggett	UT 50MWe VP-1 at 393°C Daggett	UT 100MWe SSe at 550°C Daggett
Civil works	€/m <sup>2</sup>	20	20	20
Solar field specific cost	€/m <sup>2</sup>	228	198	210
Power block / HTF system / BOP	€/kW <sub>e</sub>	1.286	1.286	973
Thermal energy storage	€/kWh <sub>th</sub>	45	45	16

As presented in Table 18 the specific cost of thermal storage would be reduced by almost a factor of three.

The present study on the costs contains a rough estimate overview of the solar field specific costs for the collectors, sometimes departing from manufacturers' specifications and others by argumentations or case studies. The analysis of these collectors presents practical boundaries that need to be established. One reason is the limitation of information and secondly because in most of the cases no solar field has been deployed yet except in theoretical studies. Therefore the cost analysis will highlight some differences compared to the later drawn baselines of the conventional EuroTrough and UltimateTrough collectors. Despite this fact, there is the advantage that manufactures also departure from a common reference regarding the specific solar field cost of a given collector, which is the current baseline at 230 €/m<sup>2</sup>. This enables a qualitative presentation of the collectors endorsed by the given sources.

The diagram in Figure 48 presents the results of the study focused on the two baselines. First, Baseline 1 is represented by the value of the EuroTrough as the known conventional collector,

which operates with thermo-oil as HTF. The solar field costs of the UltimateTrough were previously estimated with a cost reduction of -23% vs. the EuroTrough, due to the scaling of the aperture and reduction of elements [45]. This was later rectified in a case study by the manufacturers with only 14% reduction, thus deferring from the starting calculations by 9% [9]. The numbers here are a 'static' representation and do not consider material price fluctuations.

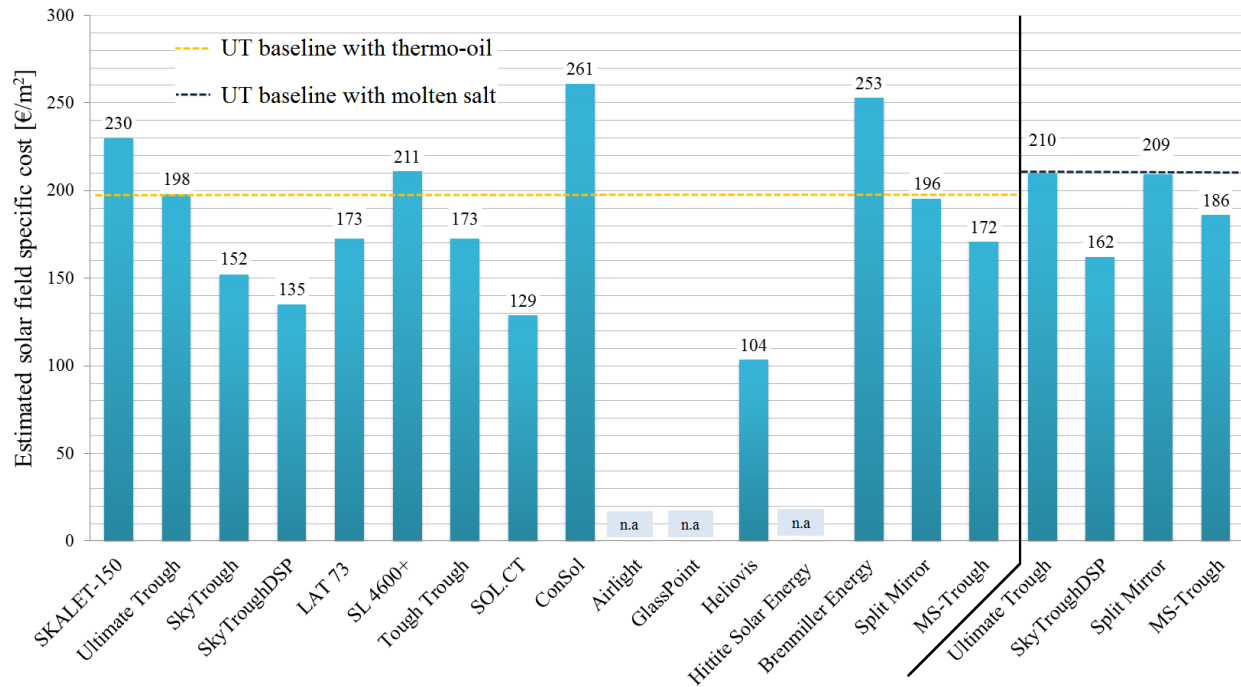


**Figure 48** Specific solar field cost estimate for different parabolic trough collectors. Supplement Table 19.

A comparison study between the UltimateTrough and SkyFuel collector, points out the sensibility of the collector price just depending on variations of the aluminum alloys. Thus a SkyFuel collector solar field could amount 152 €/m<sup>2</sup> for an aluminum alloy cost of 2.04 €/kg, while the cost would increase to 187 €/m<sup>2</sup> for an alloy price of 3.36 €/kg [58]<sup>17</sup>. This represents about 19% increase of the total costs. Therefore, with the acknowledgement of this scenario, it is to understand that given numbers could also be influenced by this effect.

Baseline 2 is introduced to differentiate those collectors operating with molten salts as heat transfer fluid. Aforementioned requirements include the material selection and the auxiliary pipe-heating system. Structural steel is holding somewhere between 0.6 €/kg to 1.6 €/kg, while stainless steel is at least around 5.9 €/kg [59]. This specially affects interconnection piping and

<sup>17</sup> Currency conversion (22.04.2019): 1 \$ ⇔ 0.89 €

ball joint elements. In the case of a EuroTrough solar field the cost for the ball joints are valued at 3.6 €/m<sup>2</sup> [18]. Considering a 44% reduction of these elements in a solar field with UltimateTrough collectors, 1.6 €/m<sup>2</sup> are estimated. In the case of molten salts the price of the stainless steel ball joints would raise at least to 5.8 €/m<sup>2</sup>. The heat transfer fluid itself represents also a cost reduction, where a solar salt type Hitec® approximately amounts 1.34 €/kg compared to 4.01 €/kg of a synthetic oil [60].

**Table 19.** Specific solar field cost estimation with different parabolic trough collectors

Category/Collector	Solar Field Costs [€/m <sup>2</sup> ]	Estimated difference to Baseline 1	Category/Collector	Solar Field Costs [€/m <sup>2</sup> ]	Estimated difference to Baseline 1	Category/Collector	Solar Field Costs [€/m <sup>2</sup> ]	Estimated difference to Baseline 2
<i>Thermo-Oil as Heat Transfer Fluid</i>			<i>Thermo-Oil as Heat Transfer Fluid</i>			<i>Molten Salt as Heat Transfer Fluid</i>		
A	SKALET-150	230	D	Airlight	n.a.	A	Ultimate Trough	210
	UltimateTrough	198		GlassPoint	n.a.	B	SkyTroughDSP	162
B	SkyTrough	152	E	Heliovis	104	E	Split Mirror	209
	SkyTroughDSP	135		Hittite Solar Energy	n.a.		MS-Trough	186
	LAT 73	173		Brenmiller Energy	253			
C	SL 4600+	211	E	Split Mirror	196			
	Tough Trough	173		MS-Trough	172			
	SOL.CT	129						
	ConSol	261						

Sources Table 19: [55]<sup>1</sup>, [9]<sup>2</sup>, [58]<sup>3</sup>, [61]<sup>4</sup>, [18]<sup>5</sup>, [62]<sup>6</sup>, [63]<sup>7</sup>, [18]<sup>8</sup>, [54]<sup>9</sup>, [64]<sup>10</sup>

Complement for Table 19, baseline 1: Thermo-Oil as heat transfer fluid

- \* **SkyTroughDSP.** This collector is a scaled generation of the previous SkyTrough with 30% larger dimensions. When scaling the EuroTrough to the UltimateTrough 40% larger dimensions were reached. It meant a 50% reduction of components in the solar field and finally decreased the costs to 14%. The estimation for SkyTroughDSP result therefore in analogy to that case in 11% less costs than the SkyTrough.
- \* **SOL.CT vs. ConSol.** While the Sol.CT concrete collector waits for the first demonstration the ConSol collector was built and evaluated. The last aimed significant cost reduction is due to the implementation of concrete. The manufacturing, transportation and assembly adjustments demonstrated, nevertheless, a total increase of 13% to baseline 1. The Sol.CT concept suggests a similar approach for which the manufacturer assures a 40% reduction to

the baseline 1. The potential of implementing concrete for the whole structure is feasible, but it requires further research.

- \* **Airlight.** The information is not available. A hypothesis based on the ConSol experience, leads to the assumption that the cost must be significantly higher than the baseline of the EuroTrough. The massive structure requires as well steel materials and the mechanical tracking system a series of robust drive components.
- \* **GlassPoint.** The information is not available. To encounter an estimate first the evident 6 m high greenhouse glass should be considered, multiplied by the number of implemented modules. Also the simplification of the tracking and bearing system can mean a reduction, but the lightweight application of the honeycomb aluminum based parabolic concentrators, might raise the price again. An assumption is that the costs represent a higher value than the baseline 1.
- \* **Heliovis.** Presents the lowest costs, with a reduction of the solar field by 55% according to the manufacturer [54]. Main drivers are the obviation of glass facets and rather the use of polymeric membranes. The estimation of this difference is debatable since the collector utilizes a significant amount of steel for its ring structure and uses as well around 10 single drives per collector. Additional auxiliary photovoltaic structures are integrated as well as wind and dust fences.
- \* **Brenmiller.** An estimate for this collector was made considering the proposed metallic structure and implementation of glass facets. The cost estimation compared to a EuroTrough is seems slightly higher, mainly because each solar collector element needs a single drive. Furthermore the railing based structure to avoid ground works, means another significant use of metallic frames increasing the field's costs. But the elimination of ball-joints and flexible elements implies also a reduction.

Complement for Table 19, baseline 2: Molten Salt as heat transfer fluid

- \* **UltimateTrough.** An increase of 12 €/m<sup>2</sup> can be seen from the UltimateTrough baseline 1 to baseline 2, corresponding on a 10% increase of the costs. The authors of the estimate, sum up in this value the heat tracing system and the stainless steel materials for a doubled in sizes solar field [9]. It is also to point out that the receivers are smaller Ø70 mm once operating salt vs. Ø90 mm with oil, also reducing the share of these costs.

- \* **SkyTroughDSP.** Departing from the results on baseline 1, a 20% increase is calculated (double than the UltimateTrough). The assumption is made due to the smaller aperture area, which requires more inter-loop connections and longer header piping. Also the heat collector elements remark a difference by implementing  $\varnothing 80$  mm receivers. The collector shows the maximal cost difference to baseline 2 with a 23% reduction.
- \* **Split mirrors.** This collector obviates the use of ball-joints and implements fiberglass facets with thin glass mirrors. The similarities to the UltimateTrough represent therefore a small difference.
- \* **MS-Trough.** About 14 €/m<sup>2</sup> for the heat tracing system and 9 €/m<sup>2</sup> for the piping material are considered in the concept [55]. Compared to the UltimateTrough, the MS-Trough accounts these components at double the value. Despite of this impression the total solar field costs are by 11.4% lower than the baseline 2. This reduction is influenced by the elimination interconnecting pipes between and at the end of the solar collector assembly. The fixed focus design allows also less robust drives and still effective for a 200 m long collector segment. The metal structure is reduced to the torque tubes, the continuous heat collector element support rail and the lighter pylons. The sandwich material facets with thin glass mirrors might lead to an increase of the costs.

From Figure 48, Table 19 and the comments reflect a clear ranking from low cost to cost intensive collectors. Though the numbers are statically presented, the tendency to less expensive innovations of the specific solar field in comparison to the applied baselines is evident.

4.1.6 Scaling Potential

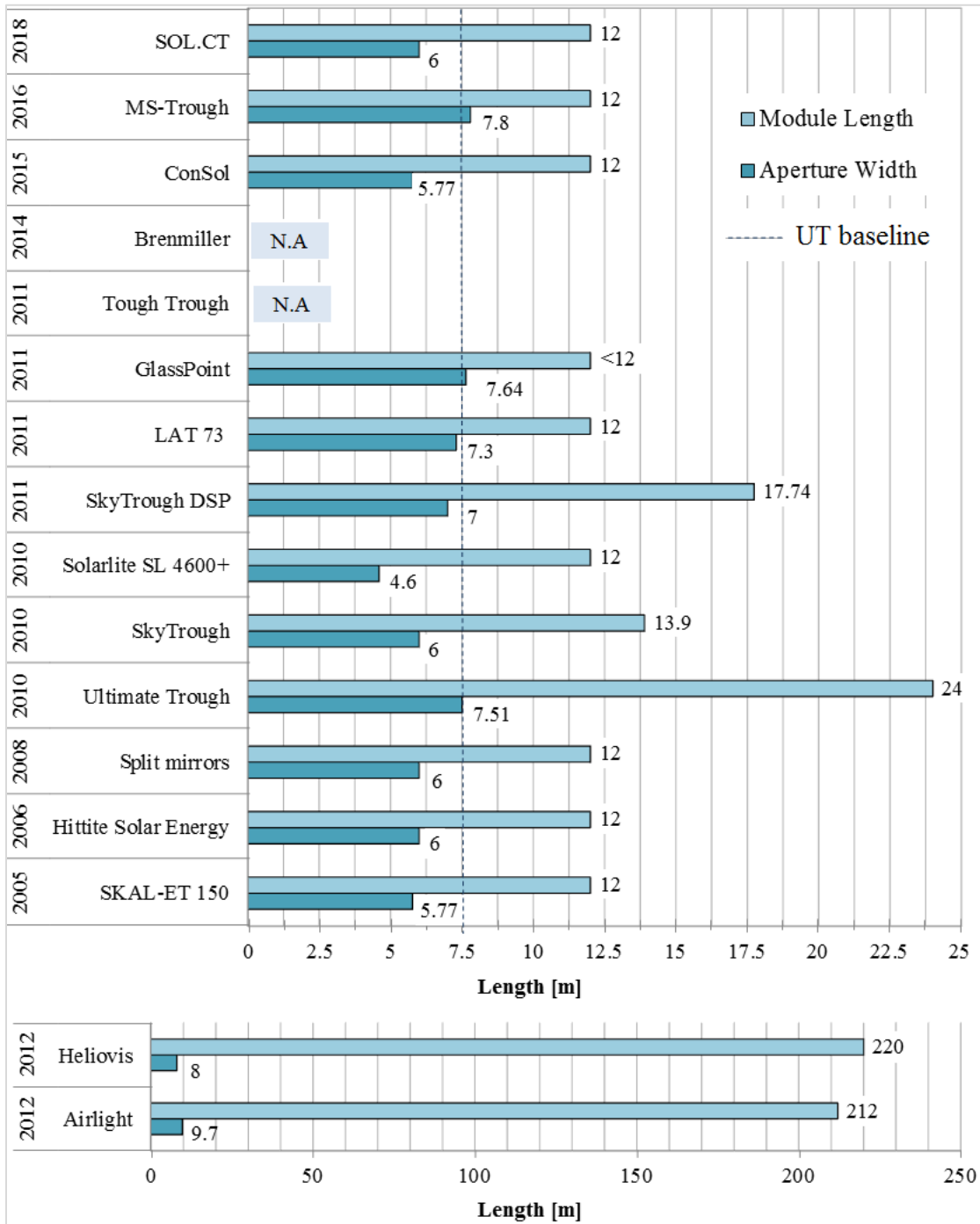


Figure 49 Dimensions comparison of innovative parabolic trough collector modules and timeline of innovations

This criterion compares the dimensional characteristics of the studied collectors. Larger apertures mean an enhanced capability to collect the solar light, but this alone is not all, since the intensity

of the concentrated solar energy also depends on the implemented receivers. Therefore not only the dimensions, but also the possible concentration ratios are compared in this section.

Particularly the module length of the innovative parabolic trough concepts with inflatable polymeric films, namely Heliovis and Airlight, exceed by almost 10 times the continuous module length of the conventional longest baseline of the UltimateTrough. Regarding the aperture width, other two collectors surpass as well this baseline, namely the MS-Trough and GlassPoint.

The scalability can be evaluated by means of the aperture area at operative scale. This aspect is therefore reduced to consider only the segment of one single loop. The value of its effective aperture area can be approximated by subtracting the projected receiver's shadow on the aperture. To estimate the value the collector and receiver length are simplified and considered as equal<sup>18</sup>.

$$A_{eff} = A_{col} - A_{rec} = l \cdot a - l \cdot d_{rec} \quad (29)$$

$A_{eff}$ :	effective aperture area [m <sup>2</sup> ]	$d_{rec}$ :	receiver diameter [m]
$A_{col}$ :	collector aperture area [m <sup>2</sup> ]	$a$ :	aperture width [m]
$A_{rec}$ :	receiver projected area [m <sup>2</sup> ]	$l$ :	approximate collector = receiver length [m]

Having the UltimateTrough and the MS-Trough, not only the longest loop, but also the widest design, they result to have greatest apertures per loop. The UltimateTrough as conventional baseline is nevertheless superior, yet with one row and two drive cross-overs. The MS-Trough instead possesses an 800 m continuous solar collector assembly.

Regarding the concentration ratio of the collectors, it might vary according to the implemented receiver diameter. This, on further considerations modifies the intercept factor on the receiver and subsequently the peak optical efficiency of the collector. For a first overview Figure 51 shows the possible geometrical concentration ratios that can be achieved with the respective aperture widths (see. 2.1 Geometry and Concentration Ratio).

---

<sup>18</sup> Gaps between mirrors, receiver bellows and cross-over elements, among others, could also reduce the effective aperture area. This depends on the manufacturer's definition.

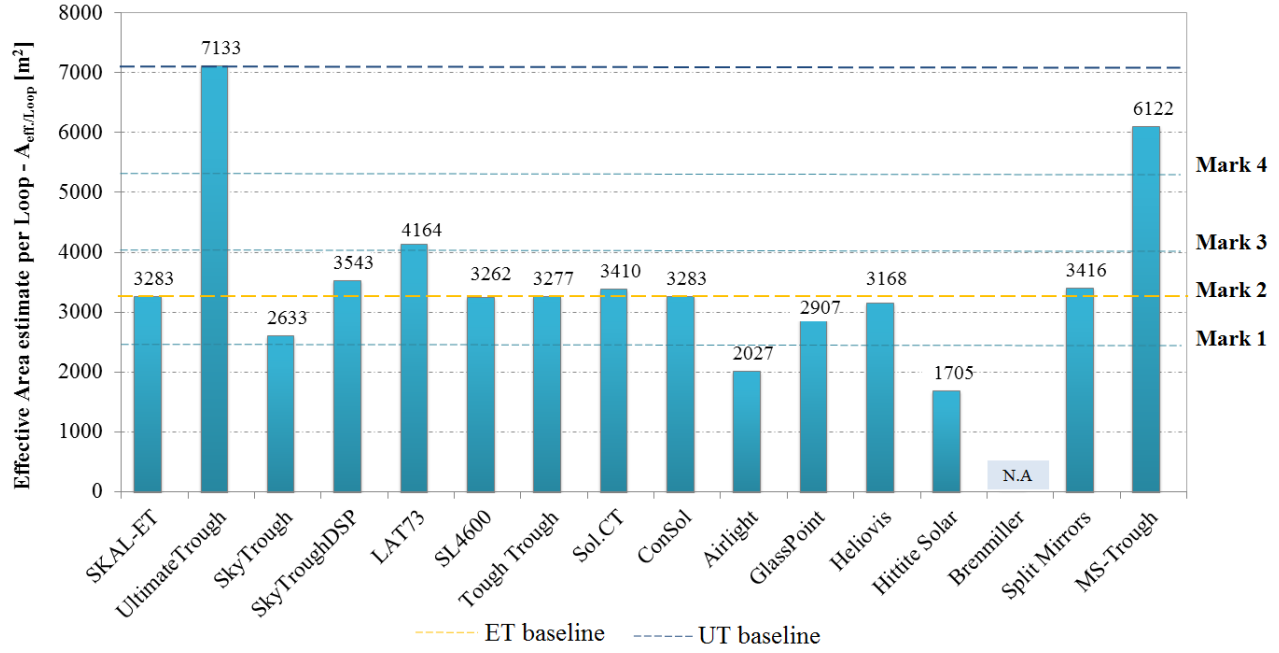


Figure 50 Effective aperture area estimate of a collector loop with subtracted receiver area

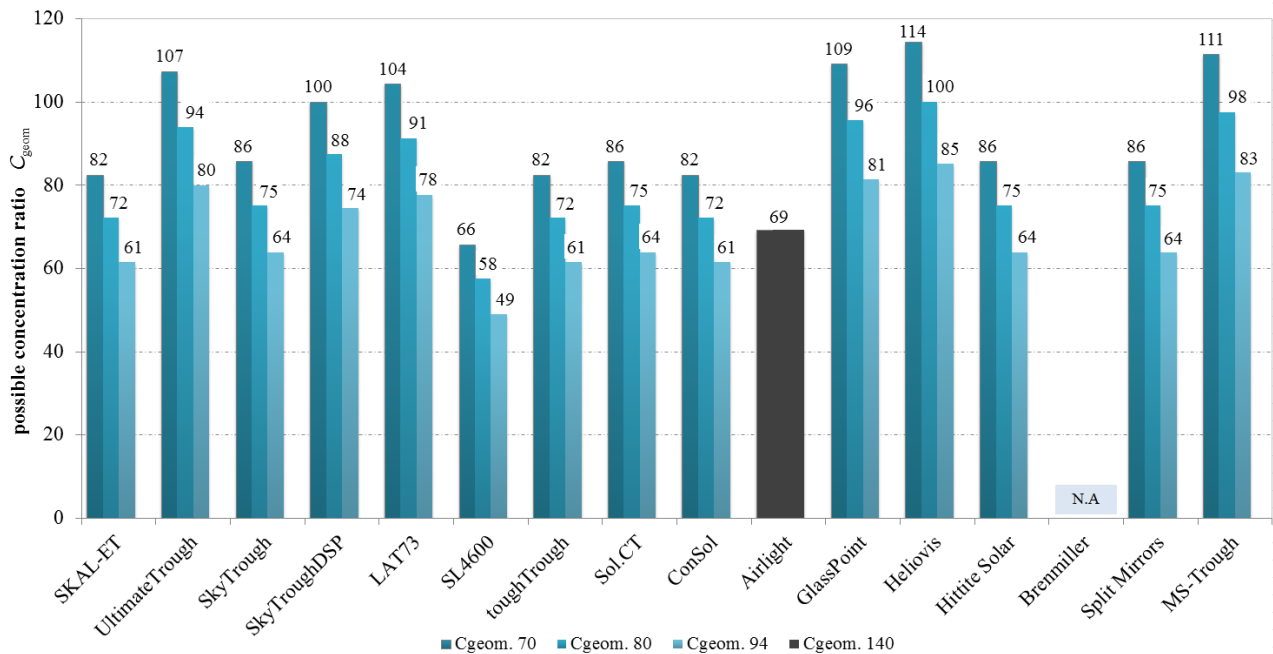
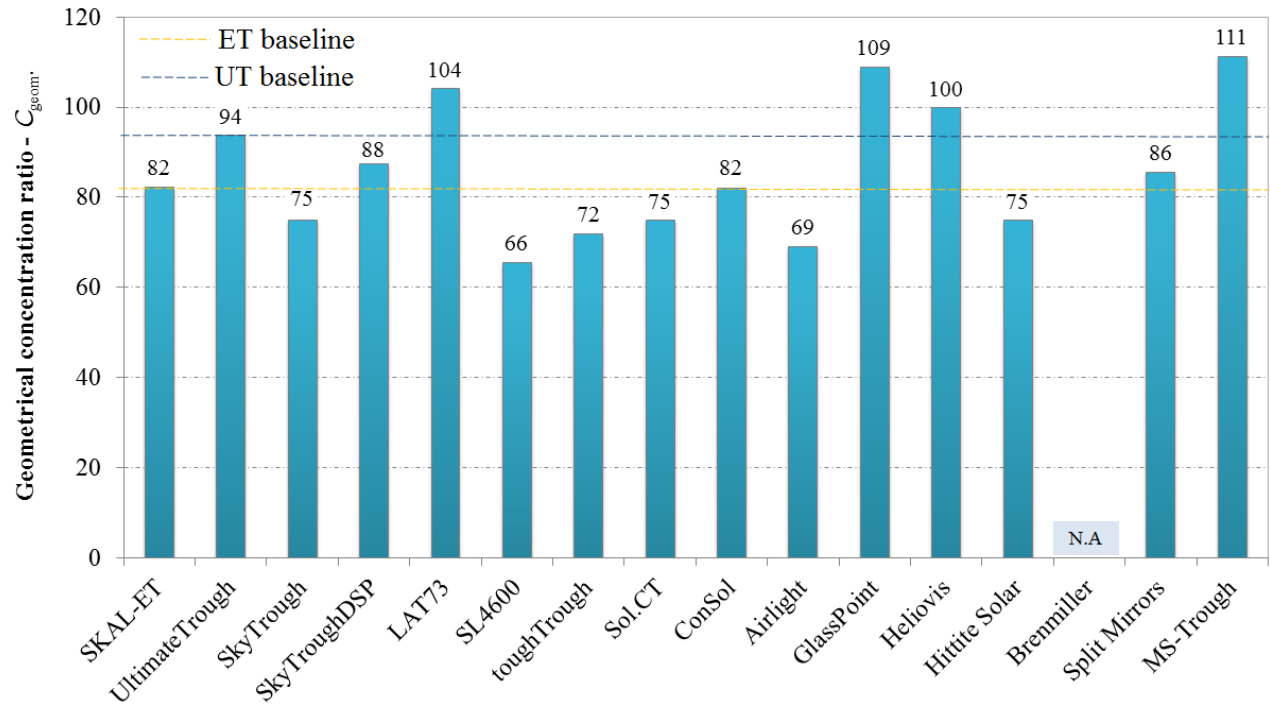


Figure 51 Possible concentration ratio of different PTC for different receiver diameters:  $\varnothing 70$ ,  $\varnothing 80$ ,  $\varnothing 94$  &  $\varnothing 140$  mm

A maximal concentration ratio of 114 can be achieved by Heliovis with the implementation of  $\varnothing 70$  mm diameter receivers, followed by the MS-Trough, GlassPoint, UltimateTrough and

LAT73. In the case of Heliovis the practical value might vary, since its design is predetermined with a secondary concentrator at receiver's height and only a portion of the reflected light intercepts directly the absorber. Therefore the next figure shows the practical values as result of the literature research and is the base for the evaluation on this criterion. The baseline is again set on the conventional collector, UltimateTrough, which possess a concentration ratio of 94 with a receiver diameter of  $\varnothing 80$  mm. The Brenmiller collector's dimensions are not available.



**Figure 52** Designed concentration ratio of innovative parabolic trough collectors

### 4.1.7 Structure

The structure criterion is analysed by comparing the intercept factor of the collectors and qualitatively in lightweight and longevity.

#### Intercept Factor

High intercept factors can only be reached, if the structure is accurate enough to concentrate the light at focal height. More than that, it is also the alignment precision of the reflectors on the supporting structure. This factor can be estimated through simulations, but further stated through photogrammetric measurement campaigns. The results regarding this criterion were considered with the same given receiver diameters as in the previous sections.

State of the art collectors possess a factor greater than 99%. It is in fact due to the central body structure and the mirror alignment, that the collectors achieve these values. For these reason the torque box, torque tube and space frames are the most recurred structures in conventional collectors. Here, Category B collector and the Category C collector SL4600+, follow the state of the art benchmark. For this criterion, the bassline is defined by the UltimateTrough with 99.2% intercept factor with an 80 mm absorber diameter [45].

**Table 20.** Intercept factor of innovative parabolic trough concepts

Category/ Collector	$\gamma$ intercept factor	Category/ Collector	$\gamma$ intercept factor
A	UltimateTrough 99.2% <sup>1</sup>	D	Airlight 74.8% -98.5 <sup>7</sup>
B	SkyTrough 99.1% <sup>2</sup>		GlassPoint N.A <sup>*</sup>
	SkyTroughDSP 98.8% <sup>3</sup>		Heliovis N.A <sup>*</sup>
C	LAT73 99.3% <sup>4</sup>	E	Hittite Solar N.A <sup>*</sup>
	SL4600 99.7% <sup>5</sup>		Brenmiller N.A <sup>*</sup>
	Tough Trough N.A <sup>*</sup>		Split Mirrors 93% <sup>8</sup>
	Sol.CT N.A <sup>*</sup>		MS-Trough N.A <sup>9</sup>
	ConSol 86% <sup>6</sup>		

Sources Table 20: [45]<sup>1</sup>, [57]<sup>2,3</sup>, [65]<sup>4</sup>, [66]<sup>5</sup>, [18]<sup>6</sup>, [67]<sup>7</sup>, [64]<sup>8</sup>, [55]<sup>9</sup>

- \* **Tough Trough.** A similar accuracy to the SL4600+ of the same category can be expected, due to the implementation of composite reflector facets.
- \* **SOL.CT.** Implements cold bent mirror reflectors into concrete preformed gaps in the parabolic frame. The ideal intercept factor of 1.0 is possible when the collector contour has the shape of an ideal parabola. In the case of the SOL.CT one can assume, that the design

entails optical errors, due to the unevenness of the concentrator surface, which cannot favour a high intercept factor (see Annex B).

- \* **ConSol.** Expected, but difficult to predict deformations during and after the casting of the concrete shell, required a manually adjustment of the receivers position to correct the intercept factor value. On the first collector's demonstration the intercept factor was measured at 46% [18]. This problematic can be also presumed of happening for the SOL.CT collector of the same Category C.
- \* **Airlight.** Analytical results are presented in Table 20 from [68]. The range is given depending on the implemented number of adjacent polymeric layers, where 98.5% are characterized for a parabolic shape. A lower than the baseline intercept factor can be expected, since the inflated reflectors deform due to the gravitational force and uneven distribution of the air in the chamber for incidence angles greater than zero degrees,  $\theta > 0^\circ$ . See Annex B.
- \* **GlassPoint.** The collector is as well a fixed focus collector. This means that the accuracy of the light's concentration is totally dependent on the reflector's suspension mechanism, yet assuming that the likewise suspended receivers are perfectly fixed and oriented. In this case a similar intercept factor to the baseline can be assumed. In another case, the thermal expansion of the receivers could modify the proper alignment in an arbitrary position, mostly since the elements are suspended from the ceiling by cables. This would decrease the intercept factor.
- \* **Heliovis.** Similar assumptions as the Airlight collector are made. Furthermore it implements a secondary reflector, which needs to be accurately installed in order to achieve a high intercept factor. The implementation of receivers with a glass envelope leads to double-refraction through its glass. The portion of deviated light could never hit the absorber.
- \* **Hittite Solar.** Due to the robust structure and implementation of thin glass facets a similar factor to the baseline can be expected. Nonetheless the counterweight in front of the aperture projects evident shading on the complete upper part of the receiver and probably on a portion of the aperture. The counterweight might as well induce a torque, which deforms the collector's structure and subsequently incrementing the slope error of the mirrors.
- \* **Brenmiller.** In analogy to the Hittite collector of the same category, the structure might enable a good intercept factor similar to the baseline. Mostly because it uses thick glass

mirror facets and two outer torque tubes, which are continuously interconnected to the adjacent modules. Slightly modifications might occur, due to the implemented single drives on each module. If the drives are not synchronized while tracking, first the torsion of the structure is susceptible to be deformed and secondly there is the hazard of receivers' breakage due to the torsion load.

- \* **MS-Trough.** The parabolic structure has been tested in a prototype and a good precision is potentially achievable [55]. Nonetheless, the great aperture proposed by the collector implies longer focal lengths from the outer regions to the absorber, which might influence the interception accuracy negatively. On the other hand the use of two torque tubes as a fix focus module combined with the thin sandwich composite parabola, could assure a constant accurate concentration in each tracking position.

### Lightweight, Wind Resistance and Longevity

**Table 21.** Specific total weight and maximal operational wind speed

Category/Collector		specific total weight [kg/m <sup>2</sup> ]	wind speed (operational) [m/s]	Category/Collector		specific total weight [kg/m <sup>2</sup> ]	wind speed (operational) [m/s]
A	SKALET-150	30.0 <sup>1</sup>	14.0 <sup>1</sup>	D	Airlight	-	16.6 <sup>9</sup>
	UltimateTrough	28.0 <sup>2</sup>	-		GlassPoint	40 <sup>10</sup>	zero wind environment
B	SkyTrough	15.5 <sup>2</sup>	12.0 <sup>3</sup>	E	Heliovis	-	-
	SkyTroughDSP	-	13.0 <sup>4</sup>		Hittite Solar Energy	-	-
	LAT 73	-	12.5 <sup>5</sup>		Brenmiller Energy	-	-
C	SL 4600+	19.8 <sup>2</sup>	14.0 <sup>6</sup>	E	Split Mirror	14.3 <sup>2</sup>	10.0 <sup>2</sup>
	Tough Trough	-	-		MS-Trough	-	-
	SOL.CT	-	37.5 <sup>7</sup>				
	ConSol	-	10.0 <sup>8</sup>				

Sources Table 21: [69]<sup>1</sup>, [70]<sup>2</sup>, [50]<sup>3</sup>, [51]<sup>4</sup>, [71]<sup>5</sup>, [66]<sup>6</sup>, [63]<sup>7</sup>, [18]<sup>8</sup>, [67]<sup>9</sup>

**Category A.** A 50 MW solar field with EuroTrough collectors corresponded to a specific total weight of 30 kg/m<sup>2</sup>, accounting the steel structure, glass mirrors, receivers and bearings [69]. An estimation by C. Prahl for the UltimateTrough accounts with 28 kg/m<sup>2</sup> [70]. The collector's receivers, reflectors and structures with the proper maintenance suppose a life time of 25 years. In the case of the UltimateTrough, due to the great aperture, wind fences need to be

implemented. The wind load on it is nevertheless reduced by 30% thanks to the gaps on the parabolic aperture [45].

**Category B.** These collectors specially target cost reductions through lightweight and standardized structures. In case of the SkyTrough a mass reduction of ca. 50% was achieved compared to the EuroTrough. The successor SkyTroughDSP is assumed to have a similar value in analogy between the EuroTrough and UltimateTrough. For the LAT73, due to the similar structural approach and the aluminum frame, a value slightly higher than 15.5 kg/m<sup>2</sup> can be expected, yet lower than the EuroTrough baseline. Reasons for this assumption are the additional longitudinal girders for the reflectors support and the reflector panels themselves.

**Category C.** The SL4600+ achieves thanks to the sandwich composite structure a 30% reduction in specific weight compared to the EuroTrough. It implements a robust torque tube, yet uses only three pairs of stamped sheet arms. The toughTrough collector might have a similar weight as the SL4600+. The concrete collectors do not offer a value on the total specific weight. An assumption is that both of them are significantly heavier than the EuroTrough collector. In an example with the ConSol collector only one of four supports weights 1995.0 kg per piece [18]. To be added is the continuous parabolic shell for two modules. Regarding the operational wind resistance the value given for the SOL.CT is evidently superior as the ConSol, which is still to be demonstrated.

**Category D.** For the GlassPoint collector a reduction of 84% in concrete, 56% in metal and an estimate of 12 kg/m<sup>2</sup> in glass elements were stated compared to Andasol 1 [72]. The final specific weight results higher than the EuroTrough. Remarkable is, nevertheless, the zero wind environment of operation, which distinguishes it over the other studied collectors. In the case of the Airlight collector, the weight is assumed to be the greatest of all given, due to its piece's dimensions, which are full concrete and steel body. Heliovis instead, represents a lightweight inflatable body made of plastic membranes. The factor that increases its weight, nevertheless, is its bearing structure. Regarding the longevity, these three collectors have a common significant risk, namely the breakage of its enclosing element. Possible hazards are strong winds, flying sharp rocks, sand/dust abrasion or degradation due to ultra-violet radiation on the surface.



**Figure 53** Degraded inflatable collector, due to a possible crack of the plastic film. Coordinates: 30°13'01.7"N 9°08'57.5"W  
(source: Google.Maps)

**Category E.** Regarding these aspects the Brenmiller collector can be close to the baseline of the EuroTrough, due to the steel structure and the use of mirror facets. The Hittite instead is assumed to be higher in weight mainly because of its massive counter weight, yet similar regarding wind resistance and longevity. The Split Mirrors collector's specific weight was estimated at around  $14.4 \text{ kg/m}^2$  and it was preliminary analysed for wind speeds of 10 m/s [64]. The MS-Trough is assumed to have similar or slightly higher specific weight values than the Split Mirrors collector, due to the thin glass and sandwich composite structures. Regarding the wind loads, its large aperture means also a mayor exposed area to the wind. Its value might range between those collectors with composite materials. In all categories longevity between 20 to 25+ years should be fulfilled, as it is state of the art.

## 4.2 Evaluation Matrix

The recurred method evaluates a row of different solutions from an economic and technical point of view. The VDI2225 guideline is a design engineering method that allows a comparative analysis of several configurations against a theoretical ideal solution, regarding performance and capital costs. After the evaluation campaign a so called “s-diagram” (*s* for *strength*) can be derived from the results to illustrate the innovative and conventional collectors versus an ideal solution.

The results of this method are strongly depended on the evaluation scale and the weight of the defined criteria. Since the categories and technologies of this study possess specific strengths, it is practically contradictory to weight each criterion, since some of them could be systematically undervalued. Therefore to avoid arbitrary results all considered criteria are weighted with the same importance as suggested in the guideline. The global scale is from ‘0’ (unsatisfactory) to ‘4’ (ideal), yet for the study additional metrics are introduced.

Two scales of type ‘I’ or type ‘II’ remark the criterion’s predominance of the baseline. Type ‘I’ is used, when the baseline is outperformed by any other technology and that of type ‘II’, when the baseline is evidently predominant. Using this and the analysis results of the previous section, a specific range is defined to evaluate each criterion as established in Table 22.

### Technical Value X

First the technical value is introduced. It values those criteria that determine aspects like performance, efficiency, structure and longevity. The ideal solution is represented for a value  $X=1.0$ , when all criteria have the maximum punctuation. In this case each criterion is valued with ‘4’ for the ideal concept and it amounts in a total of ‘48’ points for 12 criteria. The evaluation with ‘0’ is due to limitations in the previous analysis that hinders a higher punctuation. The method implements following equation to calculate the technical value of each collector [73]

$$X = \frac{p_1 + p_2 + p_3 + \dots + p_x}{n * p_{max}} = \frac{\bar{p}_x}{p_{max}} \quad (30)$$

$X$ :	technical value [-]	$p_{max}$ :	sum of all $p_x$ values [-]
$p_x$ :	value of criteria $x$ [-]	$n$ :	number of evaluated criteria [-]
$\bar{p}_x$ :	mean value [-]		

A technical value above 0.8 is generally to be considered as very good, 0.7 as good and below 0.6 as unsatisfactory. Results of this parameter aim to give a general overview of the different concepts and it only expresses, whether the chosen solutions promise success at least in technical terms [73].

### Economic Value Y

For this parameter the specific solar field cost is the main criterion. Also here an ideal scenario is set, yet based on a market survey. One strategy is to identify current low prices with a conventional state of the art collector and to put it in relation to the innovations and the consequent baseline of this study, namely the UltimateTrough. From this survey a specific solar field cost of 82.50 €/m<sup>2</sup> (92.00 \$/m<sup>2</sup>) is stated as the lowest price for the conventional collector ST8.2 (see Annex B) [74]<sup>19</sup>. Another strategy is to recognize the economic value of the lowest costs found among the studied innovations and set this as reference. In the latter case the Heliomis collector presents the lowest specific solar field costs with 104 €/m<sup>2</sup>.

According to the VDI2225 guideline the economic value is defined as followed:

$$Y = \frac{H_{M,\min}}{H} = \frac{\beta \cdot H_{\text{baseline}}}{H} \quad (31)$$

Y:	economic value [-]	$H_{\text{baseline}}$ :	baseline cost, i.e. UltimateTrough [€/m <sup>2</sup> ]
$H_{M,\min}$ :	market lowest achievable cost [€/m <sup>2</sup> ]	$\beta$ :	solar field cost levelling factor [-]
H:	solar field cost of collector concept [€/m <sup>2</sup> ]		

The cost levelling factor  $\beta$  is the result of the ratio between the solar field costs baseline reference and of the market lowest achievable costs. In this study Heliomis as reference represents the most suitable approach, for which a value of  $\beta=0.52$  is used. This means that the economic value of the UltimateTrough baseline corresponds to 52% of the ideal specific costs.

### Results

The results of this methodical approach are shown in Table 23 and are evaluated according to the metrics established in Table 22. The S-Diagram is followed in Figure 54 and is the tool to discuss the present work.

<sup>19</sup> The study was conducted under the SunShot initiative in the SolarMat project

Table 22. Evaluation metrics of the criteria and sub-criteria

Criteria and Subcriteria / Optical Performance	Value		4	3	2	1	0	Reference	
	(I)	(II)							
Peak Optical Efficiency			82-78	77-73	72-68	67-60	n.a	Table 10	
Reflector Type			Thin Glass	Thick Glass	i. Enclosed Coated Aluminium ii. Polymeric Reflector	i. Enclosed Polymeric Reflector ii. Coated Aluminium	n.a	Table 1 & 9	
<b>Thermal Performance</b>									
Scenario 1: Length Estimation	(I)		0% - 10%	>10% - 30%	>30% - 60%	>60% - 80%	n.a	Table 12	
Scenario 2.1: Loop Power Losses per produced Megawatt with Thermo-Oil as HTF	(I)		< 4%	> 4% - 5%	> 5% - 6%	> 6%	n.a	Table 13	
Scenario 2.2: Loop Power Losses per produced Megawatt with Molten Salt as HTF	(I)		< 7%	> 7% - 8%	> 8% - 9%	> 9% - 10%	n.a	Table 14	
<b>Parasitic Consumption</b>									
With Thermo-Oil vs. Molten Salt	(I)		0% - 0.5%	> 0.5% - 1.5%	> 1.5% - 2%	> 2%	n.a	Table 15 & 16	
<b>Global efficiency</b>									
with Thermo-Oil vs. Molten Salt	(I)		45% - 43%	42% - 40%	39% - 37%	36% - 33%	n.a	Table 13 & 14	
<b>Scaling Potential</b>									
Effective Aperture	(II)		Mark 4	Mark 3	Mark 2	Mark 1	n.a	Figure 50	
Concentration Ratio	(I)		> 100	< 100 - 90	< 90 - 75	< 75	n.a	Figure 52	
<b>Structure</b>									
Intercept Factor	(II)		99.9% - 95%	< 95% - 90%	< 90% - 80%	< 80% - 70%	n.a	Table 20	
Operational Wind Speed [m/s]	(I)		zero environment	17 - 12	12 - 10	10 - 5	n.a	Section 4.1.7	
Lighthouse [kg/m <sup>2</sup> ]	(I)		10 - 20	20 - 30	30 - 40	> 40	n.a	Section 4.1.7	
Longevity	(I)		Objective argumentation according to respective Category in Section 4.1.7: State of the Art Baseline are 25 years						Section 4.1.7
<b>Type of Scale</b>									
	(I)		Surpasses Baseline 1	Baseline 1	Lower than Baseline 1	Strong Difference to Baseline 1	Not Evaluable	Base line 1 Ultimate/Trough	
	(II)		Baseline 1	Between Baseline 1 and Baseline 2	Baseline 2 or Lower	Strong Difference to Baseline 1	Not Evaluable	Base line 2 Euro/Trough	
<b>Type of Scale according to VDI 2225</b>									
			Very Good (Ideal)	Good	Sufficient	Acceptable	Unsatisfactory	Ideal Solution	

**Table 23.** Evaluation matrix of innovative parabolic trough concepts for large scale application

Collector	Criteria	Category	A					B					C					D					E				
			UltimateTrough	SkyTrough	SkyTroughDSP	LAT 73	SL -4600+	Tough Trough	SOL CT	ConSol	Airight	GlassPoint	Heliolis	Hittite Solar	Brenmiller	Split Mirrors	MS-Trough	UltimateTrough (MS)	SkyTroughDSP (MS)	Split Mirrors (MS)	MS-Trough (MS)						
	<b>Optical Performance</b>		8	6	7	5	5	7	4	1	2	2	4	3	4	3	4	3	4	7	8	6	5	7	8		
	Peak Optical Efficiency		4	3	4	3	3	3	0	0	1	1	2	2	2	0	0	3	4	3	4	3	3	3	4		
	Reflector Type		4	3	3	2	2	4	4	1	1	2	1	2	1	4	3	4	4	3	4	3	2	4	4		
	<b>Thermal Performance</b>		8	5	7	4	6	2	0	0	3	0	6	7	0	0	5	8	7	5	4	7	5	4	8		
	Scenario 1: Length Estimation		4	2	4	2	3	4	1	0	0	1	0	3	4	0	2	4	3	2	4	4	3	2	4		
	Scenario 2: Loop Power Losses per produced MW		4	3	3	2	3	2	1	0	0	2	0	3	3	0	3	4	3	2	4	3	2	2	4		
	<b>Parasitic Consumption</b>		4	3	2	4	3	1	3	0	0	3	0	4	3	0	3	3	4	4	3	4	4	4	4		
	<b>Global efficiency</b>		4	3	3	2	2	2	0	0	1	0	1	1	0	0	2	2	4	3	3	4	3	3	4		
	<b>Scaling potential</b>		8	4	7	4	4	7	3	4	4	2	6	6	3	0	4	8	4	4	8	8	4	4	8		
	Effective Aperture		4	2	4	2	2	3	2	2	2	1	2	2	1	0	2	4	4	2	4	4	2	2	4		
	Concentration Ratio		4	2	3	2	2	4	1	1	2	1	4	4	2	0	2	4	2	4	4	2	2	4	4		
	<b>Structure</b>		16	13	14	13	13	15	15	7	7	6	11	10	10	13	12	13	14	13	13	14	13	13	13		
	Intercept Factor		4	3	4	4	4	4	4	2	2	2	2	2	3	4	2	3	4	4	3	4	4	3	3		
	Windload Resistance		4	3	3	3	3	3	3	2	2	2	4	3	2	3	3	3	3	3	3	3	3	3	3		
	Lighthweight		4	3	3	4	4	4	4	1	1	2	3	2	3	2	3	4	3	4	4	3	4	4	4		
	Longevity		4	4	4	2	2	4	4	2	2	1	3	2	3	3	3	3	4	2	3	4	2	3	3		
	<b>Sum:</b>		48	34	40	32	33	34	32	22	12	20	32	30	17	16	33	42	43	34	35	43	34	35	45		
	<b>Technical Value X</b>		0.71	0.83	0.67	0.69	0.71	0.67	0.46	0.25	0.42	0.21	0.67	0.63	0.35	0.33	0.69	0.88	0.90	0.71	0.73	0.94	0.71	0.94			
	<b>Economic Value Y</b>		0.45	0.52	0.68	0.77	0.60	0.49	0.60	0.80	0.40	0.00	0.00	1.00	0.00	0.41	0.53	0.60	0.49	0.64	0.56	0.64	0.49	0.56			
	Reference Costs (i.e. Heliolis) [€/m <sup>2</sup> ]		104	230	198	152	135	173	211	173	129	261	n.a.	104	n.a.	253	196	172	210	162	209	186	186	186			
	Solar Field Cost Leveling Factor β		0.52	120	104	79	90	110	90	67	136	n.a.	n.a.	54	n.a.	132	102	90	110	85	109	97	97	97			

**Categories:** A - Conventional Collector    B - Metal Structures & Sheet Reflectors    C - Non-Metallic Materials  
D - Enclosed Aperture    E - Fix Focus

Thermo-Oil as HTF  
Molten Salt as HTF

4.3 Evaluation Results

The s-diagram computes the X and Y values of each collector concept from Table 23, which indicate the techno-economic strength  $s$  of their respective design. The line ranging from point (0, 0) to  $s_i(1, 1)$  is the ideal development line, which describes an equal technical and economic value until the ideal solution. The results close to the development line represent an ideal feasibility of the concept, yet stronger, if they are closer to the ideal point  $s_i$ .

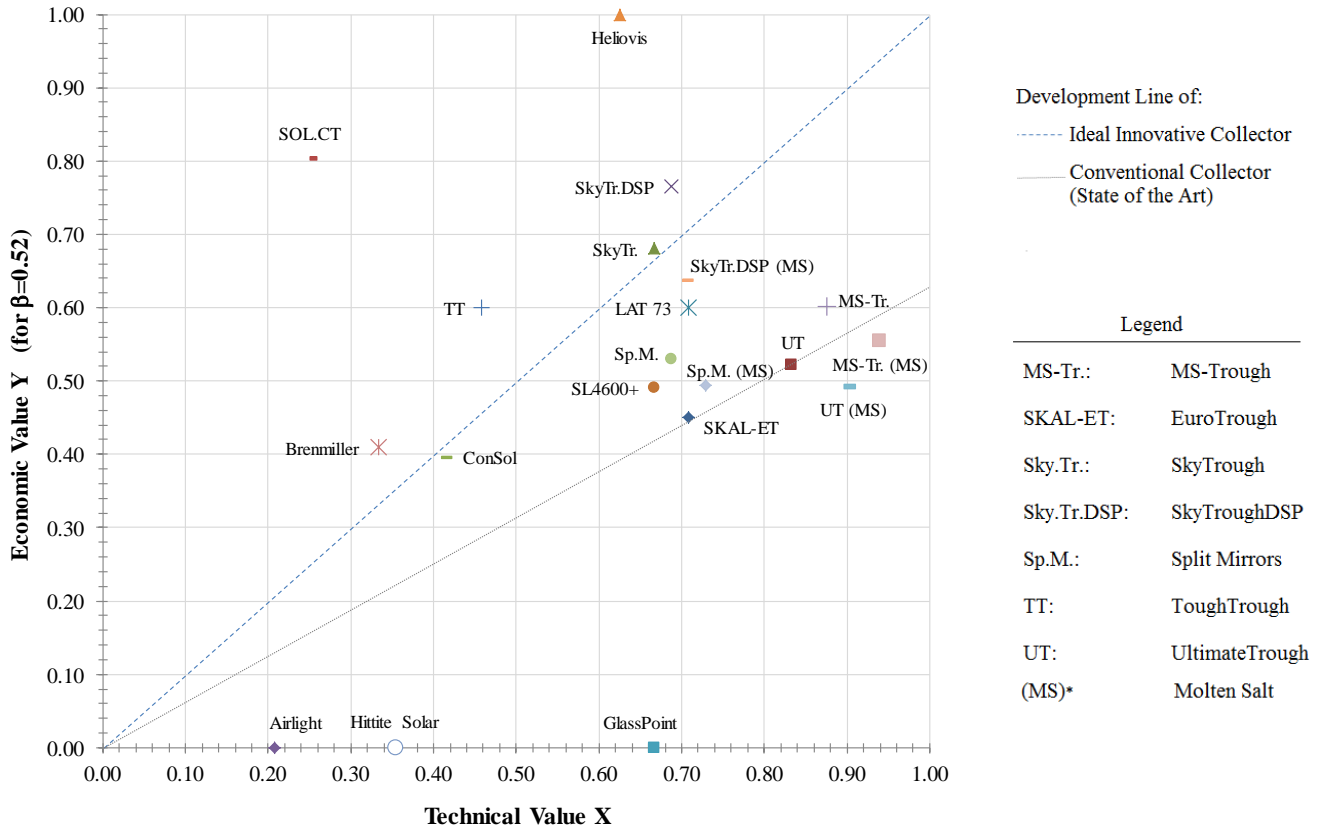


Figure 54 S-Diagram for the evaluation of innovative parabolic trough collectors

Figure 54 includes also the state of the art development line, which is approximated by observing the UltimateTrough and the SKAL-ET. This indicates a roughly estimate of the current conventional collectors’ development tendency.

The economic value Y of the concepts ranges in the graphic from the lowest to the highest limit. On one hand the Heliovis collector shows the highest economic results (Y=1.0), since it is set as lowest price basis and it has the lowest specific solar field costs within the study’s scope. On the other hand the Hittite Solar, Airlight and GlassPoint collectors result on the lowest values of

( $Y=0.0$ ), due to lack of accurate information about their solar field costs. Assumptions for the two latter collectors could expect values lower than the SKAL-ET or even lower than the ConSol collector (see 4.1.5 Costs Scenario). The graph also shows that the innovations tend to improve the specific costs of the solar field compared to conventional collectors. The development line drawn between the SKAL-ET and UltimateTrough is overburden by the concepts with higher values for  $Y$ . From all concepts 50% are above the UltimateTrough baseline.

The technical value  $X$  is not as widespread as the economic value. It ranges from  $X=0.21$  for the Airlight collector and  $X=0.94$  for the MS-Trough operating with molten salt as heat transfer fluid. In this range 70% of the concepts are better than the unsatisfactory technical value  $X=0.6$  and 1% results in an equal or higher than the optimal value of  $X \leq 0.9$ . A result of the graph is also that only few concepts surpass the technical value of the UltimateTrough baseline operating with thermo-oil. One of them is the MS-trough operating with both heat transfer fluids and the other again the UltimateTrough, but with molten salts.

There is a concentration of collectors around the development line, which mainly includes Category B collectors. Among them, the LAT73 with thermo-oil has better technical values, than the SkyTrough and the SkyTroughDSP with thermo-oil. The implementation of the SkyTroughDSP (MS) with molten salt equalizes its technical performance and enhances the economic value. In fact, all collectors operating with molten salt as heat transfer fluid state an increment on the technical value compared to their versions operating with thermo-oil. Nevertheless at the expense of increasing costs expressed by the decrease of the economic value.

Results of the collectors below the economic and technical value of the SKAL-ET do not necessarily express the inferiority of the concepts. The method rather aims to show the direction of development to which a concept must be steered to.

To summarize, the results show two outstanding concepts regarding the two values separately. On the one hand in the economic part is the Heliolis collector with its enclosed aperture the most economically important option. And on the other hand, stronger in terms of technical value, is the MS-Trough fix focus collector operating with molten salts.

#### 4.4 Evaluation Discussion

The evaluation's results highlight the technical-economic degree of current conventional and innovative parabolic trough collector concepts. It is important to mention that the panorama presented in Figure 55 shows partial results considering that the evaluation does not include all possible criteria, but it does contain those within the framework of requirements attributed to innovations<sup>20</sup>. Hence it is possible to identify which collectors are of interest for large scale power generation according to the evaluated criteria.

For the analysis and evaluation, collectors suitable for two heat transfer fluids were previously differentiated. On the one hand those collectors with thermo-oils, which correspond to the state of the art HTF and on the other hand those that can operate with molten salts. In the comparison, collectors with molten salts possess HTF specific advantages in anticipation on two criteria. One of them is the higher operating temperatures from up to 550°C or 580°C, which enable an increase of the solar power plant's global efficiency. The second is the parasitic power of the cycle, since the characteristic density and viscosity of the fluid favour the heat transfer pumps' performance. The calculated parasitic power values are lower with molten salts compared to thermal-oils. This could be observed at the UltimateTrough loop example, where the change from thermo-oil to molten salts result on parasitic power values going from 1.8% to 0.42%<sup>21</sup>.

These collectors also have a practical disadvantage in the framework of the evaluation, since only the specific solar field costs were included to establish a common baseline. It is important to have the awareness that the same fluid in the solar field and in the thermal storage block can reduce the costs of the overall solar power plant. The specific costs of the storage block could be reduced by up to a factor of 3<sup>22</sup> and also up to 23% less costs of the adjacent blocks together (i.e. BOP, power block, HTF system) [9]. The present thesis demonstrates the certain increase of the solar field costs with this medium, however it is necessary to emphasize that the true cost-efficient factor is defined together with the thermal storage block. These aspects represent the reason why it was necessary to differentiate both operating fluids. Thus the best collectors for thermo-oils and molten salts can be sorted.

---

<sup>20</sup> See Chapter 3.

<sup>21</sup> See 4.1.3 Parasitic Consumption

<sup>22</sup> Counting the scale effects from a 50 MW to 100 MW solar power plant with UltimateTrough collectors

About the UltimateTrough reference base line, it can be seen that its techno-economic relevance is already relatively competent even among the innovations. If its economic factor could be improved, an ideal concept would be approached. Unlike this one, Category B collectors that implement space frames do have an enhanced economic scenario at equally robust structures. On the one hand, the installation of standardized elements in the main structure has a significant influence on the manufacturing, assembly and installation costs, reducing on the specific solar fields' costs. On the other hand, the implementation of polymeric reflectors clearly favours the lightweight of the concept. However it is also its weak point in terms of durability and optical performance.

Close to that category there are the sandwich composite structures collectors. Category C collectors have the strong advantages of their robust structure, good optical performance and longevity, but at the expense of high manufacturing costs that can result at large scale application. In the case of the SL4600+ a disadvantage is also the scaling potential, which is limited by its aperture and concentration ratio. Its installation would require a larger number of modules in a solar field and also of absorber tubes. This not only affects the thermal efficiency of the collector, but also causes higher investment costs. It should be noted that this technology has been industrially approved and that the approach with sandwich composite materials can still be optimized, with wider apertures and thinner facets, in order to save on material and weight.

The latter aspect is precisely addressed with the Split Mirrors fix focus collector of Category E, which proposes the use of similar facets to those of the SL4600+. This collector presents slightly improved results compared to the SL4600+ mainly due to the thermal behaviour favoured by the enlarged aperture and the format of the loops. The proposal of this collector is certainly innovative. However it has structural technical challenges that need to be projected, by means of the torque body and heat collector element support bearings.

Following Category E collectors, the MS-Trough specially designed for the operation with molten salts at high temperatures, sustains the most outstanding technical value of the study. In response to the current demand for an optical collector that adapts to the requirements for this format, the MS-Trough proposes features that favour both the cost-efficiency and performance of the solar plant. Its fix focus design enables the elimination of flexible interconnection elements, thus mitigating components with a tendency to frequent breakdowns. The mass distribution of

the concept reduces the loads on the motors and their required nominal power. As far as the optical design is concerned, a value is estimated between the conventional EuroTrough and UltimateTrough collectors. The other collectors in this category, Hittite and Brenmiller, are fairly similar designs in structure and result in a similar technical value. However, an important feature that differentiates them is the mass distribution. Hittite employs a counterweight in its structure which facilitates the fixation of the receiver and separation of the collector tracking movement. This reduces the torque load on the tubes but makes the modules heavier and causes additional shading on the receiver.

From Category D, the Heliolis collector has the economic superiority over the other concepts. It proposes an extreme lightweight with its inflatable collector tube and a flexible implementation for industrial process heat, enhanced oil recovery and electricity generation. At the moment the optical and thermal performance were estimated and are being verified at the demonstration unit<sup>23</sup>. In analogy to the Airlight collector, a reduction in the intensity of the incident energy flux through the top membrane can be expected. Light deviations due to reflection effects by the cover and reflector layers disadvantage the module's intercept factor. It is also assumed that the enclosing membrane is susceptible to breakage by flying sharp objects brought by strong winds.

Among the innovations, the least salient collectors are those with a concrete structure. Of the three included in the study, only two have been built: the Airlight and the ConSol collectors. The third concept and yet to be demonstrated is the SOL.CT. A main advantage of these concepts is the universal accessibility of the material. As far as the structure is concerned, the concepts do not support a good optical performance, mainly due to the deformation of the material in the hardening process and also at wind load. The ConSol project demonstrated nevertheless the possibility of building this type of collectors and it can be considered as a milestone for the development process of these collector types.

---

<sup>23</sup> Integrated module to a company of agricultural processes, *Mercajucar*, Spain

## 5. Conclusion and Outlook

This thesis investigated the state of the art of parabolic trough collectors. For this purpose, a classification was made between conventional and innovative collectors. A description of the main components that define their optical and thermal performance was included. The data collected from each collector was used to simulate the effective thermal energy output with thermal oils and molten salts in their respective loops.

One of the goals was to identify those collector concepts that aim to increase the overall efficiency, while reducing the parasitic power consumption of a solar plant. The results showed that the UltimateTrough collector can achieve an overall efficiency of 43% by operating with molten salts instead of 40% with thermal oils. Only superior in this sense was the MS-Trough reaching 44% with molten salts. As for the parasitic behaviour of these collectors, both reduce the impact up to 0.19% in the case of MS-Trough and up to 0.42% in the case of Ultimate-Trough. These two collectors were the most salient concepts of the study in terms of performance.

Another goal was to estimate the collectors' economic impact on the solar field. Regarding this the Heliovis collector turns out to be the most remarkable innovative concept proposing a reduction of 55% compared to the EuroTrough baseline [54]. However, its technical performance is distant from that of the collectors mentioned above, mainly because it combines polymeric reflectors and a transparent membrane that reduce the intercept factor onto the receivers.

The study highlights the potential of the operation with molten salts as heat transfer fluid. This implies a significant reduction of the solar power plants' investment by up to a factor of 3 in the storage block and also up to 23% less of the costs in the adjacent blocks together (i.e. balance of plant (BOP), power block and heat transfer fluid system) [37]. However, this technology not only benefits from the use of molten salts, but is also attached to its operational boundaries. Currently there is the technology to maintain the temperature of the salts in its liquid phase at more than 270°C in the pipes, receivers and storage tank by means of heat tracing and auxiliary heaters. However, it is also cost intensive. For this reason, studies of molten salts are being undertaken to reduce their solidification temperature properties, thus counterbalancing to the risk of operation.

In the solar field especially the sealing of flexible interconnection elements such as ball-joints or swivel hoses mean a weak point of high risk freezing of the medium. For this purpose only two concepts mitigate this risk, namely the collectors MS-Trough and Split Mirrors. Because of their fixed focus design both collectors can eliminate these components allowing a fixed interconnection between the modules and the header piping to the storage tanks. This property is only found in Category E collectors.

The study, in conclusion, analysed and evaluated the collectors in their technical and economic aspects to reflect the development tendencies and the progress of their potential. The collectors capable of operating with molten salts demonstrated superior technical relevancy, among them the MS-Trough, the UltimateTrough and the SkyFuelDSP. That is mainly for their performance and second for their economic impact on the overall cost of a solar power plant. The three collectors benefit from the scale-up effects of their wide apertures, but more importantly they have the potential to integrate the cycle of the solar field with that of the thermal storage block in one.

The thesis offers a comprehensive overview of large-scale parabolic trough collectors for large scale energy generation. The content can be used as a market survey of current options, which highlights those technologies with the potential to have a major breakthrough in the sector. The objective is, in fact, that of incentivising the prevalence and competitiveness of the technology within the framework of sustainable renewable energies. Mainly research institutions, renewable energy associations, investors and inventors can benefit from this work for the promotion of new parabolic trough collectors concepts.

It is likely that concentrated solar power technology with parabolic trough collectors will not become as conventional as, for example, photovoltaics. However, any technological advance that can optimize processes to generate clean energy is relevant for the common good of reducing the use of fossil fuels to mitigate the concentration of greenhouse gases on earth.

## 6. Bibliography

- [1] R. Pitz-Paal, J. Dersch, B. Milow, F. T  lez, A. Ferriere, U. Langnickel, A. Steinfeld, J. Karni, E. Zarza and O. Popel, "Development Steps for Parabolic Trough Solar Power Technologies With Maximum Impact on Cost Reduction," *Journal of Solar Energy Engineering*, vol. 129, no. DOI: 10.1115/1.2769697, p. 8, 2007.
- [2] N. Janotte, "Requirements for Representative Acceptance Tests for the Prediction of the Annual Yield of Parabolic Trough Solar Fields", Germany: Shaker Verlag, 2012.
- [3] L. C. Enriquez, "Nueva generacion de centrales termosolares con colectores solares lineares acoplados a ciclos supercriticos de potencia," Universidad Politecnica de Madrid, tesis doctoral , Madrid, 2017.
- [4] REN21, "Renewables - Global Status Report," REN21 Community, 2018.
- [5] UNCC, "<https://unfccc.int/>," United Nations Climate Change -The Paris Agreement: Essential Elements, [Online]. Available: <https://unfccc.int/process-and-meetings/the-paris-agreement/the-paris-agreement>. [Accessed 05. 08. 2019].
- [6] SolarPaces and IEA, "<https://www.solarpaces.org/>," 2019. [Online]. Available: <https://www.solarpaces.org/wp-content/uploads/status.jpg>. [Accessed 08. 05. 2019].
- [7] ISE, "Current and Future Cost of Photovoltaics. Long-term Scenarios for Market Development, System Prices and LCOE of Utility-Scale PV Systems," Agora Energiewende & ISE Fraunhofer Institute, Ettlingen, 2015.
- [8] IRENA, "Renewable Energy Technologies:," *International Renewable Energy Agency*, vol. Vol. 1, no. 2/5, p. 48, 2012.
- [9] T. Ruegamer, H. Kamp, T. Kuckelkorn, W.Schiel, G.Weinrebe, P. Nava, K.Riffelman and T.Richtert, "Molten salt for parabolic trough applications: system simulation and scale effects," *Energy Procedia, Elsevier*, vol. 49, pp. 1523-1532, 2014.
- [10] S. N. Vijayan and S. S. Kumar, "Theoretical Review on Influencing Factors in the Design of Parabolic Trough Collectors," *International Journal of Mechanical and Materials Engineering*, vol. 11, no. 11, p. 6, 2017.
- [11] GIZ, "Solar Thermal Heat & Power - Parabolic Trough Technology for Chile," GIZ Brasil , Santiago de Chile, 2014.
- [12] Y. Makoto Nakauchi, "Making the most of solar thermal energy," 2015. [Online]. Available: <https://www.ee.co.za/article/making-solar-thermal-energy.html>. [Accessed 05. 08. 2019].

- [13] G. Edevane, “mashable.com,” 07. 02. 2016. [Online]. Available: <https://mashable.com/2016/02/06/moroccan-solar-plant/?europe=true>. [Accessed 02 02. 2019].
- [14] HelioTrough. [Online]. Available: <http://www.heliotrough.com/>.
- [15] M. Röger, P. Potzel, J. Pernpeintner and S. Caron, “A Transient Thermography Method to Separate Heat Loss Mechanisms in Parabolic Trough Receivers,” *Journal of Solar Energy Engineering*, vol. 136, no. 011006-1, p. 9, 2014.
- [16] M. Günter, M. Joemann and S. Csambor, “Advanced CSP Teaching Materials - Chapter 05: Parabolic Trough Technology,” EnerMENA and German Aerospace Center [DLR], -, 2011.
- [17] S. Meyen, E. Lüpfert, J. Pernpeintner and T. Fend, “Optical Characterisation of Reflector Materials for Concentrating Solar Power Technology,” in *15th International SolarPaces Symposium*, Berlin, Germany, 2009.
- [18] DLR, T. Kaiserslautern, RUB, Solarlite, Almeco, Stanecker and Pfeifer, “Ergebnisbericht: ConSol - Concrete Solar Collector,” DLR, Germany, 2018.
- [19] AGC Glass Europe, “AGC Solar Mirror Thin Datasheet,” [Online]. Available: [https://www.agc-yourglass.com/sites/default/files/agc\\_docs/SolarMirrorThin\\_EN.pdf](https://www.agc-yourglass.com/sites/default/files/agc_docs/SolarMirrorThin_EN.pdf). [Accessed 15. 03. 2019].
- [20] H. Price, E. Lüpfert, D. Kearney, E. Zarza, G. Cohen, R. Gee and R. Mohaney, “Advances in Parabolic Trough Solar Power Technology,” *Journal of Solar Energy Engineering*, vol. 120, no. doi: 10.1115/1.1467922, p. 17, 2002.
- [21] Skyfuel, “ReflechTech Product Information (Data Sheet),” 2017. [Online]. Available: [http://www.skyfuel.com/downloads/brochure/Brochure\\_ReflecTech.pdf](http://www.skyfuel.com/downloads/brochure/Brochure_ReflecTech.pdf). [Accessed 30. 11. 2018].
- [22] B. Usmani and S. Harinipriya, “Chapter 15: High-Temperatur Solar Selective Coating,” in *Systems Thinking Approach for Social Problems: Proceedings of 37th National Systems Conference, December 2013 (pp.9)*, Springer, 2015.
- [23] Archimede Solar Energy, “HCEMS11 Molten Salt Receivers Datasheet,” [Online]. Available: [http://www.archimedesolarenergy.it/en\\_hcems-11-sali-fusi.htm](http://www.archimedesolarenergy.it/en_hcems-11-sali-fusi.htm). [Accessed 23. 02. 2019].
- [24] A. Ambrosini, “High-Temperature Solar Selective Coating Power Tower Recievers,” 2015. [Online]. Available: [energy.gov/sunshot](http://energy.gov/sunshot). [Accessed 07. 12. 2018].
- [25] Walraven, “Thermisch bedingte Längenänderung bei Rohren,” [Online]. Available: <https://www.walraven.com/de/technische-informationen/thermisch-bedingte-laengenanderung-bei-rohren/>. [Accessed 15. 03. 2019].
- [26] P. Gooda, G. Zanganeha, G. Ambrosettib, M. Barbatoc, A. Pedrettib and A. Steinfeld, “Towards a Commercial Parabolic Trough CSP System using Air as Heat Transfer Fluid,” in *SolarPaces*

- Conference*, Las Vegas, 2013.
- [27] D. Jähning, “Entwicklung und Optimierung eines Parabolrinnekollektorsystems zur Erzeugung von Prozesswärme für industrielle Produktionsprozesse, Fabrik der Zukunft,” 2005. [Online]. Available: [www.aee-intec.at/0uploads/dateien26.pdf](http://www.aee-intec.at/0uploads/dateien26.pdf). [Accessed 06. 08. 2019].
- [28] U. Baudis, “Technologie der Salzsammelze. Wärmebehandlung, Härtetechnik, Wärmeübertragung, Reinigung,,” Landsberg, Lech , 2001.
- [29] P. H. Wagner, “Thermodynamic simulation of solar thermal power stations with liquid salt as heat transfer fluid,” Technisch Universität München, Lehrstuhl für Energiesysteme, München, 2012.
- [30] D. Kearney, “Assessment of a Molten Salt Heat Transfer Fluid in a Parabolic Trough Solar Field,” *Journal of Solar Energy Engineering*, vol. 125, pp. 170-176, 2003.
- [31] M. Eickhoff, M. Meyer-Grünefeldt and L. Keller, “New operating strategies for molten salt in line focusing solar fields - Daily drainage and solar receiver preheating,” in *AIP Publishing*, Tabernas, 2015.
- [32] M. Wittmann, “Optimization of Molten Salt Parabolic Trough Power Plants using different Salt Mixtures,” in *SolarPaces2012*, Morocco, 2012.
- [33] J. F. Feldhoff, M. Eickhoff, L. Keller, J. L. Alonso, M. Meyer-Grünefeldt, L. Valenzuela, J. Pernpeintner and T. Hirsch, “Status and first results of the DUKE project – Component qualification of new receivers and collectors,” *Energy Procedia, Elsevier* , vol. 49, no. SolarPACES 2013, p. 1766 – 1776, 2014.
- [34] H. Schenk and M. Eck, “Yield Analysis for Parabolic Trough Solar Thermal Power Plants - A Basis Approach,” DLR, Cologne, 2012.
- [35] N. Janotte, G. Feckler, J. Kötter, S. Decker, U. Herrmann, M. Schmitz and E. Lüpfer, “Dynamic performance evaluation of the HelioTrough® collector demonstration loop towards a new benchmark in parabolic trough qualification,” Elsevier by SolarPaces , Cologne, 2013.
- [36] E. Bellos and C. Tzivanidis, “Alternative Designs of Parabolic Trough Soalr Collectors,” *Process in Energy and Combustion Science, Elsevier*, vol. 71, pp. 81-117, 2018.
- [37] E. Lüpfer and B. Schiricke, “QUARZ Zentrum –Übersicht der entwickelten Prüfmethode im DLR-Test- und Qualifizierungszentrum für konzentrierende Solartechnik,” DLR, 2009.
- [38] S. Jones, “TRNSYS Modeling of the SEGS VI Parabolic Trough Solar Electric Generating System,” in *Solar Forum 2001: Solar Energy: The Power to Choose*, 2001.
- [39] P. Viebahn, S. Kronshage, F. Trieb and Y. Lechon, “Final report on technical data, costs, and life cycle inventories of solar thermal power plants,” 2008.

- [40] European Academies Sciences Advisory Council (EASAC), “Concentrating solar power: its potential contribution to a sustainable energy future,” The Clyvedon Press Ltd, Cardiff,, Halle, 2011.
- [41] C. Hemauer and R. Keller, ““No1 Sun Engine”, Art Project, 11th Cairo International Biennalet,,” December 20th – February 20th, 2008. [Online]. [Accessed <http://www.sun1913.info>,].
- [42] F. Schuman and C. Boys, “Sun Boiler”. Sun Boiler\_ Patent US1240890, 30. 11. 1912.
- [43] M. Eickhoff, “U4: Parabolic Trough and Fresnel Collectors - Capacity Building Course eM-CB01,” DLR, enerMENA.
- [44] Abengoa Solar, “A New Generation of Parabolic Trough Technology,” SunShot CSP Programm Review, Phoenix, 2013.
- [45] K. Riffelmann, T. Richert, P. Nava and A. Schweitzer, “Ultimate Trough® – A significant step towards cost-competitive CSP,” in *Energy Procedia, Elsevier, SolarPaces*, Cologne, 2013.
- [46] D. Benitez, “Potential of developing a manufacturing industry for CSP/CST in Chile,” DLR, Almería, 2017.
- [47] R. Blümner, “Development and Testing of a Design Optimization Routine for Concentrating Solar Power Collectors,” Berlin Institute of Technology, Almería, 2012.
- [48] Federal Highway Administration, “Material Property Characterization of Ultra-High Performance Concrete,” U.S. Department of Transportation , Gorgetown Pike, 2006.
- [49] W. Schiel, “Next Generation Parabolic Trough,” in *Kölner Sonnenkolloquium*, Jülich, 2011.
- [50] SkyFuel, “SkyTrough Product Information (Data Sheet),” 2017. [Online]. Available: <http://www.skyfuel.com/downloads/brochure/SkyTroughBrochure.pdf>. [Accessed 29. 11. 2018].
- [51] SkyFuel, “SkyTroughDSP Product Information (Data Sheet),” 2017. [Online]. Available: <http://www.skyfuel.com/downloads/brochure/SkyTroughDSPBrochure.pdf>. [Accessed 30. 11. 2018].
- [52] J. R. Raush and T. L. Chambers, “Initial field testing of concentrating solar photovoltaic (CSPV) thermal hybrid solar energy generator utilizing large aperture parabolic trough and spectrum selective mirrors,” *International Journal of Sustainable and Green Energy*, vol. 3, no. (6), pp. 123-131, 2014.
- [53] Glass Point Solar, “Fact Sheet GlassPoint Collector,” California, 2013.
- [54] Heliomis AG, “Frequently Asket Questions,” Heliomis, Wiener Neudorf, 2018.
- [55] DLR, “MS-Trough Report,” 2015.

## 6. Bibliography

---

- [56] M. Eickhoff, M. Hauke and E. Lüpfer, “Collector-Efficiencies of the 75m-EUROTROUGH-Collector with UVAC absorber tubes,” DLR, Tabernas, 2002.
- [57] G. Hoste and N. Schuknecht, “Thermal efficiency analysis of SkyFuel’s advanced, large-aperture, parabolic trough collector,” in *International Conference on Concentrating Solar Power and Chemical Energy Systems, SolarPaces 2014*, Arvada, 2015.
- [58] P. Kurup and Craig S. Turchi, “Parabolic Trough Collector Cost Update for the System Advisor Model (SAM),” National Renewable Energy Laboratory (NREL), Denver, 2015.
- [59] D. Wallace, “Sciencing,” 09. 01. 2018. [Online]. Available: <https://sciencing.com/about-6711987-price-steel-vs--stainless-steel.html>. [Accessed 05. 07. 2019].
- [60] C. Turchi and M. Mehos, “Current and Future Costs for Parabolic Trough and Power Tower Systems in the US Market,” National Renewable Energy Laboratory (NREL), Perpignan, 2010.
- [61] 3M and Gossamer SpaceFrames, “3M and Gossamer Space Frames to Inaugurate World’s Largest Aperture Parabolic Trough Installation - A New Benchmark in Solar Collectors,” 3M, St. Paulo, 2012.
- [62] R. Stancich, “toughTrough: From renewable to invincible,” *CSP Today*, p. 3, 18. 05. 2012.
- [63] Alto.Solutions, “High performance and highly cost-competitive parabolic trough,” 2018.
- [64] C. Prahll and A. Pfahl, “A New Concept For Line-Concentrating CSP Collectors,” SolarPaces, Tabernas, 2009.
- [65] 3M and Gossamer Space Frames, “Large Aperture Trough (LAT) 73 - engineered by Gossamer Space Frames and 3M,” 3M, St. Paul, 2012.
- [66] Solarlite GmbH, “Solar Trough Technology - SL4600, Technical Datasheet,” Solarlite, Duckwitz, 2010.
- [67] Airlight Energy, “Concentrated Solar Power Thermal Collector Data Sheet,” Airlight Energy, Biasca.
- [68] R. Bader, “Optical and thermal analyses of an air-based solar trough concentrating system,” ETH Zurich Research Collection, Zurich, 2011.
- [69] CIEMAT, CRES, DLR, F. Solar, F. Solar, INABENSA and SBP, “Development of a new Low Cost European Parabolic Trough Collector,” Non Nuclear Energy Programme, Tabernas, 2001.
- [70] C. Prahll, “Solar Power Plant Costs Estimation with differnt Modells,” 2009.
- [71] D. T. Chen, G. Reynolds and A. Gray, “Nest Generation Parabolic Trough Solar Collectors fro CSP,”

- in *Proceedings of the 6th International Conference on Energy Sustainability*, St. Paul, 2012.
- [72] B. Bierman, C. Treynor, J. O'Donnell, M. Lawrence, M. Chandra and A. Farver, "Performance of an Enclosed Trough EOR System in South Oman," in *SolarPACES 2013*, -, 2013.
- [73] VDI-Richtlinie, "VDI2225 - Konstruktionsmethodik, Technisch-Wirtschaftliches Konstruieren, Technisch-Wirtschaftliche Bewertung (Blatt 3)," Verein Deutscher Ingenieure, Düsseldorf, 1998.
- [74] D. O'Rourke, "Improved Large Aperture Collector Manufacturing," Abengoa Solar LLC, Lakewood, 2015.
- [75] A. Fernández-García, E. Zarza, L. Valenzuela and M. Pérez, "Parabolic-trough solar collectors and their applications," *Elsevier*, p. 27, 2010.

## Annex A

### A. Department internal survey: questionnaire & results

#### 1) In which fields of activity do you deal with parabolic trough collectors?

Anzahl Teilnehmer: 14

12 (85.7%): Forschung & Entwicklung

1 (7.1%): Betrieb & Instandhaltung

2 (14.3%): Inbetriebnahme

5 (35.7%): Testsdurchführung

- (0.0%): Dienstleistung

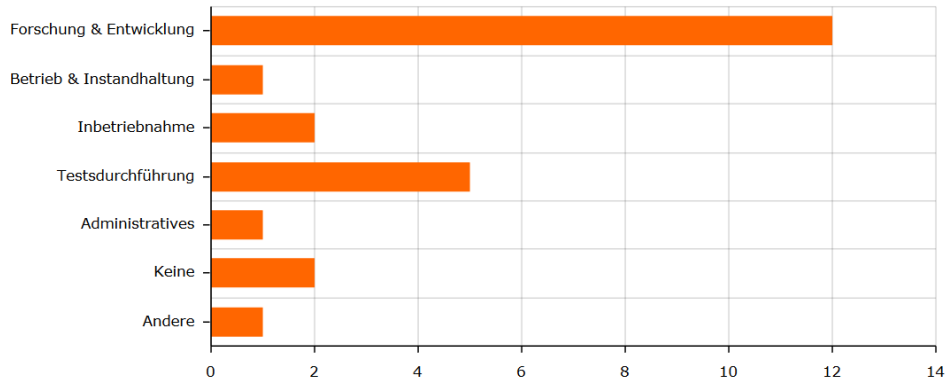
1 (7.1%): Administratives

2 (14.3%): Keine

1 (7.1%): Andere

Antwort(en) aus dem Zusatzfeld:

- Marktbeobachtung



#### 2) Which of these collectors for large scale solar fields is known to you?

Anzahl Teilnehmer: 14

12 (85.7%): EuroTrough

11 (78.6%): HelioTrough

9 (64.3%): UltimateTrough

1 (7.1%): SpaceTube ST

7 (50.0%): SenerTrough

8 (57.1%): Skyfuel [DSP]

4 (28.6%): Airlight

8 (57.1%): Solarlite SL4600

7 (50.0%): Fix-Focus-Trough mit geteiltem Parabelspiegel

3 (21.4%): Aalborg Trough

4 (28.6%): ToughTrough

5 (35.7%): MS-Trough [Molten Salt]

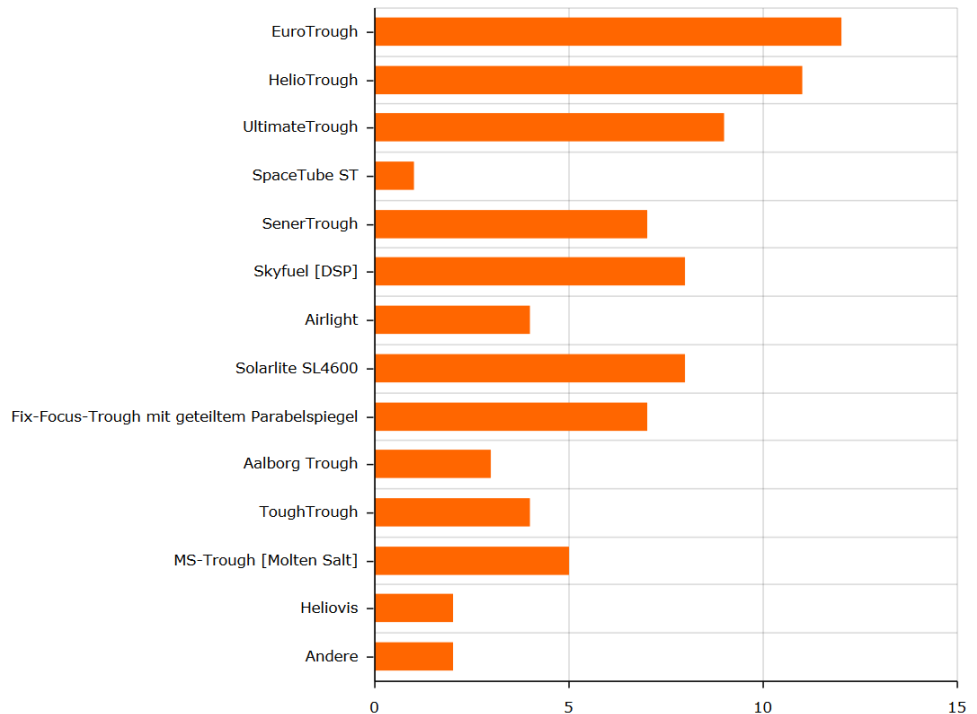
2 (14.3%): Heliovis

2 (14.3%): Andere

Antwort(en) aus dem Zusatzfeld:

- HelioPoint

- SEGS



**3) Do you know an innovative/alternative concept of parabolic trough collectors? If yes, please mention.**

- There was once a development for foldable collectors about 15 years ago from the DLR environment (Olaf Göbel). But is not further pursued m. W.
- Fix Focus trough by Christoph Prah

**4) Which specific components or aspects could be particularly relevant for increasing the efficiency and reducing the costs of parabolic trough collectors?**

- Lightweight dimensionally stable mirrors with high permanent reflectivity; Lightweight (low cost material...) dimensionally stable support structure; Improved HTF
- ball joint susceptibility; - monitoring of absorber tubes; - monitoring of pollution; - monitoring of mirror shape and alignment
- Maintenance (tracking, optical and thermal efficiency). Introduction of external systems to minimize wind loads and pollution; Automatic, water-saving cleaning system.
- BOP and solar field control; automated control; HTF (higher temperatures, HTF without need of freeze protection); optimized operation with memory (Peaker power plant)
- -Heavy and expensive EuroTrough torque box, which was simply copied in many new collector developments; - expensive self-supporting mirrors (as with EuroTrough) could be replaced by thin glass mirrors

**5) Do you recognize a weak point in the technology of parabolic troughs?**

- Lower temperature than towers, therefore more limited field of application
- Complex control. Use of sensitive components that are either expensive themselves, or expensive to repair (especially in the frequency they occur).
- High operating costs (a lot of personnel, many mechanical and hydraulic components, complex control and needs DNI), susceptible absorber glass breakage
- Very distributed hydraulic system (e.g. critical for leakages or Molten Salt)

**6) 'Last but not least': Would you like to make a free contribution to the topic?**

- I think parabolic troughs should be used more in the low process heat at medium temperature (200 - 400°C) or should be optimized for it. I.e. develop e.g. smaller, simpler, modular systems, which can be used "plug-and-play" in various industrial applications; for power generation, tower systems with molten salt currently offer a high potential for improvement.
- Compared to tower power plants, I find parabolic trough technologies much simpler and modular
- I think that CSP power plants in general have an affirmation of existence due to the storage tanks. The mass of solar power, however, will remain PV. With parabolic troughs, switching to a new HTF could do a lot. This could be salt or silicon oils.
- Large Aperture Trough with Molten Salt or Silicone Oils

## **Annex B**

# **Supplement of Master Thesis**

## **Parabolic Trough Collectors for Large Scale Application**

### **Conventional and Innovative Concepts**

**Thesis Title (german):**      Konzentrierende Solarenergie: Vergleich und Bewertung von innovativen Parabolrinnenkollektor-Konzepten für die Anwendung im großen Maßstab

**Thesis Title:**              Concentrating Solar Power: A comparison and evaluation of innovative parabolic trough collector concepts for large scale application

Author:                              José Rolando Fredriksson Chaves

Student number:                121042235

Study group:                    MM/15

Supervisor:                      Prof. Dr. rer. nat. Lutz Giese

Second assessor:              Prof. Dr. rer. nat. Michael Herzog

Institute advisor:              Dipl. Ing. Martin Eickhoff  
German Aerospace Center (DLR)  
Institute for Solar Research

Submitted on:                  11.08.2019